UNIVERSITY OF SANTIAGO DE COMPOSTELA

SCHOOL OF ENGINEERING (E.T.S. E.)

Department of Chemical Engineering

APPLICATIONS OF SURFACE ACTIVE IONIC LIQUIDS

Doctoral Thesis submitted, as compendium of publicatons, by IAGO RODRÍGUEZ PALMEIRO for the degree of Doctor in Chemical and Environmental Engineering to the University of Santiago de Compostela.

Santiago de Compostela, September 2016.

USC
UNIVERSIDADE
DE SANTIAGO
DE COMPOSTELA

Authorization for submission by the thesis directors (in Spanish)

Ana M. Soto Campos, Catedrática de Universidad, y **Eva Rodil Rodríguez**, Profesora Titular, del Departamento de Ingeniería Química de la Universidad de Santiago de Compostela

INFORMAN:

Que la presente memoria titulada *"Applications of Surface Active Ionic Liquids"*, que para optar al grado de Doctor en Ingeniería Química, Programa de Doctorado de Ingeniería Química y Ambiental, presenta **Iago Rodríguez Palmeiro,** fue realizada bajo nuestra inmediata dirección en el Departamento de Ingeniería Química de la Universidad de Santiago de Compostela.

Considerando que constituye trabajo de Tesis, y que su presentación como compendio de artículos es adecuada, autorizan su presentación a la Comisión de Tercer Ciclo de la Universidad de Santiago de Compostela.

Y para que así conste, firman el presente informe en Santiago de Compostela a 1 de Septiembre de 2016.

Ana M. Soto Campos Eva Rodil Rodríguez

USC
UNIVERSIDADE
DE SANTIAGO
DE COMPOSTELA

Acknowledgements

Looking back on the last few years, what I can see is a very important period of my life; full of experiences that helped me to be the man I am today. During these years, I had the great privilege of being part of the Group of Phase Equilibria and Separation Processes of the University of Santiago de Compostela working as a PhD student. Thus, I would like to express my acknowledgements to all the people that in one way or another walked this path by my side.

In first place I would like to thank Professors Alberto Arce and Ana Soto for the great opportunity of being part of this family. They lead the ship with honesty, being an example of professionalism, and giving everyday meaning to the expression “hard-working”. I am certainly indebted to them.

This acknowledgement is also extended to Eva Rodil. She brings me her knowledge on nanotechnology, and was helpful and patient. I also thank Héctor Rodríguez, he really was a “big brother” in the lab, always ready to help, putting his great experience in ionic liquids at the service of all group members. In the same way, I want to thank Óscar Rodríguez and Alberto Arce Jr. for their kind dedication and useful advice.

When I first joined the group I found the open arms of Sara, Alicia and Borja. I can undoubtedly say that I have found true friends in them. Although both Iria and Maria arrived later, we all quickly became not only good lab mates but also a great family. I would also thank Cristina, Jara, Adrián, Elio, Marlén, Raquel, Xiana and Manuel, I realized how lucky I was having such a good working environment; they were surely responsible for that.

Of course I don´t want to forget the RIAIDT staff for their quick and thorough work, and the Department members for their collaboration and help.

My recent short stay at TU Bergakademie Freiberg (Germany) meant not only a great professional and academic experience, but also a stage of personal growth. I want to thank Professor Mohammed Amro for allowing me to form part of his excellent group. I can´t forget Sven, Christin and Martina for their teachings as well as their warm and friendly welcome.

And finally I want to remember my family and friends. They are everything, the most important thing in my life. I thank my parents, brothers and sisters, for their unconditional support and for being an example and reference. I want to thank Irene, my wife, for every day we spend together. All of them add meaning to my life. I hope they can feel proud of me.

I want to close these lines by thanking the Ministry of Economy and Competitiveness of Spain for financial support throughout project CQT2012-33359 (including European Regional Development Fund advanced funding), and finally to express my gratitude to the University of Santiago de Compostela.

Iago Rodríguez-Palmeiro

Santiago de Compostela, September 2016.

Abstract

The overall objective of this thesis is to take advantage of the existence of polar/non-polar domains in ionic liquids, specifically surfactants, to develop new applications of these salts.

Silver chloride nanoparticles were synthesised using solely the surfactant ionic liquid trihexyl(tetradecyl)-phosphonium chloride and AgCl bulk powder. The nanoparticles were characterised and tested as nanocatalysts in the photodegradation of Orange II. An almost complete degradation can be achieved, in optimal conditions, and the nanoparticles can be recycled.

The same method of synthesis was used to prepare ionanofluids consisting of AgI nanoparticles in the ionic liquid trihexyl(tetradecyl)phosphonium chloride. High concentrate and stable nanofluids were obtained and characterised. The use of this method, with a careful consideration in the selection of the ionic liquid and nanoparticles, allows obtaining nanofluids of enhanced properties.

The capability of 1-alkyl-3-methylimidazolium surfactant ionic liquids to improve surfactant enhanced oil recovery methods was analysed. Liquid–liquid equilibria of water + $[C_n mim][NTf_2]$ (n = 10 or 12) + n-dodecane ternary systems were measured at 298.15 and 348.15 K. These systems can be classified as Winsor III. Some drawbacks were detected to use these ionic liquids in oil recovery. However the PC-SAFT equation of state was able to predict the equilibria. Thus, this model can be a fast and cheap initial method for the screening of possible surfactants for this application. The bistrifluoromethylsulfonylimide anion of the previously tested ionic liquids was changed for acetate. The dynamic interfacial tensions between several formulations, containing the ionic liquid, and crude oil (Saharan blend) were evaluated by the spinning drop method. The results obtained significantly improve upon previous results obtained up to with other ionic liquids.

Surfactant ionic liquids can be used for the synthesis of nanoparticles and ionanofluids, and are promising alternatives to evaluate for oil recovery.

Keywords: surfactant ionic liquids, nanoparticles, ionanofluids, enhanced oil recovery.

Resumen (Spanish)

El objetivo global de esta tesis es aprovechar las ventajas de los dominios polares y no polares existentes en líquidos iónicos, específicamente surfactantes, para desarrollar nuevas aplicaciones de estas sales.

Se sintetizaron nanopartículas de cloruro de plata utilizando únicamente el líquido iónico surfactante cloruro de trihexil(tetradecil)fosfonio y AgCl sólido volumétrico. Las nanopartículas fueron caracterizadas y probadas como nanocatalizadores en la fotodegradación del colorante naranja de β-naftol. En condiciones óptimas la degradación es prácticamente completa. Las nanopartículas son reciclables.

El mismo método de síntesis se utilizó para preparar ionanofluidos consistentes en nanopartículas de AgI en cloruro de trihexil(tetradecil)fosfonio. Se obtuvieron nanofluidos muy estables de alta concentración que fueron caracterizados. El uso de este método, con la selección adecuada de nanopartículas y líquido iónico, permite obtener nanofluidos de propiedades mejoradas.

Se analizó la capacidad de líquidos iónicos surfactantes con catión 1-alquil-3-metilimidazolio para mejorar los métodos de extracción mejorada del petróleo. Se determinó el equilibrio líquido-líquido de los sistemas ternarios agua + $[C_n mim][NTf_2]$ (n = 10 o 12) + n-dodecano a 298.15 y 348.15 K. Se encontraron sistemas Winsor tipo III. Se detectaron algunos inconvenientes en el uso de estos líquidos iónicos para la extracción de crudo, sin embargo, la ecuación de estado PC-SAFT fue capaz de predecir los equilibrios. Por lo tanto, esta ecuación puede convertirse en un método rápido y barato de preselección de surfactantes de interés para esta aplicación. Se cambió el anión bistrifluorometil-sulfonilamiduro de los líquidos iónicos probados por el acetato. Se determinaron tensiones interfaciales dinámicas entre diversas formulaciones (con estos líquidos iónicos) y crudo, obteniéndose reducciones en la tensión interfacial muy superiores a las presentada hasta el momento en la bibliografía.

Los líquidos iónicos surfactantes pueden utilizarse para la síntesis de nanopartículas y nanofluidos, y son además interesantes alternativas a evaluar para la recuperación de crudo.

Palabras clave: líquidos iónicos surfactantes, nanopartículas, ionanofluidos, extracción mejorada del petróleo.

Resumo (Galician)

O obxectivo global desta tese é aproveitar as vantaxes dos dominios polares e non polares existentes nos líquidos iónicos, especificamente surfactantes, para desenvolver novas aplicacións destes sales.

Sintetizáronse nanopartículas de cloruro de prata utilizando unicamente o líquido iónico surfactante cloruro de trihexil(tetradecil)fosfonio e AgCl sólido volumétrico. As nanopartículas foron caracterizadas e probadas como nanocatalizadores na fotodegradación do colorante laranxa β-naftol. En condicións óptimas a degradación é practicamente completa. As nanopartículas son reciclables.

O mesmo método de síntese utilizouse para preparar ionanofluídos consistentes en nanopartículas de AgI en cloruro de trihexil(tetradecil)fosfonio. Obtivéronse nanofluídos muy estables de alta concentración que foron caracterizados. O uso deste método, coa selección adecuada de nanopartículas e líquido iónico, permite obter nanofluídos de propiedades melloradas.

Analizouse a capacidade de líquidos iónicos surfactantes con catión 1-alquil-3-metilimidazolio para mellorar os métodos de extracción mellorada do petróleo. Determinouse o equilibrio líquido-líquido dos sistemas ternarios auga + $[C_n mim][NTf_2]$ (n = 10 ou 12) + n-dodecano a 298.15 e 348.15 K. Atopáronse sistemas Winsor tipo III. Detectáronse algúns inconvenientes no uso destes líquidos iónicos para a extracción de cru, con todo, a ecuación de estado PC-SAFT foi capaz de predicir os equilibrios. Por tanto, este modelo pode converterse nun método rápido e barato de pre-selección de surfactantes de interese para esta aplicación. Cambiouse o anión bistrifluorometilsulfonilamiduro dos líquidos iónicos probados polo acetato. Determináronse tensións interfaciales dinámicas entre diversas formulacións (con estes líquidos iónicos) e cru, obténdose reducións na tensión interfacial moi superiores ás presentada ata o momento na bibliografía.

Os líquidos iónicos surfactantes poden utilizarse para a síntese de nanopartículas e nanofluidos, e son ademais interesantes alternativas a avaliar para a recuperación de cru.

Palabras clave: líquidos iónicos surfactantes, nanopartículas, ionanofluídos, extracción mellorada do petróleo.

CONTENTS

1. OBJECTIVES....1
2. INTRODUCTION....7
2.1. IONIC LIQUIDS....9
2.1.1. Definition....9
2.1.2. Origin and generations....10
2.1.3. Properties of ILs....11
2.1.4. Applications of ILs....12
2.1.4.1. Electrochemistry....12
2.1.4.2. Synthesis and catalysis....13
2.1.4.3. Separation processes....15
2.1.4.4. Synthesis of nanomaterials....17
2.1.4.5. Other applications....17
2.1.5. Surface Active Ionic Liquids (SAILs)....18
2.2. NANOTECHNOLOGY....23
2.2.1. Definition....23
2.2.2. History....23
2.2.3. Classification of the nanostructures and effects of the nanometric scale....25
2.2.4. Nanoparticles....27
2.2.4.1. Definition....27
2.2.4.2. Conventional synthesis of nanoparticles....28
"Bottom-up" methods.....28
"Top-down" methods....29
2.2.4.3. Ionic liquids in the synthesis of nanoparticles....30
2.2.4.4. Applications of nanoparticles....32
2.2.5. Nanofluids....36
2.2.5.1. Definition....36
2.2.5.2. Synthesis of nanofluids....36
2.2.5.3. Ionanofluids....38
2.2.5.4. Application of nanofluids....39
2.3. ENHANCED OIL RECOVERY....42
2.3.1. Introduction....42
2.3.2. Oil Recovery Stages....42
2.3.3. Enhanced Oil Recovery methods....43
2.3.4. Surfactant and microemulsion flooding....47
2.3.4.1. Phase equilibria related to surfactant EOR methods....48
2.3.5. SAILs in EOR.....51
3. PUBLICATIONS....55
3.1. Synthesis of AgCl nanoparticles in ionic liquid and their application in photodegradation of Orange II....57
3.2. Synthesis and characterisation of highly concentrated AgI–$[P_{6\,6\,6\,14}]$Cl ionanofluids....67

3.3. Measuring and PC-SAFT modelling three-phase behaviour 75
3.4. Characterisation and interfacial properties of the surfactant ionic liquid 1-dodecyl-3-methylimidazolium acetate for enhanced oil recovery 93
4. GENERAL DISCUSSION 101
5. CONCLUSIONS 109
LIST OF SYMBOLS 115
REFERENCES 121
APPENDIX: RESUMEN (Summary, in Spanish) 143

1. OBJECTIVES

USC
UNIVERSIDADE
DE SANTIAGO
DE COMPOSTELA

Along with the peculiar and interesting set of physico-chemical properties of ionic liquids (ILs), these salts also show a complex local organization with self-aggregating polar and non-polar domains. The high-charge density parts of cations and anions create a polar network and the low-charge density residues, that are present in the ions as alkyl side chains, are segregated from the polar network forming non-polar domains. This structuration between polar and non-polar regions implies the existence of differentiated and complex interactions not only in pure ILs but also in their mixtures with other compounds. Moreover, the amphiphilic nature of these salts makes them potential surfactants. A surfactant or surface-active ionic liquid (SAIL) reduces the surface tension of solvents to a significant extent. In surfactant systems, the polar and non-polar domains can arrange themselves in a variety of assemblies (micellar systems, microemulsions and liquid crystals). In the case of SAILs, this situation is particularly significant due to the high degree of structural and charge anisotropy of ions.

The overall objective of this Thesis is to take advantage of the existence of polar/non-polar domains, specifically in SAILs, to develop new applications of these salts. More explicitly, SAILs will be used for the synthesis of nanoparticles and nanofluids by a dissolution-reprecipitation method. Moreover, the suitability of using these surfactants to improve enhanced oil recovery (EOR) methods will also be investigated. The above-mentioned specific objectives are presented below in detail.

– **Synthesis of AgCl nanoparticles in ionic liquid and their application in photodegradation of Orange II**

The objective of this work is the synthesis of AgCl nanoparticles. A method based on the dissolution of the bulk powder and reprecipitation in the nano-domains of the IL trihexyl(tetradecyl)phosphonium chloride, $[P_{6\ 6\ 6\ 14}]Cl$, will be used. The nanoparticles will be then precipitated from the dispersion. The aim is the use of these nanoparticles as photocatalyst for the degradation under UV radiation of an azo dye, Orange II, usually found in textile wastewaters. The parameters of the process (catalyst loading, pH solution, operation times, etc.) will be optimised, and the recyclability of the catalyst evaluated.

– **Synthesis and characterisation of highly concentrated AgI–[$P_{6\,6\,6\,14}$]Cl ionanofluids**

In this case, the dissolution-reprecipitation method will be used for the synthesis of an ionanofluid consisting of AgI nanoparticles dispersed in the IL trihexyl(tetradecyl)-phosphonium chloride, [$P_{6\,6\,6\,14}$]Cl. The aim is to obtain an ionanofluid of enhanced thermal and conductivity properties in comparison with the IL used for the synthesis. The ionanofluids synthesised and their constituent nanoparticles will be characterised. The physical properties of the nanofluids (such as density, viscosity, electric conductivity, refractive index, and specific heat capacity) will be measured and compared to those of the pure IL at several temperatures. A comparison between these properties for both IL and ionanofluid will show if the goal is achieved.

– **Measuring and PC-SAFT modelling three-phase behaviour**

The main mechanism of surfactant EOR is reducing interfacial tension, which has been linked to water and oil solubilisation and the presence of a third, immiscible, microemulsion phase. Thus, the determination of phase behaviour and interfacial tension between phases in equilibrium is necessary as a fundamental study to evaluate the use of SAILs in EOR. Therefore, the goal of this work is to determine the phase diagram of the ternary systems water + 1-decyl-3-methylimidazolium bis(trifluoromethylsulfonyl)-imide, [C_{10}mim][NTf_2] + *n*-dodecane and water + 1-dodecyl-3-methylimidazolium bis(trifluoromethylsulfonyl)imide, [C_{12}mim][NTf_2] + *n*-dodecane, as a first step on the application of these SAILs in oil recovery. PC-SAFT will be applied to predict the phase behaviour, and results will be compared with the experimentally obtained phase diagrams.

– **Characterisation and interfacial properties of the surfactant ionic liquid 1-dodecyl-3-methylimidazolium acetate for enhanced oil recovery**

The objective of this work is to synthesise and characterise the SAIL 1-dodecyl-3-methylimidazolium acetate, [C_{12}mim][OAc]. Its suitability to improve surfactant EOR methods will be tested. To analyse its capacity to reduce the interfacial tension between water and oil, the dynamic interfacial tensions between the aqueous solutions of this SAIL and crude oil (Saharan blend) will be evaluated. The

effect of different variables (temperature and concentration of SAIL and NaCl) will be analysed looking for the best formulation to be used in EOR.

USC
UNIVERSIDADE
DE SANTIAGO
DE COMPOSTELA

2. INTRODUCTION

USC
UNIVERSIDADE
DE SANTIAGO
DE COMPOSTELA

2.1. IONIC LIQUIDS

2.1.1. Definition

There are many slightly different definitions in literature for ionic liquids (ILs). The most widespread claims that ILs are salts composed solely of ions, having a melting point below 373.15 K [1-4]. Many of them are also liquids at room temperature, so they are called “room temperature ionic liquids” (*RTILs*).

The reduced coordination between the ions that form the ILs (due to the asymmetry of the cation with respect to the anion) decreases the lattice energy of the crystalline form of the salt, and it is responsible for the significantly low melting point of these compounds compared to conventional salts [5].

The ILs often comprise large and unsymmetrical organic cations and organic or inorganic anions. Within the wide variety of cations present in ILs, the most significant are those formed by nitrogen or phosphorus-containing molecules with different alkyl chains. In the case of anions, they can be reduced-size molecules such as halides, but also greater and more complex structures. Figures 2.1 and 2.2 show the most common cations and anions, respectively, that form part of the structure of the ILs. Due to all of the possible combinations of different ions, the potential for research and synthesis of new ILs is virtually unlimited [6]. Among them, protic ILs are formed by proton transfer from an acid to a base. As these ILs may contain a reduced proportion of molecular species, their vapour pressure is not as negligible as in the case of aprotic ILs.

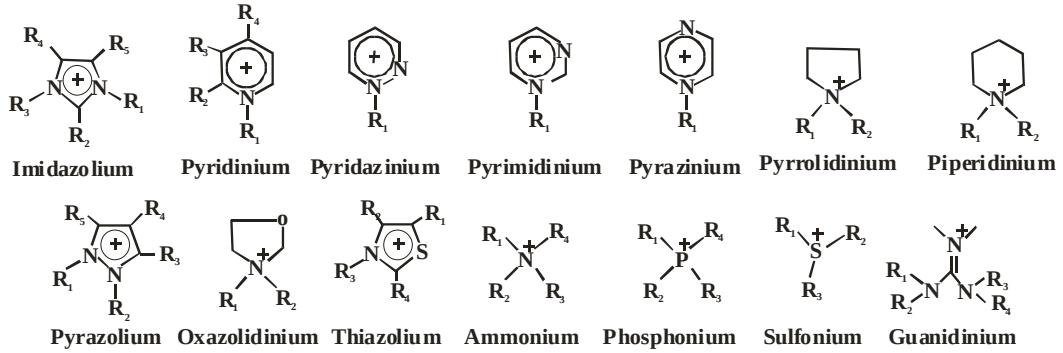

Figure 2.1. Most common cations in ILs.

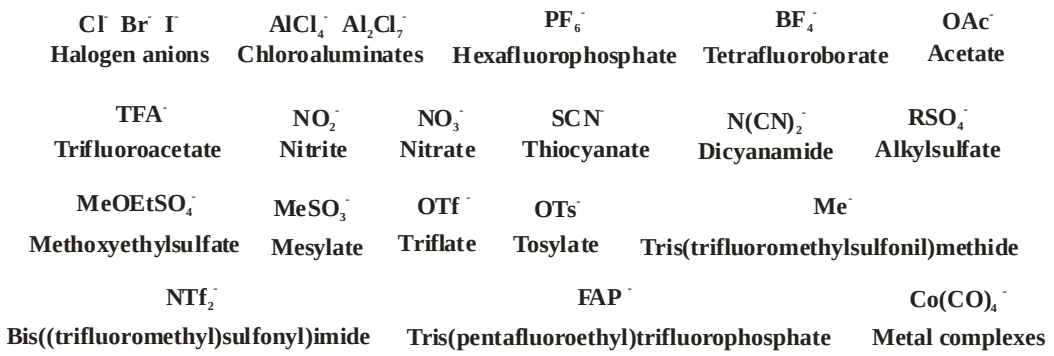

Figure 2.2. Most common anions in ILs.

2.1.2. Origin and generations

In 1877 Friedel-Crafts reported the formation of a "red oil" during a series of alkylation and acylation reactions [7]. That compound, that could not be determined at that time, was identified in 1976 by Nambu [8] as an IL composed of an alkylated aromatic ring cation and a chloroaluminate anion. In the early 1880s, Gabriel and Weiner [9] reported the discovery of a protic IL, ethanolammonium nitrate, with a melting point of 325.15-328.15 K. It was probably the first organic salt with a melting point lower than 373.15 K.

However, it is considered that the birth of the ILs took place in 1914 with the publication of the synthesis of ethylammonium nitrate by Walden [10]. This IL, with a melting point of 285.65 K, is known as the first RTIL described in the literature. Nonetheless, the explosion in research on ILs only took place in the late 20th Century, resulting in an exponential increase in the publications on the topic.

The haloaluminate-based ILs comprise the first generation. Wilkes reported the use of dialkylimidazolium chloroaluminates in 1982 [11]. These kinds of ILs have been studied widely as solvents and catalysts for several organic reactions. However, their reactivity with water implies that they have to be handled in a dry-box. The second generation includes the non-haluminated ILs which have been extensively used in organic chemistry as solvents. In 1992, Wilkes and Zaworotko [12] reported the synthesis of 1-ethyl-3-methylimidazolium ILs with weakly coordinating anions such as tetrafluoroborates, [BF_4^-], and hexafluorophosphates, [PF_6^-]. Although it was initially believed that they were stable in water, it is shown that under certain conditions they

undergo hydrolysis forming hydrogen fluoride. Bonhôte and co-workers reported in 1996 [13] the synthesis of hydrophobic ILs by using the bis(trifluoromethylsulfonyl)imide anion, [NTf_2^-]. These ILs are stable in the presence of air and water. The so-called third generation of ILs appeared in the early 2000s and comprises task-specific, designed salts to have specific properties or reactivity, and chiral ILs.

Given the current emphasis on environmentally friendly chemistry and the sustainable use of resources, an area of current interest is the design of ILs that are based on low-toxicity natural products (e. g. choline). Furthermore, biodegradability is another key factor in the development and acceptation of ILs as solvents of the future.

2.1.3. Properties of ILs

ILs exhibit many properties which make them potentially attractive compounds as an alternative to traditional organic solvents. Among the most important, the following should be mentioned [7, 14]:

- They are liquids below 373.15 K, by definition, and many of them at room temperature. Furthermore, in general ILs present far higher liquid range than molecular solvents.
- Their vapour pressure is negligible. This property generates a great amount of interest in ILs from the point of view of green chemistry. As non-volatile solvents, air pollution is avoided and the upper limit of their liquid range is determined by their thermal decomposition temperature.
- In general, they are thermally stable compounds and they are usually not flammable. This means that ILs can be used at high operating temperatures without solvent degradation.
- The stability of ILs in water varies widely. Many are stable in the presence of water but there are important exceptions, such as haloaluminate-based ILs and others containing [BF_4^-] or [PF_6^-] anions.
- In general ILs present a wide electrochemical window and high conductivity values.
- ILs can dissolve substances of different natures. The existence of polar and non-polar domains in the molecule of the IL is responsible for different molecular

interactions, depending on the nature of the chemical species dissolved in such medium.

In addition to these general properties, ILs may present specific properties. On one hand, different combinations of cations and anions can be used. On the other hand, the structure of the cation and/or anion can be modified by changing the length of the alkyl chain or by the introduction of different functional groups. This fundamental aspect makes that ILs are considered to be "designer solvents" [6]. An IL with physical and/or chemical specific properties can be designed depending on the requirements of the application in which it is going to be used. For instance, the miscibility of ILs in water is determined by the forming ions, being the coordination capacity of the anion a key factor in the hydrophobicity of the IL [4]. Some ILs with specific functional groups can act not only as solvents but also as catalysts in certain reactions [7, 15]. The presence of long chain alkyl structures in the cation and/or the anion can give the ILs surfactant character [16].

2.1.4. Applications of ILs

Given this range of possibilities offered by ILs, it is logical that in recent years there has been an enormous interest, from the scientific community, in order to apply these promising compounds in different processes, mainly as an alternative to conventional volatile organic compounds (VOCs) [17, 18].

VOCs have been used in a variety of industrial applications. As a result of their volatile nature, these compounds easily evaporate into the environment. The use of these compounds implies a risk to people working with them. Furthermore, VOCs have been strongly implicated in causing changes to the global climate as well as being identified as a source of ozone depletion. Many industries and organizations have been forced to re-evaluate their chemical operations, due to the environmental impact caused by the use of VOCs. ILs are being evaluated as a possible solution to these problems.

2.1.4.1. Electrochemistry

One of the first areas where ILs have been proposed is electrochemistry. Their high ionic conductivity and wide electrochemical window have led to different electrochemical applications [19, 20]. Important work is being carried out on

the use of ILs as electrolytes for batteries, solar cells, fuel cells, and other chemical devices (actuators, supercapacitors, etc.) Other applications consist of their use as solvents for electrochemical redox reactions or electrolytes for the electrodeposition of metals.

2.1.4.2. Synthesis and catalysis

Another main application of ILs is their use as synthesis media, replacing VOCs, and as catalysts in several reactions [21, 22]. There is an innumerable amount of reactions where ILs have been tested: energy transfer, electron transfer, acid-base, substitutions (S_N1, S_N2, nucleophilic aromatic...), eliminations, additions (electrophilic, nucleophilic, oxidative, 1,4-conjugate additions, Diels-Alder, metal alkyl and aryl addition reactions), acid-catalysed, base/nucleophile-catalysed, transition-metal-catalysed reactions, etc. It has been found that the performance, in terms of selectivity and reaction rates, for many of these reactions when ILs are used, is better than using conventional organic solvents. The solvent-solute interactions in the ILs, as well as their physical properties such as the liquid range, heat capacities, viscosities, and so on, are important parameters for the performance of a reaction within ILs.

IONIC LIQUIDS VERSUS ORGANIC SOLVENTS

ORGANIC SOLVENTS	IONIC LIQUIDS
▪ Sometimes difficult to find the desired solvent	▪ Ionic liquids have high solubilisation capacity
▪ Products and by-products are usually soluble in the solvent	▪ Mutual solubilities of ionic liquid, products and byproducts can be adjusted to optimise the process
▪ Homogeneous catalysis: difficult separation	▪ Often, the reactions are robust and work in the presence of water
▪ Difficult solvent recycling	▪ Homogeneous catalysis: simple separation
▪ Solvent loss by evaporation: exposure, environmental concerns, cost	▪ Catalyst dissolved in the ionic liquid, biphasic system, advantages of homogeneous and heterogeneous catalysis
▪ Problems with solvent flammability, toxicity, biodegradability	▪ Often easy solvent recycling
	▪ No solvent loss by evaporation
	▪ Most ionic liquids are non flammable
	▪ ILs can be designed: low toxicity, biodegradability

Figure 2.3. Advantages of ILs versus organic solvents in chemical reactions

The properties of ILs make them suitable as reaction media for a wide variety of reactions. Moreover, they are particularly attractive for monophasic and biphasic catalysis. In monophasic catalysis, the substrate and the catalyst are dissolved in the IL. The role of the IL can be the solvent, the catalyst, the co-catalyst or even the solvent and the catalyst or co-catalyst simultaneously. However, the separation of the products of the reaction and the IL can be a problem. In spite of the negligible vapour pressure of these compounds, high energy demand could be required to make the separation through distillation. This problem is overcome in the case of the biphasic catalysis. In biphasic systems, the catalyst is dissolved in the IL and the reactants and products dissolved in a second phase immiscible with the IL. The products can be easily separated by decantation and the IL-catalyst solution can be re-used. These two-phase or biphasic catalytic processes offer the benefits of both homogeneous (good contact between phases) and heterogeneous (easy separation) catalysis [4]. Heterogeneous catalysis, supported IL catalysis, or supported IL phase catalysis have also been proposed as applications of ILs. Figure 2.3 shows the advantages of ILs versus organic solvents in chemical reactions.

These advantages led to processes that have been or are being developed at industrial scale. From 1996 until 2004, Eastman Chemical Company run a process for the isomerization of 3,4-epoxybut-1-ene to 2,5-dihydrofuran [17]. The process used trialkyl iodide as a Lewis catalyst and a Lewis basic tetralkylphosphonium iodide IL, $[P_{8\ 8\ 8\ 18}]I$, as co-catalyst. The original process used a high boiling solvent that led to several undesired side reactions. The plant was shutdown because the decay of market for furan products. BASF (*Badische Anilin- und Soda-Fabrik*) developed in 1998 the BASIL (Biphasic Acid Scavenging Utilizing Ionic Liquids) process [23]. The process is used for the production of the generic photoinitiator precursors alkoxyphenylphosphines. In the original process (303.15 K) triethylamine was used to scavenge the acid forming the insoluble waste by-product triethylammonium chloride. Replacing triethylamine with 1-methylimidazole results in the formation of 1-methylimidazolium chloride, an IL, which separates out of the reaction mixture as a discrete phase. The new process (363.15 K) requires a much smaller reactor than the initial process and the yield has increased from 50% to 98%. 1-Methylimidazole is recycled via base decomposition.

Another example of reaction carried out commercially is the Difasol process developed by IFP (*Institut Français du Pétrole*) [24]. This process, an example of biphasic catalysis, is used for the dimerization of *n*-butene. It employs a catalyst (nickel salt) dissolved in an acidic chloroaluminate IL. The advantages in comparison with the classic process (Dimersol) are: a reduced catalyst disposal and cost, smaller reactor, higher yield and better dimer selectivity. The possibility of integrating the Difasol process into existing Dimersol plants is also an advantage.

2.1.4.3. Separation processes

ILs are playing an increasingly important role in separation science [25-29]. In the framework of analytical chemistry, ILs are selective stationary phases in gas chromatography. They are also being used as mobile phase modifiers or stationary phases in high performance liquid, planar, supercritical or counter-current chromatography. Moreover, new separation methods in which ILs are used as run buffer additives, and as wall-coated stationary phases, have significantly improved electrophoretic separations in capillary electrophoresis and capillary electrochromatography [25].

At an industrial level, ILs may be suitable replacements for the toxic, flammable and volatile organic compounds that are currently used in liquid-liquid extraction processes. Figure 2.4 shows the properties that define an ideal solvent and the properties of ILs that adhere to those requirements [26].

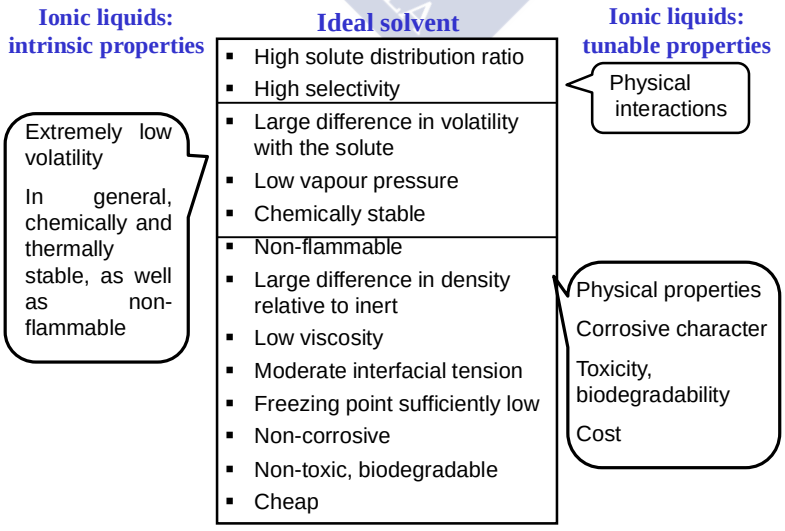

Figure 2.4. Required properties for an ideal solvent in comparison with ILs properties [26].

Separation of aromatic and aliphatic hydrocarbons (through the substitution of the classical solvents) and desulphurisation of fuel oils (proposing a liquid-liquid extraction unit instead of the hydrodesulphurisation process) are the most widely studied separations with ILs. Other separations also related to refineries where ILs are being tested are: bitumen recovery from oil sands, desalting, metals removal, and deasfalting [26]. ILs are also suitable as entrainers in extractive distillation. They combine the advantages of both organic solvents and salts increasing the relative volatility of one of the components and reducing the solvent-to-feed ratio by the salting out effect without the disadvantages of a solid salt [27]. In spite of the enormous number of publications found in relation to these topics, there is a serious lack of experiments carried out at a pilot plant level.

Aqueous biphasic systems (traditionally formed by two polymers or a salt and a polymer) can also be formed with a conventional salt and an IL. These systems are especially interesting for the extraction and purification of biomolecules and other substances that require an aqueous medium.

The processing of biomass (via solid-liquid extraction) is another area of research of great interest where ILs could mean an important revolution. The emphasis of most of the works resides, in one hand, in obtaining value-added compounds from plants, and secondly, in the dissolution and fractionation of lignocellulosic materials for the recovery of the major constituent biopolymers [28, 29].

From all the separation processes a special mention is required for the called Hycapure-Hg that has been installed in full-scale commercial on-shore gas terminals in Malaysia (Kerteh, Bintulu...), successfully producing sales-quality natural gas. It is a system for removing metals, particularly mercury, from hydrocarbon gases (also applicable to liquids) developed by the Queen's University Ionic Liquids Laboratories (QUILL) in collaboration with Petronas [30]. In the process, the mercury-containing hydrocarbon fluid feed is contacted with an IL (as a liquid or supported into a solid) having the formula $[Cat^+][M^+][X^-]$. $[Cat^+]$ and $[X^-]$ represent the common cations and anions of the ILs, and $[M^+]$ represents one or more transition metal cations having an oxidation state of +2 or greater. The ILs oxidise elemental mercury and organomercury species to highly soluble mercury ions and

extract them. The exiting hydrocarbon fluid has a reduced mercury content.

2.1.4.4. Synthesis of nanomaterials

The synthesis of inorganic matter in ILs is a rather new development, which has roughly emerged over the last decade [31-34]. Various approaches to the fabrication within ILs of inorganic solids, mostly nanoparticles and porous framework materials, with unprecedented and sometimes unique structures and properties have been reported.

Electrochemical methods have been among the first to be used for the fabrication of inorganic particles and nanostructured films in ILs. The properties of ILs allow the electrodeposition of metals and semiconductors at room temperature. The traditional hydrothermal or solvothermal reactions used in the synthesis of nanoparticles, transform into the ionothermal reactions (reactions that are conducted in ILs at high temperature) with the main advantage of taking place at ambient pressure. The obtaining of novel structures (that are not accessible with other conventional methods) can be expected, as the chemistry of ionothermal reactions is quite different from hydrothermal or solvothermal conditions. In other cases, the IL does not play only the role of the solvent but also they act as molecular precursor or template. They are the so-called solvent–reactant or solvent–template–reactant systems. The classical sol-gel route for the synthesis of inorganic materials has also been proved as successful when it is used with ILs. Another technique of synthesis of nanomaterials uses emulsions or microemulsions. In this case, the IL can play the role of the water, the organic solvent or the surfactant.

ILs possess highly organised structures, through mainly hydrogen bonds, that induce structural directionality. This structural organisation of imidazolium ILs can function as an "entropic driver" for spontaneous, well-defined, and extended ordering of nanostructures [34].

2.1.4.5. Other applications

Due to the active work of research groups, as well as the interest of companies, the number of applications where ILs are being tested is immeasurable [4]. It can be cited: reprocessing agents for nuclear fuels, energetic materials and

propellants, lubricants [35-38], optical immersion fluids, thermometers, pharmaceutical ingredients... among many others.

2.1.5. Surface Active Ionic Liquids (SAILs)

The surface tension of a liquid changes when other substances are dissolved in it. The surface activity of a solute is its ability to change the surface tension of solvents. Solutes that reduce the surface tension of a solvent have positive surface activity, and those that do so to a significant extent are known as surface-active agents, or surfactants for short. Such molecules are generally amphiphilic, possessing both a hydrophilic polar moiety with affinity for polar solvents and a hydrophobic (lipophilic) non-polar moiety (generally a hydrocarbon chain). However, amphiphiles do not have surface activity if their interactions with solvents are dominated by either their hydrophilic or their lipophilic moiety.

The steric mismatch that makes ILs having melting points below 373.15 K, is generally due in large part to the attachment of alkyl side chains to the charged head-group of the cation and/or anion. At least one of the ions of an IL is thus amphiphilic, and therefore a potential surfactant. Surfactant ILs (hereinafter SAILs), as conventional ionic surfactants, can be classified as anionic, cationic, catanionic or zwitterionic (positive and negative charge in the head group).

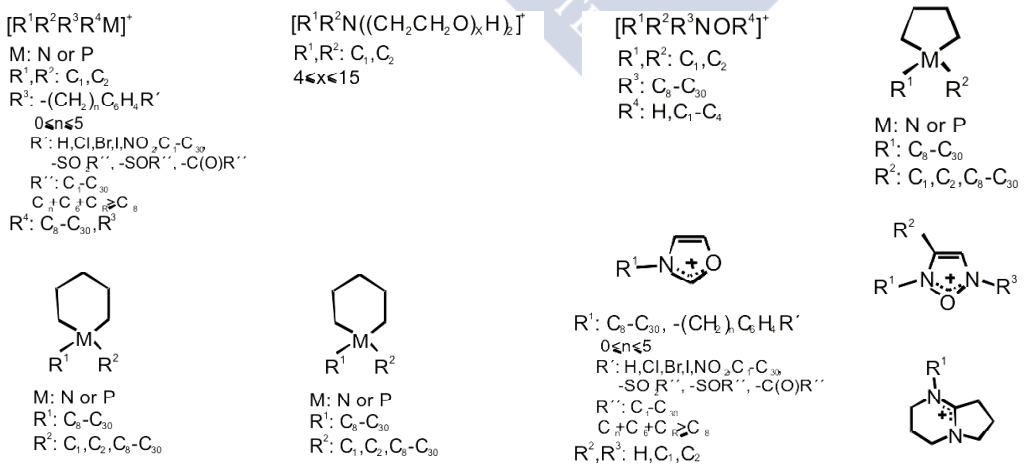

Figure 2.5. Typical cationic components of SAILs [39].

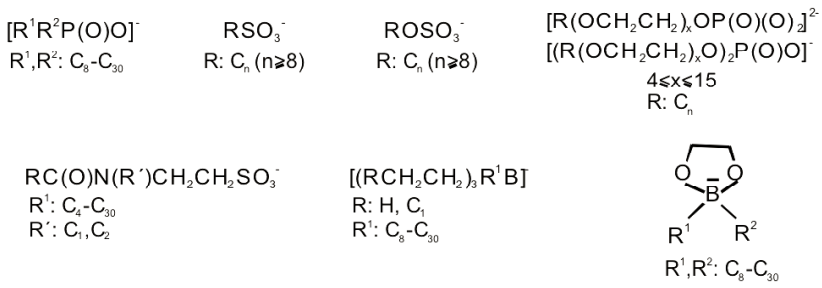

Figure 2.6. Typical anionic components of SAILs [39].

Figures 2.5 and 2.6 exhibit a number of typical SAILs, in this case taken from a patent application that cites as an advantage of the invention their ability to form stable microemulsions without any need for a cosurfactant or salt [39]. Possible applications cited include the preparation of foams for mobility control in gas or gas condensate reservoirs, the dispersion of oil spills, and use as emulsifiers or wetting agents in cleaning agents and personal hygiene products, as hydrophobic solvents, as lubricants or heat transfer agents in drilling fluids, as inhibitors of gas hydrates or corrosion in oil production, as recovery-enhancing additives in oil well flooding operations, as lubricants, hydraulic fluids, milling or cutting fluids, phase transfer agents or drug delivery agents, and as chemical reaction media (e.g. for micellar catalysis). A rough indication of the suitability of a particular SAIL for one or another application is given by its hydrophilic-lipophilic balance index (see Table 2.1).

Table 2.1. SAILs utilities corresponding to various ranges of hydrophilic-lipophilic balance value (HLB).

HLB	Applications
1-3	Anti-foaming agents
3-8	For w/o emulsions
7-9	Wetting agents
9-18	For o/w emulsions
15-20	Solubilising agents

So far, most SAILs research has concerned ILs in which the cation is amphiphilic and the anion is not, and which are thus classifiable as cationic surfactants. However, increasing attention is being paid to SAILs with amphiphilic anions and to catanionic SAILs in which both the anion and the cation are amphiphiles. For example, Blesic *et al.* [40] reported that whereas alkylimidazolium methylsulphates, $[C_nH_{2n+1}mim]$-$[MeSO_3]$, behaves as a cationic surfactant with $n>8$, alkylimidazolium alkylsulphates SAILs of the form

$[C_nH_{2n+1}mim][C_mH_{2m+1}SO_3]$ with *n,m* = 4,8 are catanionic and have greater surface activity

Two other classes of SAILs that must be mentioned are the gemini and polymeric SAILs. Gemini SAILs feature two linked replicates of an amphiphilic moiety, like that shown in Figure 2.7. Polymerisation raises melting points. Nevertheless, the formed polyelectrolyte from a SAIL can sometimes keep both IL and surfactant behaviour, although their surface properties have not been investigated in depth [41].

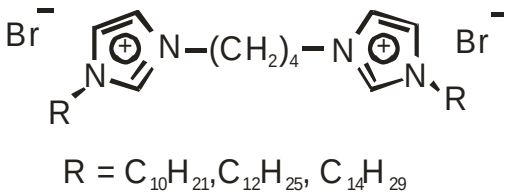

R = $C_{10}H_{21}$, $C_{12}H_{25}$, $C_{14}H_{29}$

Figure 2.7. A gemini SAIL.

Besides the already mentioned advantages of the ILs, the delocalised charges associated to the special head-groups of these compounds, can also deliver special interfacial properties to the systems. The surfactant character of a SAIL, as in the case of traditional surfactants, is usually tested through its behaviour in water. The surface tension of water falls abruptly upon addition of even small concentrations of surfactant. As more surfactant is added, the surface tension continues to fall until, at the critical micelle concentration (cmc), surfactant micelles begin to form and surface tension remains practically constant (Figure 2.8). Since micelle formation also affects other physical properties of the solution, cmcs can be determined not only by measuring surface tension (although this is one of the most common methods) but also by a number of other techniques, including conductimetry, fluorescence spectroscopy, isothermal titration calorimetry, small-angle neutron scattering, and NMR spectroscopy.

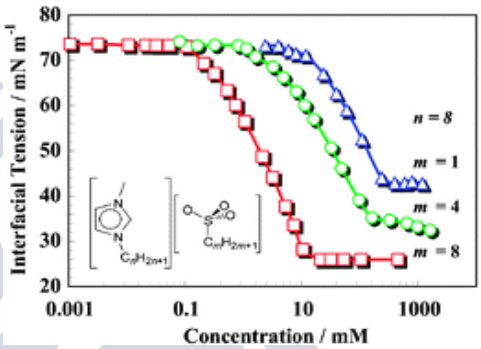

Figure 2.8. Cmc of several SAILs in water [42].

Like other aspects of ILs, their micelle-forming characteristics have in fact been studied mainly in regard to $[C_nmim^+]$ salts. cmcs can be determined for n>6 (as can aggregation numbers, i.e. the numbers of molecules per

micelle), but not for smaller molecules, although [C_4mim^+] does exhibit certain signs of aggregation [43]. The aggregation number and the cmc are important parameters influenced by the length and shape of the alkyl chain, the type of polar head group, and the nature and size of the counter-ion [42-48].

The term micelle refers to aggregates composed of a single layer of amphiphilic molecules constituting a closed surface. It is understood that the micelle surface has the hydrophobic moieties of its constituent molecules on its inside and their hydrophilic moieties on its outside. In inverse micelles, the reverse arrangement holds. A micellar solution is an isotropic, transparent phase in which micelles, with or without hydrophobic content, move freely in a polar solvent. In an oil-in-water (o/w) microemulsion, the dispersion of droplets of a hydrophobic liquid in water is stabilized by their confinement in micelles, while in a water-in-oil (w/o) microemulsion inverse micelles achieve the opposite configuration. Bicontinuous microemulsions consisting of interpenetrating networks of each phase are likewise stabilised by surfactants. Many applications of traditional surfactants and SAILs are related to these microemulsions because certain organic compounds that are insoluble in water do dissolve in aqueous solutions of micelles or o/w microemulsions, being taken into the hydrophobic micelle lumen. Similarly, compounds that are insoluble in non-polar solvents can sometimes be dissolved in solutions of inverse micelles or w/o microemulsions.

When the amphiphile concentration of a micellar solution or microemulsion exceeds a certain threshold, the density of micelles becomes too great for their free motion, and multi-micellar structures with long-range order are formed. As the micelle density increases, cubic structures composed of globular micelles give way to hexagonal structures composed of cylindrical micelles, and then to lamellar structures composed of plate-like micelles. Like conventional surfactants, SAILs are able to form mesophases that can be quite complex. This behaviour can be studied by small angle X-ray scattering, polarized optical microscopy, ^1H NMR, and rheology, among other techniques.

As has often been emphasized, one of the most attractive characteristics of ILs is that they can be modified in significant ways that “fine-tune” their behaviour without changing their IL nature. SAILs are no exception: their

aggregation behaviour in water can be tuned not only through mechanisms common to conventional surfactants, such as the addition of salts, alcohols, or other (conventional) surfactants, but also by chemical modifications that alter their interactions.

Most applications of SAILs derive from the two fundamental properties of surface active agents in aqueous solution: adsorption at the surface or interface, and aggregation. By reducing surface tension, adsorption at the air/water interface modifies the wetting and foam-forming properties of the surfactant-containing water, while adsorption at oil/water interfaces is the first step in emulsification, and adsorption at the interface of water with suspended solids can lead to flocculation and coagulation. The aggregation of SAILs like that of other surfactants, is the basis of applications involving the formation of micelles, microemulsions and liquid crystals.

A number of the currently most widespread applications of SAILs in fact concern conventional ionic surfactants that have only relatively recently been seen as ILs, being salts with melting points below 100˚C. Dodecyldimethylbenzyl-ammonium chloride, $[C_{12}mim]Cl$, for example, is widely used as a bactericide, and cetylpyridinium chloride, $[C_{16}py]Cl$, as a mouthwash. Other more recent examples of the applications of SAILs are: foaming and antifoaming agents [49], antimicrobials [49], solubilisation of drugs [50,51], demulsification of crude oil [52], Enhanced Oil Recovery (EOR) [53], extraction of natural products [54], chromatographic and electrophoretic separations [55], synthesis of new materials (mesoporous inorganic materials, nanocomposites, nanoparticles and microcrystals) [56,57], and microemulsion-based reactions [51].

2.2. NANOTECHNOLOGY

2.2.1. Definition

Nanotechnology literally means any technology on a nanoscale (Figure 2.9) that has applications in the real world. Nanotechnology encompasses the production and application of physical, chemical and biological systems at scales ranging from individual atoms or molecules to submicron dimensions, as well as the integration of the resulting nanostructures into larger systems [58]. Working at the nanoscale changes the way that the matter interacts with its surroundings. In that sense nanomaterials are designed to provide improved properties over bulk solids. The reason for such interesting behaviour is that when characteristic structural features are intermediate in extent between isolated atoms and bulk macroscopic materials, the objects may display physical attributes substantially different from those displayed by either atoms or bulk materials [59]. Nanotechnology can be used across all scientific fields, such as chemistry, biology, physics, materials, and engineering.

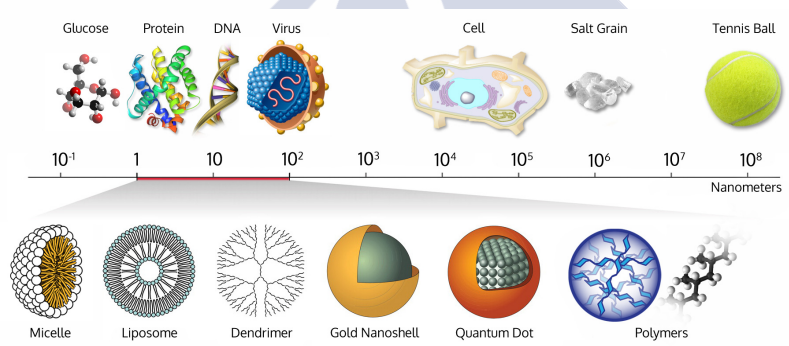

Figure 2.9. Nanoscale [60].

2.2.2. History

Humans have used nanotechnology since The Premodern Era. Mayan blue is a blue pigment developed in the 9th Century by the Mayan and Aztec cultures (Figure 2.10a). It is a hybrid compound composed of nanoparticles of organic (indigo derived from indigo leaves) and inorganic (a phyllosilicate found in some clays) materials. As a result an extremely resistant dye was obtained. The Lycurgus cup (Figure 2.10b) was made around the 4th Century BC in Rome. In daylight the mythological scene is displayed in green and opaque. But when the cup is illuminated from within it becomes red and

translucent shades. Gold and silver nanoparticles, from which the cup is made, are responsible for these colour changes [61].

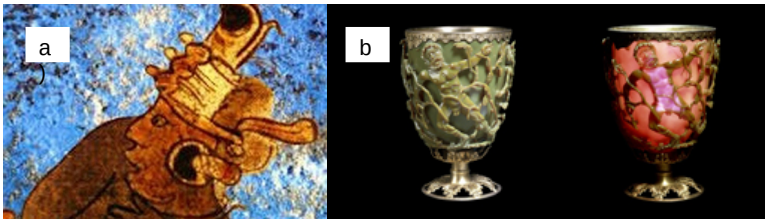

Figure 2.10. First applications of nanotechnology [61].

Alternate-sized gold and silver particles created colours in the stained glass windows of medieval European cathedrals and churches (6th-15th Centuries). “Damascus” sabre blades (13th-18th Centuries) contained carbon nanotubes (CNTs) and cementite nanowires, an ultrahigh-carbon steel formulation that improves strength and resilience.

The first development in nanotechnology in the Modern Era was carried out by Michael Faraday who in 1857 discovered colloidal “ruby” gold, demonstrating that nanostructured gold under certain lighting conditions produces different-coloured solutions. In the early 20th Century (1902), Zsigmondy carried out a further study of solutions of gold and other nanomaterials under 10 nm, being the first size measurements of nanoparticles that were performed. For that purpose, an ultramicroscope was employed, using the method of "dark field". Zsigmondy was the first to use the term "nanometer" explicitly to characterize particle size as one millionth of a millimetre [62].

The unlimited possibilities of nanotechnology were already being imagined some years after, in 1959, when Feynman, from the California Institute of Technology, enlightened the world with his famous talk entitled "There's plenty of room at the bottom" at a meeting of the American Physical Society. The ability to handle individual atoms and molecules was then described. Nevertheless, the term "nanotechnology" was first used in 1974 by Taniguchi, from the Tokyo University of Science, in a paper on the ion-sputtering machine [63]. Since then, there has been remarkable interest by the scientific community in the development of this area. Wiles and Open discovered, in 1979, small rolls of carbon atoms, which they later called

nanotubes. In 1981 Binning and Roherer, from the IBM Corportation, developed the electronic scanning tunnelling microscope (STM), which enabled the visualization of individual atoms and later their manipulation. Four years after, in 1985, the buckminsterfullerene (a molecule with 60 carbons of 0.7 nm) was discovered by the Rice University researchers Kroto, O'Brien, Curl, and Smalley who were awarded with the Nobel Prize in 1996. The carbon nanotubes (CNTs) were discovered by Iijima (NEC laboratories) in 1991. Researchers at Massachusetts Institute of Technology in 1993 synthesised semiconductor nanoparticles that emit light in quantum packs, and that can bind to molecules in the body to help doctors to locate diseases. In 1997 Engineers at the US Company Lucent Technologies in New Jersey built a silica transistor of 60 nm. One year later a CNT was turned into a nanopen that could be used to write [63].

It was at the beginning of the 21st Century when researchers at Cornell University extracted a bio-molecular engine of 80 nm from a cell and added a metal rotor creating a nanomechanical motor. Researchers at IBM in New York and the University of Delft in the Netherlands (2001) built a logic circuit using CNTs. In 2003 Halas, West, Drezek and Pasqualin, from Rice University, developed gold nanoshells used as a platform for integrated discovery, diagnosis and treatment of breast cancer. In 2009 Seeman and coworkers created several nanoscale devices with a robotic DNA construct. Also Seeman (in collaboration with researchers at the Nanjing University of China) created a "DNA assembly line", obtaining the Kavli Nanoscience Prize in 2010. In the same year, IBM used a silicon tip measuring only a few nanometers at its apex to chisel a substrate material and create a complete 3D nanoscale map of the world, showing a powerful methodology to generate nanoscale patterns and structures, and opening new perspectives for the fields of electronics, optoelectronics and medicine. Also in 2010 the Nobel Prize was received by Geim and Novoselov for the synthesis of graphene [61]. Currently, nanotechnology is a strategic research field encouraged in all developed countries.

2.2.3. Classification of the nanostructures and effects of the nanometric scale

The classification of nanostructured materials and systems essentially depends of the number of dimensions which lie within the nanoscale [59]:

- Systems confined in one dimension, include discs or platelets, ultrathin films on a surface and multilayered materials.

- Systems confined in two dimensions, include nanowires, nanorods, nanofilaments and nanotubes.

- Systems confined in three dimensions, include nanoparticles and nanopores.

Extrinsic materials properties are continuously modified as a function of system size. Intrinsic properties should be independent of specimen size, however, many of the intrinsic properties of matter at the nanoscale are not predictable from those observed at larger scales. This is due to the appearance of the phenomenon known as quantum confinement, which causes changes in the electronic structure, the presence of wave transport processes, or the predominant electron interfacial effects. Thus, when particle size is adjusted to nanoscale, properties such as melting point, fluorescence, electrical conductivity, magnetic permeability, and chemical reactivity change as a function of the size of the particle.

The increase in surface area and surface free energy with decreasing particle size leads to changes in interatomic spacing. The increased surface area to volume causes, in certain atoms, a different magnetic coupling with neighbouring atoms, modifying the initial magnetic behaviour [64]. While bulky ferromagnetic materials usually have several magnetic domains, magnetic nanomaterials tend to have only one magnetic domain, exhibiting superparamagnetism. Magnetic nanomaterials have a great range of applications, such as ferrofluids, biotreatments, cooling devices or magnetic memory devices with high capacity.

The thermal behaviour is also affected by quantum confinement [65]. As heat is transported in materials by lattice vibration waves (phonons) and free electrons, when the system length scale is reduced to the nanoscale, there are quantum confinement and classical scattering effects. The presence of nearby surfaces of nanometric size cause changes in the distribution of the phonon frequencies, as well as in the appearance of surface phonon modes, which leads to changes in the way that heat is transferred.

Mechanical properties such as hardness are determined by the absence of defects in the structure, as well as the difficulty in their formation and propagation. As the system size decreases, the capacity for defects is also decreased, causing the mechanical properties to be affected accordingly. CNTs exhibit high mechanical compression elastic limits, which gives them flexibility and reversible mechanical deformation [66]. Many nanostructured metals and ceramics are superplastic, supporting greater deformation without presenting fractures.

Optical absorption and emission are dependent on the transitions between HOMO (Highest Occupied Molecular Orbital, especially the valence band) and LUMO (Lower Unoccupied Molecular Orbital, especially the conduction band) states. These energy states are modified due to the effect of the nanoscale on the electronic structure. Metals and semiconductors, for example, show large changes in colour depending on particle size [67].

The chemical reactivity is affected by the ionization potential. This potential for atomic clusters is greater than for the bulk solid, and also changes significantly with the particle size. Nanostructures have a high surface area/volume ratio, which can lead to a drastic alteration in chemical reactivity. So nanoparticles typically present different chemical behaviour to materials on a larger scale. The use of nanoparticles as catalytic agents [68] may increase the selectivity and efficiency of many chemical reactions, such as combustion, synthesis or photodegradation processes.

Changes in the electronic properties are produced by decreasing the size of the nanomaterial [69] due to the shortage of scattering centers and the influence of the wave behaviour of electrons (quantum mechanics). This phenomenon is used e.g. to make components for electronics and optoelectronics and new types of transistors.

2.2.4. Nanoparticles

2.2.4.1. Definition

As aforementioned, nanoparticles are particles with all of their dimensions at the nanometer scale. Thus, a nanoparticle can be defined as an aggregate of atoms bonded together with a radius of between 1 and 100 nm.

2.2.4.2. Conventional synthesis of nanoparticles

There are different methods for the synthesis of nanostructures (Figure 2.11). Globally, these methods can be classified as "bottom-up", atom-by-atom, or "top-down", which involve the reorganization or withdrawal of atoms [59].

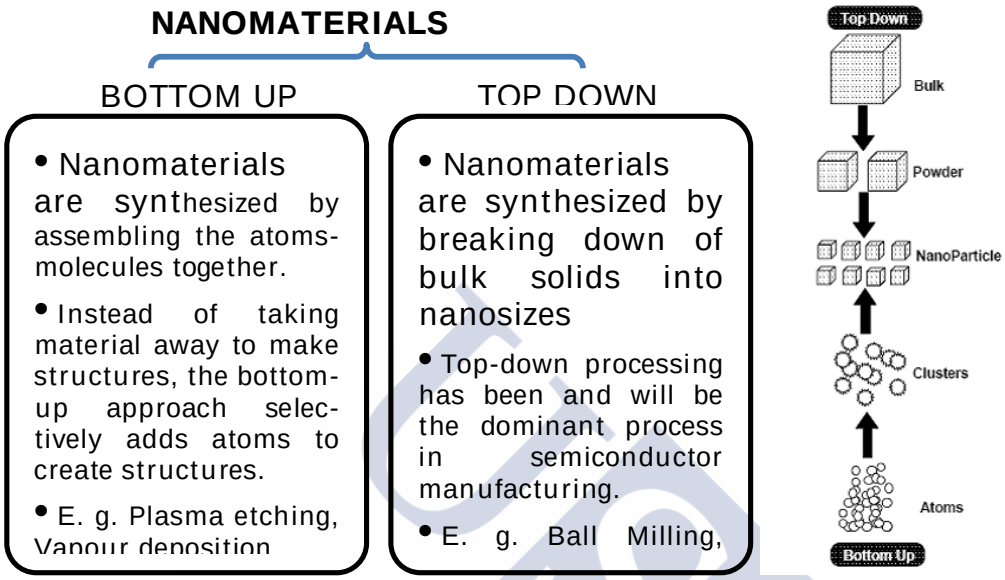

Figure 2.11. Schematic representation of the building up of nano-structures [59].

"Bottom-up" methods

In "bottom-up" processes, the starting materials are atoms, molecules and particles as building blocks for creating complex nanostructures. The size of these elements determines the properties of the final structure. Therefore, these materials can be designed according to their future application by controlling the size of the building blocks, its internal and surface chemistry, and its organization and assembly. Some "bottom-up" processes are: deposition methods, molecular beam epitaxy, liquid phase techniques, colloid techniques, sol-gel techniques and electro-deposition.

- *Deposition methods:* These methods are divided into two groups:

  - Physical Vapour Deposition: This process implies a solid-to-vapour conversion of the material by physical methods, followed by its deposition over a substrate.

- Chemical Vapour Deposition: produced by chemical reaction or thermal decomposition at high temperatures (773.15-1273.15 K) of the material, followed by its deposition over a substrate.

- *Molecular beam epitaxy:* This is a crystal-growing technique whereby, starting from a semiconductor material crystal face, a uniform layer of low thickness grows. This layer presents the same crystal structure as the starter material.

- *Liquid phase techniques:* These techniques are based on the reaction between precursors in a liquid medium. The precursors react or self-assemble, achieving a supersaturated solution. UV-radiation, catalysts, stabilizers or even ultrasound are often used to improve the reaction mechanism. Thermodynamic and kinetic factors determine the shape and structure of the nanoparticles formed after the nucleation process.

- *Colloid techniques:* This involves the precipitation of nanometric particles in a matrix solvent, forming a colloidal solution. The colloidal material tends to aggregate due to Van der Waals attractive forces. The use of microemulsions in the synthesis of nanoparticles further improves on the set of colloid techniques.

- *Sol-gel techniques:* Here a set of chemical reactions irreversibly transform a homogeneous solution of precursor reagents (sol) into a three-dimensional polymer (gel).

- *Electrodeposition:* This method is based on chemical reactions carried out by applying a certain voltage in an electrolytic aqueous solution. The electrodeposition may be cathodic or anodic, depending on where the material is deposited. The substrate must obviously be conductive.

"Top-down" methods

The "top-down" processes involve the division of a bulk solid. This approach refers to slicing or successive cutting of a bulk material to get nano-sized particle. The most common "top-down" processes employed are grinding, lithographic or machining processes.

- *Grinding processes:* The granulated powder material is mechanically crushed in a controlled atmosphere to avoid

oxidation problems. Repeated deformation may cause significant reductions in grain size. This technique is applicable to large scale.

- *Nanolithographic processes:* The lithographic processes are used to create nanostructures by etching on the substrate. These methods use UV or visible radiation, X-ray, electrons or ions to project an image with the design to be produced on the substrate surface coated with a photoresin.

- *Machining processes:* Similar techniques to conventional machining allow tridimensional engravings to be obtained. The resolution limits of conventional machining processes are in the order of 5 microns. Nevertheless, in recent years a new technology has been developed to mould directly in the micron and submicron scales [70].

2.2.4.3. Ionic liquids in the synthesis of nanoparticles

As aforementioned in section 2.1.4.4, ILs can play a key role in the synthesis of inorganic solids. The presence of nano-domains in their structure and the capacity to form hydrogen-bonded and highly structured systems, make them suitable media for the synthesis of nanoparticles. This structural organization allows orderly and well-defined nanostructures to be obtained [34]. Several mechanisms, in which ILs play different roles, can be found in the literature [31] for the preparation of nanoparticles. Those methods involve both “bottom-up” and “top-down” technologies.

Electrochemical reactions were conducted to obtain inorganic nanoparticles and nanostructured films in ILs. The properties of these salts opened the door to the electrodeposition, of metals and semiconductors, at room temperature. The electrodeposition of Ag, Cd, Cu and Sb in 1-butyl-3-methyl-imidazolium tetrafluoroborate, $[C_4mim][BF_4]$, 1-ethyl-3-methyl-imidazolium chloride, $[C_2mim]Cl$, or 1-ethyl-3-methylimidazolium tetrafluoroborate, $[C_2mim][BF_4]$, was reported [71-74]. Also nanoporous Au, Pt, and Ag structures were obtained by electrodeposition of a binary alloy such as gold-zinc, platinum-zinc and silver-zinc and subsequently electrochemical dealloying in a lewis acidic zinc chloride-1-ethyl-3-methyl-imidazolium chloride IL ($ZnCl_2$-$[C_2mim]Cl$) [75-77].

The non-volatile, non-flammable, and thermally stable character of ILs make possible reactions in open reactor. Thus, hydrothermal and solvothermal reactions for the synthesis of nanomaterials can be substituted by ionothermal reactions, with the main advantage of taking place at ambient pressure, avoiding safety problems related to high pressure. For instance, an imidazolium-based IL (1-butyl-3-methyl-imidazolium bis(trifluoromethylsulfonyl)imide, [C_4mim][NTf_2]) was used for the synthesis of CoPt nanorods at high-temperature [78]. Another interesting study combines imidazolium-based ILs with oleic acid as capping agent to successfully prepare Ag and Pt nanoparticles [79].

Several ILs (especially those containing ions like sulphate, phosphate, carbonate, chloride, and metal cations) can act as reactive precursors to obtain inorganic matter. In these cases, the ILs do not only play the role of the solvent but also act as molecular precursor with a well-defined composition, structure, and reactivity. They are the so-called solvent–reactant systems. Furthermore, depending on the structure of the molecule, ILs may exhibit long-range order interactions and liquid crystallinity (IL crystals, ILCs) [80]. Due to the fact that ILCs form ordered domains, within which the reaction occurs, they provide an additional way of reaction control for the inorganic chemistry. In analogy to the solvent–reactant ILs mentioned above, ILCs act at the same time as precursor, template, and reactant (solvent–template–reactant systems). The main advantage of using ILs or ILCs as precursors is their virtually unlimited flexibility of combinations of anions and cations, which implies different phase behaviour, chemical composition and reactivity. Thus ILs provide a flexible toolbox for obtaining inorganic nanomaterials with specific properties simply by designing the appropriate precursor [81, 82].

The use of emulsions or microemulsions (thermodynamically stable media formed by immiscible liquids which are stabilized by surfactants) represents one of the most extensively applied routes of synthesis of nanomaterials. In this case, the IL can play the role of the water, the organic solvent or the surfactant (SAILs), providing highly polar environments for the synthesis of inorganic nanoparticles. An example of this method of preparation of nanoparticles is the synthesis of CaF_2 nanocubes and hollow rods, obtained from an emulsion of the SAIL 1-methyl-3-octyl-

imidazolium hexafluorophosphate, [C_8mim][PF_6], in an aqueous solution of $CaCl_2$ [83].

Recently, the Separation Processes´ group of the University of Santiago de Compostela, where this Thesis is developed, has patented [84] a method of synthesising nanoparticles. Only an IL and the bulk powder of the material of the target nanoparticle are used, thus avoiding the utilization of volatile solvents or solid precursors, which lead to by-products. The method is very simple: first, a mixture of the bulk solid material and the IL is heated and stirred, then the mixture is allowed to cool down, and it is centrifuged to remove any excess of the bulk material from the generated nanodispersion. The suitability of the method depends critically on the appropriate selection of the IL. The existence of polar/non-polar domains in the structure of the ILs, allow a process of dispersion/fragmentation mechanism of the solid material that leads to the formation of the nanoparticles. This route avoids the use of volatile solvents, high temperature or high pressure. The method has been successfully used to synthesise different kinds of nanoparticles [85-87]. The procedure works with different ILs, however, SAILs have been proved as the most effective according to the number of nanoparticles synthesised and their homogeneity.

2.2.4.4. Applications of nanoparticles

Nanotechnology has numerous applications in sectors as diverse as medicine, food industry, material science and manufacturing, organic catalysis, energy, electronics, environmental treatment processes, etc [88-102]. Therefore, nanoparticles are currently present in many different aspects of the everyday lives of human beings.

One of the fields where nanotechnology has a greater impact is medicine. One exciting research area is the synthesis of nanoparticles that deliver anti-cancer drugs [88]. Nanoscience allows developing customized nanoparticles that can deliver drugs directly to diseased cells. This method can greatly reduce the damage that several treatments, such as chemotherapy, produce to a patient's healthy cells. Drug delivery systems are also of great interest for cosmetic and personal care products. Nanoparticles can be used to break up clusters of bacteria as an effective treatment of chronic bacterial infections [89]. The surface change of protein filled nanoparticles affects the ability of the nanoparticle to

stimulate immune responses, allowing their use in vaccines [90]. Several nanoparticles can also act as an antioxidant to remove oxygen free radicals that are present in a patient's bloodstream following a traumatic injury [91]. Moreover, nanotechnology is not only useful in drug delivery, therapy techniques or anti-microbial medicines, but also in monitoring and diagnostic techniques [92].

Food nanotechnology is an area of emerging interest and opens up a whole universe of new possibilities for the food industry. Shekhon published a review [93] showing that nanoparticles have the potential to improve food packaging (improving plastic materials barriers, incorporating active components that can deliver functional attributes beyond those of conventional active packaging, and through the sensing and signalling of relevant information), and food industry (detecting bacteria, producing stronger flavours, better colour quality, and safer products).

Nanotechnology can change the properties of many materials, from increasing the strength to increasing their reactivity. Composites with nanosized particles or fibres allow the improvement of textile mechanical properties without a significant increase in weight, thickness, or stiffness [94]. Moreover, textiles can provide a suitable substrate to grow microorganisms, especially at appropriate humidity and temperature when are in contact with the human body. Inorganic nanostructured materials and their nanocomposites allow anti-microbial modification of textiles [95]. Nanoparticles can also be dispersed in industrial coatings to protect wood, plastic, and textiles from exposure to UV radiation [96]; applied to pipes used in the oil industry to provide resistance to corrosion; used in coating to prevent oxidation, etc. Many other applications in materials science and manufacturing could be mentioned. Some of the most widely studied are conducting film composite materials (polymeric composites containing metal nanoparticles); single and multilayer nanostructures applied in microelectronic device manufacturing; magnetic nanostructures showing giant magnetoresistance; ceramic nanomaterials for the production of components operating at high temperatures, etc. [97]

Focusing on the change of reactivity of materials, catalysis of chemical reactions is an important field of application of metal, alloy and semiconductor nanoparticles.

High catalytic activity of small particles is attributed to the higher specific surface area. Nanostructured catalysts lead to high activity, selectivity, and durability in many different types of reactions [98]. However, nanoparticles exhibit catalytic activity in a very narrow size range. Such a high sensitivity of the catalytic action to the size and distribution of small particles demonstrates the importance of the development of selective procedures for the preparation of nanoparticles with a very narrow size distribution range.

Nanomaterials have large potential to contribute to a sustainable energy system, both through more efficient use of current energy sources and by enabling breakthrough solutions towards novel energy sources and systems [99]. Nanotechnology is expected to have a profound impact on new or improved schemes for light harvesting such as solar photovoltaics (e.g. the performance of dye-sensitized solar cells critically depends on nanoscale components) or solar water splitting (photoelectron-chemical water decomposition using solar energy to produce hydrogen as an energy source). Fuel cells are electrochemical devices that convert a fuel such as hydrogen or methanol directly to electricity through an electro-catalytic process. Nanoparticles are used to improve the electrodes, membranes and catalysts. Also the improvement of electrodes with nanoparticles and nanocomposites can increase battery power and reduce the recharge time of batteries [100, 101].

There are many ways in which nanoscience may play a key role in environmental treatment processes. Nanomaterial-based technologies can improve the performance of catalysts used to transform vapours escaping from cars or industrial plants into harmless gasses, with the aim of controlling air pollution. Additionally, several types of detecting elements such as nanoparticles, CNTs and nanowires, can be used in nanotechnology-based sensors. Due to the small size of these nanomaterials, a few gas molecules are sufficient to change the electrical properties of the sensing elements. This allows the detection of a very low concentration of chemical vapours [102].

High reactivity and high degree of functionalization of nanomaterials makes them suitable for applications in wastewater treatment and for water purification. Thus nanotechnology has been applied to remove contaminants

such as organic or inorganic materials, pathogens, heavy metals or other toxins [103].

Of special interest are studies on photodegradation using nanoparticles. Photodegradation is the photochemical transformation of a molecule into lower molecular weight fragments, usually in an oxidation process. This term is widely used in the destruction (oxidation) of pollutants by UV-based processes. Photolysis is the cleavage of one or more covalent bonds in a molecular entity resulting from absorption of light, or a photochemical process in which such cleavage is an essential part. In the case of photolysis of water, using the high energy associated with UV radiation, yields powerful oxidizing and reducing radicals that can degrade contaminants in water [104]. Photocatalysis is the change in the rate of a chemical reaction or its initiation under the action of UV, visible or infrared radiation in the presence of a substance (the photocatalyst) that absorbs light and is involved in the chemical transformation of the reaction partners. Thus, photocatalysis can be used as an effective method to degrade water pollutants such as industrial dyes, pharmaceuticals or emerging contaminants.

Nanometric photocatalysts present a higher specific surface area, improving the degradation performance. Several authors have studied the effect of the catalysts size. Xu *et al.* [105] reported the influence of particle size of TiO_2 in the degradation of Methylene Blue, concluding that increasing the particle size from 30 nm to 49 µm, the average lifetime of the dye increases from 2 min to 15 min. Many examples can be used to show the efficacy of nanoparticles in wastewater treatment. TiO_2 nanoparticles in several forms (anatase, rutile and P-25 Degussa) are likely to be the nanocatalysts most frequently used in the degradation of contaminants such as carbamazepine [106], Orange II [107], Reactive Blue 19 [108], endocrine disruptors, pharmaceuticals and personal care products [109, 110]. SiO_2 nanoparticles are used in the photodegradation of carboxylic acids [111] or Methyl Red dye [112]. ZnO is used as a catalyst for the photodegradation of azorubine (food colouring) [113] or Reactive Blue 19 [108]. Rhodamine B and 4-nitrophenol were successfully degraded by using Fe_2O_3 nanoparticles [114]. Focusing on the use of AgCl as the photocatalyst for dye degradation, most of the papers found in the literature use silver/silver halide composites [115-122].

As part of this Thesis, AgCl nanoparticles synthesised from the corresponding powder material and the IL trihexyl(tetradecyl)phosphonium chloride, $[P_{6\ 6\ 6\ 14}]Cl$, are proposed to degrade Orange II dye [87]. The method of degradation has been proven to be effective also with other dyes [123].

2.2.5. Nanofluids

2.2.5.1. Definition

The preparation of isolated solid materials is not the only objective of nanotechnology. The term nanofluid was first used in 1995 by Choi [124]. They are defined as stable dispersions of nanomaterials on a base fluid (frequently water, oils or glycols). Nanofluids are fundamentally characterised by the fact that Brownian agitation overcomes any settling motion due to gravity. Thus, a stable nanofluid is theoretically possible as long as particles stay small enough (usually <100 nm). Thus, the problems of corrosion or deposition along pipes through which the nanofluid circulates can be minimized or avoided. Maintaining this size, however, can be a challenge since particles frequently come into contact with each other, potentially leading to the formation of agglomerates which can settle out of suspension. Nanofluids have the peculiarity of presenting enhanced properties (favoured with the increasing of specific area) over the base fluid. Primarily, this advantage has been used to develop fluids with significantly increased conductive and convective heat transfer properties

2.2.5.2. Synthesis of nanofluids

There are two primary methods to prepare nanofluids: the single-step preparation process, and the two-step preparation process [125, 126]. The first method implies that the processes of nanoparticle synthesis, surface modification for stabilization, and transport/mixing with the host liquid are all achieved in a single batch process. This can be carried out by vacuum evaporation onto a running oil substrate, chemical reaction (with or without microwave irradiation), nano-emulsification, laser and electric arc ablation in liquids, etc. An advantage of the one-step synthesis method is that nanoparticle agglomeration is minimized. An inherent difficulty with this approach is the removal of unwanted chemicals from the nanofluids after synthesis.

A nanofluid can also be synthesised by simply mixing a nanopowder in a liquid (two-step preparation process). Nanoparticles can be purchased or previously synthesised. Sonication (at high intensity and over extended periods of time) is usually sufficient to break up the agglomerated powders and form a well-dispersed nanoparticle suspension. However, a stabilizing agent (for instance a surfactant) is normally required to avoid re-agglomeration of the nanoparticles in the nanofluid and it can affect the desired properties of the final fluid.

Table 2.2 shows several examples of nanofluids obtained by both one-step and two-step methods [127]. Dispersed nanoparticles can be metals, metal oxides, carbides or CNTs, among others. Base fluids can also be of different natures (e.g. water, glycols, hydrocarbons, oils, etc).

Table 2.2. Examples of nanofluids [127].

System	Synthesis	Concentration (%vol)	Particle size (nm)
Cu/EG	Single-step	0.3	10
Cu/H_2O	Single-step	0.1	75 ~ 100
Cu/H_2O	Two-step	7.5	100
Fe/EG	Single-step	0.55	10
Ag/toluene	Two-step	0.001	60 ~ 80
Au/toluene	Two-step	0.00026	10 ~ 20
Au/ethanol	Two-step	0.6	4
Fe_3O_4/H2O	Single-step	4	10
TiO_2/H2O	Two-step	5	15
Al_2O_3/H2O	Two-step	5	20
Al_2O_3/EG	Two-step	0.05	60
CuO/H2O	Two-step	5	33
SiC/H2O	Two-step	4.2	25
CNTs/engine oil	Two-step	2	20 ~ 50
CNTs/poly oil	Two-step	1	25 × 50000
CNTs/EG	Two-step	1	15 × 30000
CNTs/H_2O	Two-step	1	15 × 30000
CNTs/decene	Two-step	1	15 × 30000
CNTs/FC-72	Two-step	12	9.8

2.2.5.3. Ionanofluids

Ionanofluids are stable dispersions of nanomaterials in ILs [128-130] or, in other terms, are nanofluids where the base fluid is an IL. The ionanofluids combine the advantages of nanofluids and ILs. Thus, they have enhanced properties, have negligible vapour pressure, and can be designed for a specific application. As in the case of nanofluids, ionanofluids can be synthesised in single-step or two-step processes and most of the studies focus in their application in heat transfer processes.

Some papers should be highlighted where ionanofluids are synthesised in a two-step process. Nieto de Castro *et al.* [128-132] reported the study of thermal properties of several IL-based nanofluids containing multi-walled carbon nanotubes (MWCNTs). The studies comprise different cations (imidazolium, [$C_n$mim$^+$], and pyrrolidiniuim, [$C_n$pyrr$^+$]) and different anions (tetrafluoroborate, [BF_4^-], hexafluoro-phosphate, [PF_6^-], bis(trifluoromethylsulfonyl)imide, [NTf_2^-], ethylsulphate, [$EtSO_4^-$] or dycianamide, [DCA^-]). These authors have proved that the tested ionanofluids present enhanced thermal properties, such as heat capacity and thermal conductivity, when comparing with the corresponding ILs. The effect of temperature and MWCNTs concentration was also studied.

Ferreira *et al.* [133] also focus on the study of transport and thermal properties (viscosity, thermal conductivity and stability, and heat capacity) of phosphonium ILs and their MWCNTs-based ionanofluids. Their results show that the presence of MWCNTs leads to an enhancement of 0.4% to 1.4% on the thermal conductivity (with a weak effect of the temperature), a drastic reduction in the viscosity (up to 83% in some cases) and an increase on heat capacity (reaching 13%), without losing the thermal stability of the systems.

Wang *et al.* [134] reported the dispersion of functionalized MWCNTs in 1-butyl-3-methylimidazolium hexafluorophosphate, [C_4mim][PF_6], as well as the study of the rheological and tribological behaviour of the synthesised ionanofluids. They show that the self-lubrication of the functionalized MWCNTs leads to a reduction in the shear viscosity and friction, implying a great advantage for lubricant applications.

Likely the most studied ionanofluids correspond to the dispersion of MWCNTs in different ILs. Nevertheless, some other nanoparticles have also been used. For instance, Paul *et al.* [135,136] studied several thermophysical properties of ionanofluids of Al_2O_3 in 1-butyl-3-methylimidazolium bis(trifluoromethyl-sulfonyl)imide, $[C_4mim][NTf_2]$, and N-butyl-N,N,N-trimetylammonium bis(trifluoromethylsulfonyl)imide, $[N_{4\,1\,1\,1}][NTf_2]$.

Regarding ionanofluids synthesised in one-step, the synthesis of stable nanofluids comprising of mixed valent copper (I, II) oxide clusters (<1nm) suspended in 1-butyl-3-methylimidazolium acetate, $[C_4mim][OAc]$, and copper (II) oxide nanoparticles (<50nm) suspended in trioctyl(dodecyl)phosphonium acetate, $[P_{8\,8\,8\,12}][OAc]$, was reported by Swadzba-Kwaśny *et al.* [137]. A facile one-pot reaction from solutions of copper (II) acetate hydrate in the corresponding IL was employed. This study also revealed different formation mechanisms, with both anions and cations of the ILs playing a significant role, as well as the influence of the particle size on the density of the nanofluids. One-phase and two-phase methods were used by Wang *et al* [138] to prepare different ionanofluids with gold nanoparticles. Thermophysical properties were measured and several theoretical studies were carried out to conclude that the research on mechanisms and potential applications of the nanofluids is still far from enough. Clarifying experimental parameters of the nanofluids and measurement conditions is paramount for investigating the heat transport in nanofluids.

In the results section of this Thesis, a paper will be presented where the aforementioned patented method for the synthesis of nanoparticles [84] will be tested for the preparation of silver iodide–trihexyl(tetradecyl)phosphonium chloride, AgI-$[P_{6\,6\,6\,14}]Cl$, ionanofluids [139].

2.2.5.4. Application of nanofluids

There are many studies in the literature about the possible applications of nanofluids. Most of these studies are focused on their application as thermal fluids. The enhanced thermal properties of nanofluids, in comparison with the corresponding base fluids, lead to a good number of applications where the nanofluids are used as heat transfer fluids: industrial cooling, refrigeration of nuclear reactors, geothermal energy extractors, etc. [140, 141].

The addition of nanoparticles to engine oils, automatic transmission fluids, coolants, lubricants, brake fluids and other automotive-related fluids can improve either thermal or tribological properties, enhancing the heat transfer and contributing to a reduction of friction and wear, reducing parasitic losses. Nanofluids can also improve the performance of fuels, increasing the total combustion heat while decreasing the concentration of smoke and nitrous oxide in the exhaust emission from the diesel engine [140].

Nanofluids are used also in cooling systems of microchips in computers, but it is not their only electronic application. The manipulation of small volumes of liquid is necessary for several electronic applications such as digital display and optical devices, and microelectromechanical systems. Electrowetting on dielectric actuation (reducing the contact angle by an applied voltage) is a very useful method of microscale liquid manipulation, and nanofluids can be good candidates for that purpose [142].

There is a new initiative in biomedical fields to take advantage of several properties of certain nanofluids to use them in cancer imaging and drug delivery. This initiative involves the use of iron-based nanoparticles as delivery vehicles for drugs or radiation in cancer patients. Magnetic nanofluids can also be used with magnets to guide the particles up the bloodstream to a tumour, allowing to deliver high local doses of drugs or radiation without damaging nearby healthy tissue. In addition, magnetic nanoparticles are more adhesive to tumour cells than to non-malignant cells and they absorb much more power than microparticles in alternating current magnetic fields tolerable in humans. However, prior to the use of magnetic nanofluids as drug-delivery systems, more research must be conducted on the nanoparticles containing the actual drugs and the release mechanism [140].

The special behaviour of nanofluids in terms of spreading and adhesion on solid surfaces opens up the possibility of using nanofluids in other processes such as detergency, soil remediation, oil recovery or lubrication.

The above mentioned applications for nanofluids are also extensive to ionanofluids, which also show the intrinsic advantages of ILs: negligible vapour pressure, usually high thermal stability, and the possibility of tuning not only by

means of the nanoparticle but also by means of the base fluid.

2.3. ENHANCED OIL RECOVERY

2.3.1. Introduction

Global energy consumption has soared since the Industrial Revolution. Energy needs required to maintain society's standard of living mean that humanity must fully exploit the energy resources at its disposal. In recent years there has been an increase in the exploitation of renewable and potentially renewable energy resources such as biomass, wind, solar, hydro, geothermal, etc. Consequently, technologies have been developed and optimised to exploit these resources. However despite the need to move to renewable energies, today's dependence on fossil fuels, especially oil, as the primary energy source is a fact. Furthermore, oil is the basis of the petrochemical industry which generates thousands of chemical compounds used in the production of plastics, adhesives, detergents, dyes, fertilizers and many other useful products to society. With the decline in oil discoveries during the last few decades, it is believed that better recovery technologies will play a key role in meeting the energy demand in years to come. Thus, there is considerable focus on renewed efforts to improve techniques that allow: better exploitation of wells that years ago were abandoned due to their poor output, the recovery of heavy oils, or taking advantage of tar sands.

2.3.2. Oil Recovery Stages

The overall process of exploitation of a well is divided into three stages [143-145]. During primary recovery, extraction of oil due to the pressure gradient existing between the interior and exterior of the well occurs. Expansion and subsequent release of the retained gas is produced. This process pushes the oil out of the well, until the pressure gradient decreases, causing a considerable decrease in the production rate. At this point, a typical production of 10-15% of the total oil reservoir is achieved, and another energy source must be applied to maintain oil production.

This "extra-energy" is applied during secondary recovery. Sometimes pumps on the surface or submerged are used to bring the oil to the surface. Other methods consist of the injection of different kinds of fluids in order to increase the pressure inside the well to maintain production. Among them, the most commonly injected fluids are water and

petroleum gases. In the case of gas injection, a decrease in the fluid density inside the well occurs, while injecting water a mobilization of the oil occurs due to viscous forces. Depending on the geological characteristics of the well and the physical properties of the crude oil, a recovery between 25-30% is achieved after the secondary recovery.

After primary and secondary recovery, approximately two thirds of the original oil remains inside the well. This is due to limitations of the processes. On one hand, the low permeability zones in the reservoir, the geometry of the well or preferential paths may cause that the injected fluid does not penetrate. On the other hand, the oil is retained discontinuously inside the pores by capillary forces.

Tertiary recovery, or Enhanced Oil Recovery (EOR), consists of a set of methods in which different materials are introduced into a well in order to continue with the extraction of crude oil by exercising control over the wettability, the fluid properties and the flow in the wellbore, the interfacial tension between oil and displacing fluid, or the pressure gradients needed to overcome the retaining forces.

When the full exploitation of reservoirs becomes economically profitable, EOR methods are the alternative to extract the difficult-to-access oil from the well. It is obvious that the economic viability of a tertiary recovery process depends on one hand on the costs of that exploitation, and on the other hand on the price of crude. A rise in oil prices implies that those wells whose production activity has ceased at the end of primary and secondary recovery processes can be subject to the application of EOR methods to continue their exploitation.

2.3.3. Enhanced Oil Recovery methods

All different EOR methods are based on at least one of the following objectives to facilitate oil extraction:

- The reduction in interfacial tension between oil and water.
- The improvement in the displacement ability of injected fluid in terms of an increase of the viscosity of the water or a decrease of the viscosity of the oil.
- The extraction of the oil by using a solvent.

EOR methods are usually classified into three groups: thermal, miscible flooding and chemical flooding methods, but also the use of microorganisms should be considered as a tertiary recovery method [145-147].

Thermal methods are based on reducing the oil viscosity in the wellbore. Several mechanisms are developed for that purpose. Steam injection (Figure 2.12) is the most common form of thermally EOR. Another method consists of the injection of oxygen-enriched air, producing propagation of a combustion zone. The reduction in the viscosity of crude oil facilitates its drive towards the production wells. In general, wells containing heavy oil or sandstone reservoirs are liable to exploitation by such methods. There have also been modifications aimed to improve the process of steam injection by the addition of solvents, chemicals, gases or foams. Furthermore, several other less usual methodologies for thermal EOR have been proposed such as electric, electromagnetic and microwave heating.

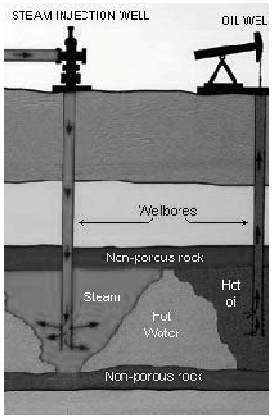

Figure 2.12. Thermal recovery by steam injection.

Miscible flooding consists of the injection of a fluid into the reservoir at pressure levels such that it is miscible with the oil. The contact between the displacement fluid and the crude oil implies that a transfer between two phases takes place. The transport of components between phases provokes a modification of the properties of both, thus mobilizing the oil. The most commonly used fluid for miscible flooding is CO_2 (Figure 2.13), but also hydrocarbons or nitrogen. The main limitation of this method lies in the reduced viscosity of the injected gas. The difference in viscosity between gas and oil implies adverse mobility ratio, and it may cause fingerings and preferential paths among the reservoir oil. The use of N_2 and hydrocarbons has been reported in several works.

Nevertheless, due to the availability of inexpensive CO_2 from natural sources, CO_2 flooding has been the most common method used in miscible flooding. Alcohols have also been tested but the cost of the injected fluid becomes quite high.

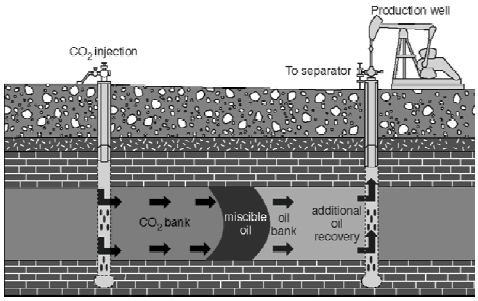

Figure 2.13. Miscible flooding using CO_2 as miscible gas.

Chemical methods [145, 148] represent an alternative to overcome the limitations that occur with the miscible flooding methods. They are based on the injection of water into the well together with chemicals of different natures. The intention with the addition of these chemicals is on one hand, to achieve a reduction in the interfacial tension between oil and water, and secondly to reduce the viscosity difference between the oil and displacing fluid through the increase of the viscosity of the latter. In these methods, polymers, surfactants and alkaline or caustic chemicals are used.

In polymer flooding, polymers are dissolved in water, increasing its viscosity and thus reducing the difference between water and oil viscosities. This fact promotes the displacement not only of crude oil but also of water from the pores. Adsorption of polymer molecules in the surface of pores also occurs, blocking some channels and avoiding the filtration of water, increasing the effectiveness of the flooding.

Surfactant flooding (Figure 2.14) involves the use of aqueous solutions of surfactants as injection fluids, in order to achieve a significant reduction in the interfacial tension between oil and water. This reduction in the interfacial tension enhances the mobility of the oil retained in the pores, allowing it to be flushed of the reservoir. It is necessary to take into account that a very low value of interfacial tension between displaced and displacing fluid is required for the mobilization of the oil through the narrow capillary pores.

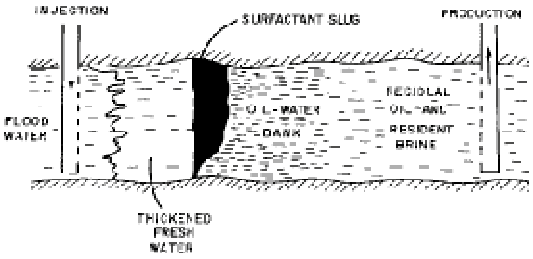

Figure 2.14. Principles of surfactant flooding [143].

Alkaline flooding is based on the formation *in situ* of surfactants by the interaction of the alkalis (from the alkaline solution flooding) with organic acids that are present in the oil. These generated surfactants reduce the interfacial tension between oil and water, and the wetting characteristics of the reservoir may also change, increasing the rate of displacement.

In most cases combined EOR methods are implemented. For instance, the Alkali/Surfactant/Polymer (ASP) flooding (Figure 2.15) combines all the advantages of the aforementioned methods.

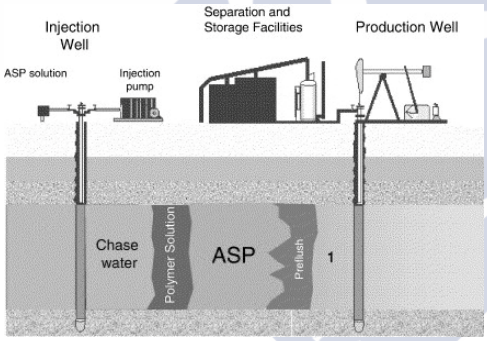

Figure 2.15. Principles of Alkali/Surfactant/Polymer (ASP) flooding.

Biological based technology can also be used in oil recovery. Microbial EOR (MEOR) processes involve the use of reservoir microorganisms or specially selected natural bacteria to produce specific metabolic events that lead to oil recovery. A variety of fermentation products are produced with different roles in EOR [149]: gases that reduce oil viscosity; bio-surfactants; bio-polymers; acids that improve the permeability and the porosity by dissolving carbonate precipitates; alcohols and ketones that are typical co-surfactants; and biomass that physically displace oil by growing between oil and rock/water surface. The injected bacteria and nutrients are inexpensive and easy to obtain and

handle in the field, but the control over the microbial system is a serious challenge.

There are also some locally applied methods, among them the hydraulic fracturing, which are usually attributed to a special group called Oil Production Intensification methods. They increase for some period of time the current oil production (recovery) but they do not usually increase the final recovery rate as EOR methods do.

2.3.4. Surfactant and microemulsion flooding

Among chemical flood recovery methods, the addition of surfactants to the extraction fluid is a promising alternative.

Surfactant flooding is a multiple-slug process involving the addition of surface-active chemicals to water. These chemicals reduce the capillary forces that trap the oil in the pores of the rock. The surfactant slug displaces the oil forming a flowing oil-water bank that is propagated ahead of the surfactant slug. As surfactant contacts rock surfaces, wettability may be changed. A slug of water containing polymer, to increase viscosity, usually follows the surfactant solution to avoid digitations.

Another chemical flood recovery method that uses surfactants is the microemulsion or micellar flooding. In this case, oil and water are displaced by a microemulsion slug consisting of oil, water, surfactant, co-surfactant, electrolytes, etc. Two approaches are normally used. In the first process, a relatively low concentration (2-4%) surfactant microemulsion is injected to reduce the interfacial tension between the water and the oil. In the second process, a high concentration (8-12%) surfactant microemulsion is injected and the micelles solubilize the oil and water in the displacing microemulsion. Inside the reservoir, the process gradually reverts to a low-concentration flood. The mobility of the microemulsion can be controlled by tuning its viscosity [148].

Although the surfactant flooding technique is promising, its application to date has been limited due to the high cost of the surfactant and the difficulty in its recovery, as a result of its adsorption onto the oil bearing formation rocks. For these reasons, there is growing interest in finding new surfactants whose properties best fit the surfactant EOR requirements, and which optimise the process.

Two important methods to produce the mobilization of the crude oil with surfactants are the reduction of the interfacial tension and the solubilization. For that reason, the determination of phase behaviour and interfacial tension between the compounds involved in these EOR processes is the first step to optimize them.

2.3.4.1. Phase equilibria related to surfactant EOR methods

A valid approach for the study of the complex systems of interest in oil extraction (which consists of a mixture of water, salts, surfactant, co-surfactant, petroleum components...) is to consider them as a pseudo-ternary mixture surfactant-water-oil.

A microemulsion is a dispersion made of water, oil, and surfactant(s) that is an isotropic and thermodynamically stable system with dispersed domain diameter varying approximately from 1 to 100 nm, usually 10 to 50 nm. In a microemulsion the domains of the dispersed phase are either globular or interconnected (to give a bicontinuous microemulsion) [150].

At constant temperature and pressure, Winsor (1954) [151] defined three types of basic diagrams (Figure 2.16).

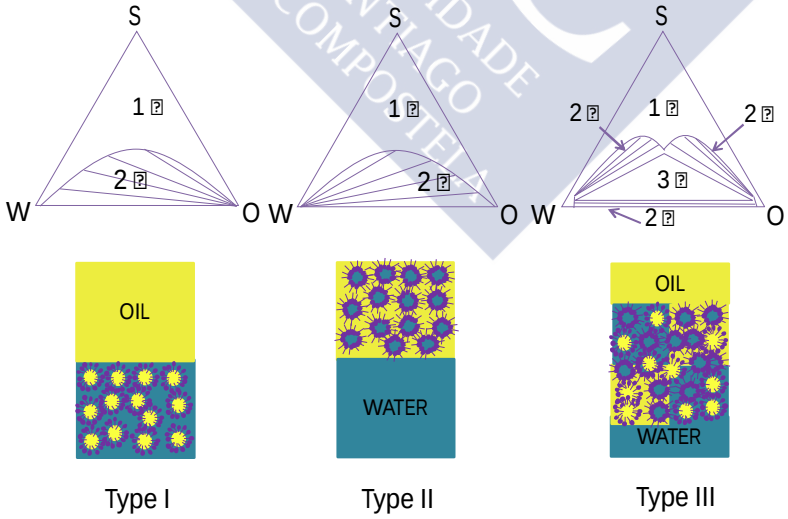

Figure 2.16. Types of Winsor diagrams. S: surfactant; W: water; O: oil.

Type I is characterised by the presence of a biphasic area (2ϕ) in the region of low concentration of surfactant, and a monophasic area (1ϕ) in which the surfactant causes

miscibility between water and oil. For this type, the affinity of the surfactant for the aqueous phases is greater than that for the oil. Any mixture within the interior of the immiscible area will split into an aqueous microemulsion in equilibrium with an excess phase of oil.

In the type II diagram, a similar situation is observed. Nevertheless, the roles of oil and water are now inverted. The affinity of the surfactant for the oil phase is the dominating one. Therefore, the biphasic systems correspond to an oily microemulsion in equilibrium with an excess phase of water.

The type III diagram comprises a 3-phase region (3ϕ) surrounded by three biphasic regions (2ϕ) and a monophasic region (1ϕ). Systems with global composition lying within any of the biphasic regions will split as in the previous cases. With regard to systems with global composition lying in the 3-phase region (3ϕ), these will split into three phases in equilibrium: an aqueous phase and an oily phase containing essentially water and oil respectively, plus an intermediate phase with density between those of the other two phases.

In the type III diagram, the interactions are equilibrated and the surfactant corresponds to what the enhanced oil recovery researchers called in the 1970s, the optimal formulation, because such physicochemical situation corresponds to an interfacial tension extremely low and, therefore, to the almost total elimination of the capillary forces that retain the oil in the porous medium [152].

Although the real systems are multicomponent and the diagrams are much more complex, the concept of optimal formulation is maintained, the study of the number of phases can be carried out visually, and the compositions of the phases can be determined by means of suitable analytical methods.

Thermodynamic modelling using the PC-SAFT equation of state

The Perturbed-Chain Statistical Associating Fluid Theory (PC-SAFT) equation of state has been utilized to calculate phase equilibria for chemical and separation processes for the last 15 years. Originally developed by Gross and Sadowski [153, 154], this equation of state adopts a hard-sphere chain fluid as a reference fluid. Thus, molecules are assumed to be

chains of equal-sized spherical segments interacting according to a repulsive/attractive potential. Besides the repulsion interactions of the hard chain fluid, attractive interactions are considered through dispersive forces and association effects. In terms of the residual Helmholtz energy (a^{res}), the general expression of the PC-SAFT model is given as a sum of three terms: the hard-chain contribution (a^{hc}), the dispersion contribution (a^{disp}) and an association contribution (a^{assoc}):

$$a^{res} = a^{hc} + a^{disp} + a^{assoc} \qquad (1)$$

The expressions to calculate these residual Helmholtz energy contributions are those used in the original PC-SAFT publication [153]. Within these terms, different parameters characterise the components and their interactions. A non-associating molecule is described by three pure-component parameters: The number of segments in the hard chain, m, the temperature-independent segment diameter, σ, and the dispersion energy between two segments u_{ij}/k_B (where k_B is Boltzmann constant). For mixtures, the parameters are calculated using the conventional Berthelot–Lorentz combining rules:

$$\sigma_{ij} = \frac{1}{2}\left(\sigma_i + \sigma_j\right) \qquad (2)$$

$$u_{ij} = (1-k_{ij})\sqrt{u_i u_j} \qquad (3)$$

One of the major advancements of the SAFT theory is the ability to account for association interactions between molecules. In order to do that, two additional pure-component parameters are required: The association energy between acceptor (A_i) and donor (B_j) sites, ε^{AiBj}/k_B, and a dimensionless parameter accounting for the associating volume, κ^{AiBj}. For mixtures of different components, combining rules from Wolbach and Sandler [155] can be used:

$$\varepsilon^{A_iB_j} = \frac{1}{2}\left(\varepsilon^{A_iB_i} + \varepsilon^{AjB_j}\right) \qquad (4)$$

$$\kappa^{A_iB_j} = \sqrt{\kappa^{A_iB_i}\kappa^{A_jB_j}}\left(\frac{\sqrt{\sigma_i\sigma_j}}{\frac{1}{2}\left(\sigma_i+\sigma_j\right)}\right)^3 \qquad (5)$$

In eqn (3), k_{ij} is a binary interaction parameter used to correct the dispersion-energy parameter u_{ij} between components *i* and *j*, and it is obtained by fitting to experimental mixture data. When $k_{ij} = 0$, the equation of state is called predictive, as only pure-component parameters are used to describe the properties of any mixture of those components.

The interest in the PC-SAFT equation is due to its ability to successfully model different types of phase equilibria (solid-liquid, liquid-liquid, vapour-liquid), even when complex compounds (biomolecules, polymers, ionic liquids...) are involved. It i swell known that the condition for phase equilibrium is the equality of chemical potential of each compound in all the phases present. This equality of chemical potential is transformed to the equality of fugacities or activities for each compound, for convenience. For *N* liquid phases in equilibrium at temperature *T* and pressure *P*, this equilibrium condition can be written as:

$$x_i^I \hat{\phi}_i^I = x_i^{II} \hat{\phi}_i^{II} = \ldots = x_i^N \hat{\phi}_i^N \qquad (6)$$

where subscript *i* refers to components, *x* is the mole fraction, $\hat{\phi}$ is the fugacity coefficient, and superscripts *I, II. . .N* are the different phases in equilibrium. The fugacity coefficients of eqn (6) can be directly calculated with the PC-SAFT equation (1) because there is a direct connection between the residual Helmholtz energy and the fugacity coefficient. And most important, this is done using the parameters of the pure components of the mixture, and the combining rules described above. Thus, the model allows relating the equilibrium compositions of the different components of the mixture through the equilibrium condition, equation (6). Together with the material balances (overall and for each compound) a system of equations is established to calculate the phase splitting for a given mixture. In this way, phase diagrams such as those of Figure 2.16 can be constructed.

2.3.5. SAILs in EOR

The first work published in open literature where a SAIL was proposed to improve surfactant EOR methods [53], due to their capacity to reduce oil/water interfacial tension and solubilise oil, was by the Separation Processes' group of the University of Santiago de Compostela where this Thesis is

developed. In that work, the phase equilibria of a ternary system involving trihexyl(tetradecyl)phosphonium chloride, $[P_{6\,6\,6\,14}]Cl$, water and *n*-dodecane (as oil) was determined and an important reduction of the interfacial tension between water and oil was found. Several advantages of SAILs over typical ionic and non-ionic surfactants were highlighted: their liquid character over a wide range of temperatures (including room temperature) which makes their handling easier; their usually high viscosity that could increase aqueous phase viscosity avoiding digitations; their design opportunities (a specific SAIL can be designed for a specific reservoir); the possibility of avoiding the use of co-surfactants because SAILs form stable aggregates due to their strong cohesive forces; their thermal stability, etc.

Since that first work, the number of publications on this topic in scientific and technical literature has increased exponentially, which is indicative of the interest of this application.

The literature covering this research is very recent and it is basically focused on two aspects. There are several papers [156-161] where SAILs are characterised determining their surface and aggregative (micelles and higher ordered structures) properties. After this characterisation, the studies focus on the reduction of the interfacial tension between water or brine and oil. The second group of papers [162-166] involves studies more focused on the practical application of the technology, basically core flooding tests. These are laboratory tests in which a fluid or combination of fluids is injected into a sample of rock at several conditions of temperature and pressure. The fluid in place at the start of the test is typically simulated as formation brine, oil or a combination of both. Injected fluids include the formulations to be tested for oil recovery. Objectives include measurement of permeability, oil recovery, formation damage caused by the fluid injection, or interactions between the fluid and the rock. Unfortunately, practically all those works lack previous more fundamental studies about phase diagrams and conditions to reach an optimal formulation. This is the reason why the obtained results are not optimal.

From the first group above-mentioned, the more relevant papers are those corresponding to Benzagouta [156] and Hezave [157, 158]. These works focus on the effect of several variables (type and concentration of SAIL, temperature

and salinity) in the interfacial tension between water or brine and crude oil. They reach maximum reductions of about 90% with 1-dodecylpyridinium chloride, [C_{12}py]Cl, but they are still far from the ultra-low values required. Moreover, this IL is solid at room temperature. These works also show that the presence of salt, contrary to classical surfactants, usually helps to reduce the interfacial tension. Hezave's studies also consider dynamic values of this property that allow the prediction of the variation of the property with time. Recently, Prof. Gardas *et al.* [159-161] also presented several studies on the influence of SAILs in the interfacial tension brine/crude oil and its variation with salinity and temperature. However, only in the first of the papers [159] are the alkyl chains of the ILs are long enough to be surface active agents. Thus, reductions found are low (between 10 to 30%, or 40% in the case of the SAIL 1-methyl-3-octylimidazolium chloride, [C_8mim]Cl), far from the required goal.

Most of the papers found in literature are experimental. The only exception is the work of Palchowdhury and Bhargava [167]. These authors use molecular dynamics simulation to study ternary systems SAIL + water + alkane and their interfacial tensions. Reductions found are always lower than 60%, again far from the ultra-low values required.

The more relevant works from a technical point of view are core flooding tests where the crude is displaced using aqueous solutions or microemulsions with SAILs. Coutinho *et al.* [162] test several non-surface active ILs (alkyl chains with 2 or 4 carbons). They obtain a moderate recovery of the crude from sand-pack columns (65%). This recovery was obtained with the IL 1-ethyl-3-methylimidazolium tosylate, [C_2mim][OTs]. The authors base this extraction on the aromatic character of the IL that produces interactions with the aromatic oil fractions, allowing a better wettability and consequent removal of the oil from the reservoir.

Better results are found when the IL used is a surface active agent. This is the case in the works published by Hezave *et al.* [163] and Benzagouta *et al.* [164, 165]. These works present an initial study about the reduction of the interfacial tension between water or brine and oil, and some core flooding tests with the most promising SAILs. In the first work an EOR of about 13 % (total recovery 60%) was found in the best conditions of salinity with 1-dodecyl-3-methylimidazolium chloride, [C_{12}mim]Cl. Benzagouta's group

suggest the use of Ammoeng 102 (tetra-alkyl ammonium sulfate), getting in the most favourable attempts an EOR of about 10%.

Gou *et al.* [166] used the combination of different SAILs with a co-polymer. The polymer, denoted as PAAD, was prepared with acrylamide, acrylic acid, and N,N-diallyl-2-dodecyl-benzenesulfonamide. The PAAD/[C_8mim]Br complex was found more effective to reduce the interfacial tension than water/[C_8mim]Br system. An EOR of about 22% was obtained with the complex brine solution. Prof. Gardas *et al.* [168] tested the combination of several methods of EOR using ILs at several temperatures and salinities. The authors carried out core-flooding experiments with sodium dodecyl sulphate (SDS), alkyl ammonium ILs, polyacrylamide and polyacrylamide after SDS/IL flood. The IL + polymer flood under high saline conditions showed significant increase in oil recovery as compared to the rest of the flooding schemes, reaching maximum recoveries of about 72% (28% EOR) with [$OHPrNH_3$][CF_3COO].

In 2015, two papers [169,170] have been published using Deep Eutectic Solvents (DESs) for EOR. DESs, also known as eutectic-based ILs, are characterized by the marked depression of freezing point when the two components of a eutectic mixture (for instance a quaternary ammonium salt with a hydrogen bond donor) are mixed. The DESs tested in those works are not surfactants, in fact they increase the interfacial tension between water and crude. The recovery is based only on the modification of the wettability oil/rock, and the concentrations used are extremely high (50%) making the process unreasonable from an economic point of view.

All the previously described papers screen several ILs (some of them with surfactant character and some others without it) for EOR, but these were not chosen by any scientific or technological reason. At the same time that these works were presented, we also continued our research on this topic [171-175], focusing on the more fundamental research on phase equilibria to find SAILs capable of forming a triphasic system, where the IL solubilizes equilibrated quantities of water and oil, with minimal interfacial tension. Some of those works are part of this Thesis and they will be presented in the corresponding section.

3. PUBLICATIONS

USC
UNIVERSIDADE
DE SANTIAGO
DE COMPOSTELA

3.1. Synthesis of AgCl nanoparticles in ionic liquid and their application in photodegradation of Orange II:

http://link.springer.com/article/10.1007/s10853-015-8917-0

3.2. Synthesis and characterisation of highly concentrated AgI–[$P_{6\,6\,6\,14}$]Cl ionanofluids:

http://link.springer.com/article/10.1007/s11051-013-1881-1

3.3. Measuring and PC-SAFT modelling three-phase behaviour:

http://pubs.rsc.org/en/content/articlelanding/2014/cp/c4cp04336g

3.4. Characterisation and interfacial properties of the surfactant ionic liquid 1-dodecyl-3-methylimidazolium acetate for enhanced oil recovery:

http://pubs.rsc.org/en/Content/ArticleLanding/2015/RA/c5ra05247e

USC
UNIVERSIDADE
DE SANTIAGO
DE COMPOSTELA

4. GENERAL DISCUSSION

USC
UNIVERSIDADE
DE SANTIAGO
DE COMPOSTELA

Ionic liquids are salts that have melting points or glass-transition temperatures below 100 ºC, and due to their tuneable and favourable properties they can be used for the preparation of materials in the nanometric size. First and second papers presented in this thesis focus in this application. A simple and very effective method, patented by the Group of Separation Processes of the University of Santiago de Compostela, was used to synthesise different type of nanomaterials, namely silver chloride nanoparticles and AgI-[$P_{6\ 6\ 6\ 14}$]Cl ionanofluids, using the SAIL trihexyl(tetradecyl)phosphonium chloride.

In the first work, silver chloride nanoparticles were prepared, using solely the corresponding powder material and the SAIL. The structure of the nanoparticles was corroborated by means of XRPD, showing the only presence of chlorargyrite, and UV-vis spectroscopy. TEM showed nanoparticles with a size in the range of 5-20 nm, homogeneous and with spherical shape. The nanoparticles were precipitated from the IL, and SEM showed that the solid was formed by big cubic agglomerates of small particles.

The ability of the obtained nanoparticles as catalyst for degrading Orange II was tested. After 30 minutes of UV irradiation, when starting from dye dissolution of 100 ppm and using 1 g/L of silver chloride nanoparticles, the degradation of the azo dye was confirmed by a remarkable decrease in the corresponding absorbance peak and from the decolouration of the dye. The UV spectra absorbances, confirmed a degradation of 79.2% under these conditions. Moreover, from the variation of these dye concentrations with time, the kinetic of the photocatalytic process was obtained and depicted by a first-order equation with a rate constant of 0.0451 min^{-1}.

The products formed after certain degradation times could be identified by LC-Q-TOF-MS and a plausible mechanism for the degradation reaction was suggested. The azo bond of the main molecule is broken and the compound is degraded (via the formation of phtalic acid and via the formation of benzenesulphonic acid) to small dicarboxylic acids and thus probably to CO_2 by the “photo-Kolbe” reaction. When using bulk solid instead of the nanosised one the effectiveness in the degradation diminished to a 42.2%, and when the nanocatalyst was used under the sunlight instead of UV irradiation, the degradation is even lower, only a 20.4%.

Moreover, when the same experiment was carried out with the UV irradiation and in the absence of catalyst the degradation achieved is 24.4%. Therefore, the combination of silver chloride nanoparticles with the UV radiation was required to obtain an effective degradation of Orange II.

A comparison was established with other commonly used nanocatalysts. To that end, the experiment was repeated by using different commercial nanoparticles. The prepared silver chloride nanomaterial was highly effective (79.2% of degradation) for the photodegradation of Orange II in comparison with the other studied nanoparticles (62.5%, 50.4% and 29.4% of degradation for ZnO, TiO_2 and Ag, respectively). The recyclability of the prepared catalyst was also proved. After a first photodegradation experiment, in which the degradation achieved was 79.2%, the photocatalytic activity slowly decreased to degradation efficiencies around 65%. The slight decrease of activity can be due to small loses of catalyst in each cycle.

To check the effect of the initial concentration of dye and catalyst concentration, different concentrations of dye in the dissolution and different amounts of catalyst were used under the UV radiation for 30 minutes. It was found that for a given amount of catalyst the degradation efficiency decreased when increasing the initial dye concentration. Moreover, when fixing this initial content of Orange II, higher amounts of catalyst meant a higher degradation performance. The degradation achieved with solutions below 100 ppm by using 10 g/L of catalyst was almost complete (≥99.9%) for all the samples. Finally, the effect of different pH in the initial solution was also tested. The degradation achieved in an acidic medium was approximately the same than at natural pH of the solution (pH = 6). Nevertheless, the degradation was really enhanced (up to 96.7%) when the pH was increased to 9 and it sharply decreased in very basic media (46.0%).

The aforementioned method was used in the second paper presented in this thesis to synthesise AgI-$[P_{6\ 6\ 6\ 14}]Cl$ ionanofluids. In this case AgI bulk powder was dispersed into the SAIL to obtain ionanofluids with nanoparticles concentration up to 50 wt%. The structure of the nanoparticles was corroborated by the same techniques used in the previous paper. XRPD confirmed the existence of iodargyrite, the hexagonal crystal system of the silver iodide, and TEM showed nanoparticles with a size in the range of 2-4

nm, homogeneous and with spherical shape. This size was also confirmed by measurements in a Zetasizer Nano ZS and using Bru's equation.

Several physical properties were measured at atmospheric pressure and different temperatures to characterise the ionanofluids. Densities and refractive indices linearly decreased with temperature and increased when increasing the concentration of nanoparticles. In the case of the viscosity, the SAIL and ionanofluids presented a Newtonian behaviour. No variation in the viscosity of the 1–20 % ionanofluids was found in comparison with the values of the pure SAIL. However, this property drastically increased for higher concentrations, especially at lower temperatures. As expected, the viscosity diminished with the increase of temperature.

Electrical conductivities and specific heat capacities of ionanofluids were also measured. It was found that the electric conductivity became higher with the concentration up to 20 % w/w of AgI. Then, the value began to decrease. This phenomenon could be explained because of the high viscosity of the more concentrated dispersions. This low mobility of the ions in the nanofluid (associated to the high viscosity) could lead to lower electric conductivity values. In the case of the specific heat capacity, the values got slightly higher with temperature, but they decreased with the increase of the concentration of nanoparticles because the specific heat capacity of the silver iodide is lower than that of the SAIL.

The following two papers that constitute this thesis are based on the capacity of solubilisation and reduction of the interfacial tension of SAILS to improve surfactant EOR methods. Useful laboratory tests to analyse the viability of a surfactant for EOR are: the determination of phase diagrams and the measurement of dynamic interfacial tensions. Each one of these methods has been applied for different SAILs in the third and fourth papers of this thesis.

In the third paper, phase equilibria of ternary systems water + *n*-dodecane + SAIL were determined at 298.15 K and 348.15 K and atmospheric. The selected SAILs were: 1-decyl-3-methylimidazolium bis(trifluoromethylsulfonyl)imide, $[C_{10}mim][NTf_2]$, and 1-dodecyl-3-methylimidazolium bis(trifluoromethylsulfonyl)imide, $[C_{12}mim][NTf_2]$. According to the classification of Treybal, ternary diagrams obtained are

Type III systems because they are composed of three pairs of partially miscible liquids. But the obtained diagrams also could be classified according to the Winsor type III system, with a triphasic region and two biphasic regions around it (the biphasic region at the bottom of the diagram is negligible), as well as a monophasic domain. A Winsor type III system contains a region in which three phases are in equilibrium: a surfactant-rich, the so-called middle phase because of its intermediate location in the test tube, and two excess phases (oil and water). However, the surfactant-rich phases obtained here contain a very high amount of IL (denser than the two other components), and thus they appear as the lower phase in the three-phase system.

With the enhanced oil recovery application in mind, physical properties like density, viscosity and interfacial tension are of critical relevance and were measured. $[C_{12}mim][NTf_2]$ caused lower interfacial tensions than $[C_{10}mim][NTf_2]$, as it was expected according to its more amphiphilic character. For both considered SAILs, the water/SAIL interfacial tension decreased with temperature and upon addition of sodium chloride. However, in the case of SAIL/*n*-dodecane, the interfacial tension was almost not affected by temperature. A similar behaviour was found for the interfaces of the three-phase systems. The middle/lower (aqueous/IL-rich phase) and the upper/middle (dodecane/aqueous) interfacial tensions decreased with temperature and upon addition of sodium chloride. The effect of NaCl is more noticeable at the highest temperature. However, the effect of both variables (temperature and addition of NaCl) is negligible for the upper/lower (dodecane/IL-rich phase) interfacial tension.

It was possible to use PC-SAFT to predict the phase diagram for the ternary systems (water + $[C_n mim][NTf_2]$ + *n*-dodecane) ternary systems. Deviations obtained between experimental data and PC-SAFT were of same magnitude than the experimental uncertainties. Increasing the temperature from 298.15 to 343.15 K slightly higher deviations were obtained. However, such deviations could be easily reduced by introducing the parameter *kij* for the (n-dodecane/IL) pair.

The objective of the fourth paper of the thesis was obtaining an optimal formulation, for surfactant EOR, based on the SAIL 1-dodecyl-3-methylimidazolium acetate, $[C_{12}mim][OAc]$. A critical micelle concentration in water of

0.81 mM was found for this SAIL by surface tension measurements and an approximated value was obtained with electrical conductivity. The aggregation effects of the SAIL were compared with literature values for the same SAIL with halide counter-ions. [C_{12}mim][OAc] presented, in general, lower cmc, better tendency for micellization over adsorption at the interface and lower spontaneity for micellization.

A Saharan crude oil was used to test the capability of the SAIL to reduce the interfacial tension. A value of 19.2 $mN \cdot m^{-1}$ was found for the Saharan crude oil/water interfacial tension. Dynamic interfacial tension measurements between crude oil and the aqueous solutions of the SAIL were carried out at 298.15 K and atmospheric pressure. The interfacial tension decreased with concentration of the SAIL, with equilibrium values of 6.91, 2.92 and 2.08 $mN \cdot m^{-1}$ for 500, 2000 and 4000 ppm concentration, respectively. There was a clear reduction in the interfacial tension with the concentration of [C_{12}mim][OAc], but the efficiency on interfacial tension reduction decreased from a certain surfactant concentration. The same behaviour has been found for other SAILs.

Various experiments were also carried out varying the salinity of the aqueous phase (NaCl concentration) from 0 to 4 wt%, while maintaining a constant concentration of [C_{12}mim][OAc] at 2000 ppm. The increase in aqueous phase salinity further reduced the interfacial tension, but NaCl concentrations in the range 2000 – 40000 ppm provided similar equilibrium values for interfacial tension. The influence of the temperature was studied working at 298.15 K, 318.15 K and 338.15 K and measuring interfacial dynamic tensions between crude oil and surfactant (2000ppm) aqueous solution. The effect of this variable was clearly different in the presence or absence of electrolyte. While for solutions of [C_{12}mim][OAc] in pure water the equilibrium interfacial tension decreased within the temperature range studied from 2.92 to 0.81 $mN \cdot m^{-1}$, in 4 wt% NaCl brine the interfacial tension increased from 1.20 to 2.03 $mN \cdot m^{-1}$.

It is known that alkalis react with components of crude generating surfactants in situ, thus producing a synergistic effect in the reduction of the interfacial tension. For this reason, a set of experiments were performed using a solution of [C_{12}mim][OAc] (2000 ppm) prepared in brine (NaCl 4 wt.%) and varying NaOH concentration (0, 0.5, 1.0 and 1.5 wt%).

Dynamic interfacial tension between these solutions and crude oil were measured at 298.15 K. The results showed a significant decrease of the interfacial tension from 1.2 to 0.30, 0.25 and 0.11 $mN \cdot m^{-1}$ with 0.5, 1.0 and 1.5 wt% NaOH. Considering the pure water/crude oil interfacial tension given before (19.2 $mN \cdot m^{-1}$), a remarkable reduction of two to three orders of magnitude is accomplished. In order to further check this effect, another alkali (sodium carbonate) was evaluated. Different solutions of $[C_{12}mim][OAc]$ (2000 ppm) in brine (4 wt.%) were prepared, varying Na_2CO_3 concentration from 0 to 1.5 wt%.. Again, a clear reduction in the interfacial tension was produced, however best results were found with the use of NaOH as alkali.

The two methods presented in the las two manuscripts that constitute this thesis are useful tools to encourage or avoid the realisation of the expensive core flooding essays as definitive tests in EOR.

5. CONCLUSIONS

USC
UNIVERSIDADE
DE SANTIAGO
DE COMPOSTELA

ILs do not behave like simple molecular solvents and form spatially heterogeneous domains. The segregation of polar/non-polar domains, noticeable in the case of SAILs, provides the possibility to elaborate high-performance materials or to take advantage of their high capacity of solvation. In this thesis two applications, based on these properties, have been tested.

The first main conclusion of this work is that several SAILs can be used for the synthesis of nanoparticles and ionanofluids. The only chemicals involved in the process are the SAIL and the bulk powder of the nanomaterial to synthesise. The synthesised nanoparticles can be used in many applications. In this work, their use as nanocatalysts in the photodegradation of dyes was tested. The second main conclusion is that the capacity of SAILs to solubilise water and oil, and to reduce the interfacial tension between them, make these surfactants promising alternatives to evaluate for the improvement of surfactant EOR methods. Specific conclusions related to the manuscripts that constitute this thesis are summarised below.

– Synthesis of AgCl nanoparticles in ionic liquid and their application in photodegradation of Orange II

Silver chloride nanoparticles can be synthesised by a dissolution-reprecipitation method using solely the SAIL trihexyl(tetradecyl)phosphonium chloride, $[P_{6\,6\,6\,14}]Cl$ and AgCl bulk powder. Only a process of stirring under moderate temperatures is required. This technique allows the production of very high concentration of nanoparticles in the IL that, once precipitated, form cubic agglomerates of small nanoparticles (<20 nm) of spherical shape.

The obtained nanoparticles have shown higher degradation rates than other commonly used nanocatalysts (Ag, TiO_2, or ZnO) to degrade Orange II, an azo dye usually found in textile wastewaters. The process requires both UV light and AgCl nanocatalyst to be effective, and pH values around nine improve the results. An almost complete degradation can be achieved and the nanoparticles can be recycled.

– **Synthesis and characterisation of highly concentrated AgI–[$P_{6\ 6\ 6\ 14}$]Cl ionanofluids**

The aforementioned method of synthesis of nanoparticles in fact first forms the ionanofluid, a stable dispersion of nanoparticles in the IL. From there, the nanoparticles can be precipitated. It is consequently evident that the method can be used both for the synthesis of ionanofluids and nanoparticles.

Specifically, in this paper the synthesis of ionanofluids, consisting of silver iodide nanoparticles in the IL trihexyl-(tetradecyl)phosphonium chloride, [$P_{6\ 6\ 6\ 14}$]Cl, can be produced with a mass percentage of up to 50 %. The nanoparticles contained in the fluid were hexagonal with sizes between 2-4 nm.

Density and viscosity increase with the concentration of nanoparticles and decrease with temperature. In this case, specific heat capacity of the ionanofluid decreases with the concentration of nanoparticles, due to the low value of this property for silver iodide, and increases with temperature. An enhancement of the electric conductivity of the IL was found but only up to concentrations of about 20% w/w of nanoparticles.

In spite of not obtaining good results in relation to the enhancement of the thermal or electrical properties of the IL, it can be concluded that the proposed method can be used for the production of very high concentrate stable ionanofluids, without the need of any surfactant of any other stabilizing agent. Taking advantage of this method of synthesis and with careful consideration in the selection of the IL and nanoparticles, fluids of enhanced properties can be obtained.

– **Measuring and PC-SAFT modelling three-phase behaviour**

The liquid–liquid equilibria of water + 1-alkyl-3-methyl-imidazolium bis(trifluoromethylsulfonyl)imide, [$C_n$mim][NTf_2] (n = 10 or 12) + *n*-dodecane ternary systems were measured at 298.15 and 348.15 K. Systems are Treybal type III, with three pairs of partially miscible pure liquid components. Due to the surfactant character of the IL, they can also be classified as Winsor type III with a three-phase region surrounded by three biphasic regions.

In the case of these ILs, the three phases appear as a consequence of the immiscibility of the three binaries. The immiscibility of the SAIL in water and the high concentration of this compound in the middle phase, where water and oil are solubilised, disfavour the use of this surfactant in oil recovery. This is also confirmed with the low reduction in the interfacial tension of water/dodecane found with the use of these ILs.

The PC-SAFT equation of state was able to predict the equilibrium involved in triphasic systems using solely pure component parameters. No fitting parameters were required. It can be concluded that the use of PC-SAFT model to predict the phase behaviour of these complex systems, could be a fast and cheap initial method for the screening of possible surfactants for EOR processes.

– *Characterisation* and interfacial properties of the surfactant ionic liquid 1-dodecyl-3-methyl imidazolium acetate for enhanced oil recovery

To get miscibility with water, the [NTf_2^-] anion of the previously tested IL was changed for [OAc^-]. Thus, a novel SAIL, 1-dodecyl-3-methyl imidazolium acetate, [C_{12}mim][OAc], was obtained. For this salt, in comparison with others with the same cation and different halide counter-ions, a noticeable lower cmc was found.

To test the validity of this SAIL in EOR applications, the dynamic interfacial tensions of aqueous solutions of [C_{12}mim][OAc] with crude oil (Saharan blend) were evaluated for different formulations and conditions. Interfacial tensions of around 0.1 $mN \cdot m^{-1}$ were found using the SAIL in combination with NaOH. It can be concluded that this IL is an interesting alternative for EOR, and that combination of SAILs with alkalis is important to further reduce interfacial tension. Adsorption and core-flooding experiments are the next steps prior to carrying out studies with the conditions of a specific well.

USC
UNIVERSIDADE
DE SANTIAGO
DE COMPOSTELA

LIST OF SYMBOLS

USC
UNIVERSIDADE
DE SANTIAGO
DE COMPOSTELA

Symbols

a	Helmholtz energy
a_1, a_2	slopes of the linear regions before and after the cmc in Carpena model
A, B	associating sites
AAD	average absolute deviation
a^s_m	minimum area per surfactant molecule at saturated interface
ASP	Alkaline/Surfactant/Polymer flooding
BASIL	Biphasic Acid Scavenging Utilizing Ionic Liquids
C	concentration
CAS	Chemical Abstracts Service
cmc	critical micelle concentration
CNT	Carbon Nanotube
D	diameter
DES	Deep Eutectic Solvent
DLS	Dynamic Light Scattering
d_p	nanoparticle diameter
e	charge of an electron
EG	Ethylene Glycol
E_g	nanoparticle band gap
$E_{g,bulk}$	bulk band gap
EOR	Enhanced Oil Recovery
h	Plack constant
HLB	Hydrophilic-Lipophilic Balance
IFT	interfacial tension
IL	Ionic Liquid
ILC	Ionic Liquid Crystal
K	capillary constant
k_{app}	pseudo-first order constant
k_B	Boltzmann constant
k_{ij}	binary interaction parameter
LC-Q-TOF–MS	liquid chromatography-quadrupole-time-offlight–mass spectrometry
LLE	liquid-liquid equilibrium
LLLE	liquid-liquid-liquid equilibrium
m	number of segments in the hard chain
m_e	effective mass of an electron
MEOR	Microbial Enhanced Oil Recovery
m_h	effective mass of a hole
MWCNTs	multi-walled carbon nanotubes

N_A	Avogadro constant
n_D	refractive index
NMR	Nuclear Magnetic Resonance
o/w	oil-in-water
p	width of the transition between both linear regions in Carpena model
pC_{20}	negative logarithm of the concentration needed to reduce surface tension in 20 mN m^{-1}
PC-SAFT	Perturbed Chain Statistical Associating Fluid Theory
PXRD	X-ray powder diffraction
R	gas constant
r	radius
RTIL	Room Temperature Ionic Liquid
SAIL	Surface Active Ionic Liquid
SEM	Scanning Electron Microscopy
S_N1	Nucleophilic Substitution 1
S_N2	Nucleophilic Substitution 2
STM	Scanning Tunneling Microscope
T	Temperature
t	time
TEM	Transmission Electron Microscopy
u	standard uncertainty
u_{ij}	dispersion-energy parameter
UV	ultraviolet radiation
UV-vis	ultraviolet-visible radiation
VLE	vapour-liquid equilibrium
VOC	Volatile Organic Compound
w	mass fraction
w/o	water-in-oil
x	mole fraction
XPS	X-ray photoelectron spectroscopy
y	kinetic energy correction

Greek letters

α	degree of micelle ionization near the cmc
β	degree of counter-ion binding
Δ	variation
ε	absolute permittivity
ε^{AiBj}	association energy parameter
ϕ	phase

$\hat{\phi}$	fugacity coefficient
γ	interfacial tension
γ	surface tension
Γ_m	surface excess concentration at saturation
η	dynamic viscosity
κ	conductivity
κ^{AiBj}	association volume parameter
λ	wavelength
ρ	density
σ	electric conductivity
σ	temperature-independent segment diameter
υ	kinematic viscosity
ω	rotational velocity

Subscripts

I, II, ...N	phases in equilibrium
i	components / molecules
j	components / molecules
m	number of carbon atoms in an alkyl substituent chain
mic	micellization
n	number of carbon atoms in an alkyl substituent chain

Superscripts

assoc	association
disp	dispersion
hc	hard-chain
res	residual

USC
UNIVERSIDADE
DE SANTIAGO
DE COMPOSTELA

REFERENCES

USC
UNIVERSIDADE
DE SANTIAGO
DE COMPOSTELA

[1] R. D. Rogers and K. R. Seddon: "Ionic Liquids - Solvents of the Future?", *Science*, 302, pp. 792-793 (2003).

[2] J. F. Brennecke and E. J. Maginn: "Ionic Liquids: Innovative Fluids for Chemical Processing", *AIChE Journal*, 47, pp. 2384-2389 (2001).

[3] R. D. Rogers and K. R. Seddon, Preface to *Ionic Liquids as Green Solvents - Progress and Prospects* (Eds. R. D. Rogers, and K. R. Seddon), ACS Symposium Series, vol. 856, American Chemical Society, Washington DC, 2003.

[4] M. Freemantle, *An introduction to ionic liquids*, RSC Publishing, Cambridge, 2009.

[5] M. J. Earle and K. R. Seddon: "Ionic liquids. Green solvents for the future", *Pure Appl. Chem.,* 72, pp. 1391-1398 (2000).

[6] K. R. Seddon: "Ionic liquids: Designer solvents?", in *The International George Papatheodorou Symposium: Proceedings* (Eds. S. Boghosian, V. Dracopoulos, C. G. Kontoyannis and G. A. Voyiatzis), pp. 131-135, Institute of Chemical Engineering and High Temperature Chemical Processes, Patras, 1999.

[7] T. Welton: "Room-Temperature Ionic Liquids. Solvents for Synthesis and Catalysis", *Chem. Rev.*, 99, pp. 2071-2083 (1999).

[8] N. Nambu, N. Hiraoka, K. Shigemura, S. Hamanaka and M. Ogawa: "A Study of the 1,3,5-Trialkylbenzenes with Aluminum Chloride-Hydrogen Chloride Systems" *Bull. Chem. Soc. Jpn.*, 49, pp. 3637-3640 (1976).

[9] S. Gabriel and J. Weiner: "Ueber einige Abkiimmlinge des Propylamins", *Chem*. *Ber*., 21, pp. 2669-2679 (1888).

[10] P. Walden: "Molecular Weights and Electrical Conductivity of Several Fused Salts", *Bull. Russ. Acad. Sci.,* 8, pp. 405-422 (1914).

[11] J. S. Wilkes, J. A. Levisky, R. A. Wilson and C. L. Hussey: "Dialkylimidazolium chloroaluminate melts: A new class of room-temperature ionic liquids for electrochemistry, spectroscopy, and synthesis", *Inorg. Chem.*, 21, pp. 1263-1264 (1982).

[12] J. S. Wilkes and M. J. Zaworotko: "Air and water stable 1-ethyl-3-methylimidazolium based ionic liquids", *J. Chem. Soc., Chem. Commun*., pp. 965-967 (1992).

[13] P. Bonhôte, A. P. Dias, N. Papageorgiou, K. Kalyanasundaram and M. Grätzel: "Hydrophobic, Highly Conductive Ambient-Temperature Molten Salts", *Inorg. Chem.,* 35, pp. 1168-1178 (1996).

[14] K. R. Seddon: "Ionic Liquids for Clean Technology", *J. Chem. Tech. Biotechnol.*, 68, pp. 351-356 (1997).

[15] R. Giernoth: "Homogeneous Catalysis in Ionic Liquids", in *In situ NMR Methods in Catalysis* (Eds. J. Bargon and L. T. Kuhn), Topics in Current Chemistry, vol. 276, pp. 1-23, Springer, Dordrecht, 2007.

[16] K. S. Rao, P. Bharmoria, T. J. Trivedi and A. Kumar: "Self-Assembly of Surface-Active Ionic Liquids in Aqueous Medium", in *Ionic Liquid-Based Surfactant Science: Formulation, Characterization, and Applications* (Eds. B. K. Paul, S. P. Moulik and W. Kunz), Wiley Series on Surface and Interfacial Chemistry, pp. 175-192, John Wiley & Songs, New Jersey, 2015.

[17] N. V. Plechkova and K. R. Seddon: "Applications of ionic liquids in the chemical industry", *Chem. Soc. Rev.*, 37, pp. 123-150 (2008).

[18] R. D. Rogers, K. R. Seddon and S. Volkov, Preface to *Green Industrial Applications of Ionic Liquids* (Eds. R. D. Rogers, K. R. Seddon and S. Volkov), Kluwer, Dordrecht, 2002.

[19] A. A. J. Torriero, *Electrochemistry in Ionic Liquids, Volume 2: Applications* (Ed. A. A. J. Torriero), Springer, New York, 2015.

[20] T. Tsuda and C. L. Hussey: "Electrochemical Applications of Room-Temperature Ionic Liquids", *Electrochem. Soc. Interface*, 16, pp. 42-49 (2007).

[21] J. P. Hallett and T. Welton: "Room-Temperature Ionic Liquids: Solvents for Synthesis and Catalysis. 2", *Chem. Rev.*, 111, pp. 3508-3576 (2011).

[22] V. I. Parvulescu and C. Hardacre: "Catalysis in ionic

liquids", *Chem. Rev.*, 107, pp. 2615-2665 (2007).

[23] M. Maase: "BASIL™ Process" in *Multiphase Homogeneous Catalysis* (Eds. B. Cornils, W. A. Herrmann, I. T. Horvath, W. Leitner, S. Mecking, H. Olivier- Bourbigou, and D. Vogt), Wiley-VCH, vol. 2, pp. 560-566, Weinheim, 2005.

[24] H. Olivier-Bourbigou and F. Hugues: "Applications of Ionic Liquids to Biphasic Catalysis", in *Green Industrial Applications of Ionic Liquids* (Eds. R. D. Rogers, K. R. Seddon and S. Volkov), NATO Science Series II: Mathematics, Physics and Chemistry, vol. 92, pp. 67-84, Springer, Dordrecht, 2002.

[25] C. M. Graham and J. L. Anderson: "Ionic Liquids in Separation Science" in *Ionic Liquids Uncoiled: Critical Expert Overviews* (Eds. N. V. Plechkova and K. R. Seddon), pp. 87-118, John Wiley & Sons, New Jersey, 2012.

[26] A. Soto: "Ionic Liquids for Extraction Processes in Refinery-Related Applications" in *Ionic Liquids for Better Separation Processes* (Ed. H. Rodriguez), pp. 39-66, Springer-Verlag Berlin Heidelberg, 2016.

[27] W. W. Meindersma and A. B. De Haan: "Separation Processes with Ionic Liquids" in *Ionic Liquids Uncoiled: Critical Expert Overviews* (Eds. N. V. Plechkova and K. R. Seddon), pp. 119-180, John Wiley & Sons, New Jersey, 2012.

[28] A. Brandt, J. Gräsvik, J. P. Hallett and T. Welton: "Deconstruction of lignocellulosic biomass with ionic liquids", *Green Chem.*, 15, pp. 550-583 (2013).

[29] A. P. Carneiro, O. Rodriguez and E. A. Macedo: "Separation of carbohydrates and sugar alcohols from ionic liquids using antisolvents", *Sep. Purif. Technol.*, 132, pp. 496-504 (2014).

[30] M. Abai, M. P. Atkins, K. Y. Cheun, J. D. Holbrey, P. Nockemann, K. R. Seddon, G. Srinivasan and Y. Zou: "Process for removing metals from hydrocarbons", *PTC Int. Appl. WO 2012046057A2*, 2012.

[31] M. Antonietti, D. Kuang, B. Smarsly and Y. Zhou: "Ionic liquids for the convenient synthesis of functional nanoparticles and other inorganic nanostructures", *Angew. Chem. Int. Ed.*, 43, pp. 4988-4992 (2004).

[32] Y. Zhou: "Recent advances in ionic liquids for synthesis of inorganic nanomaterials", *Curr. Nanosci.*, 1, pp. 35-42 (2005).

[33] A. Taubert and Z. Li: "Inorganic materials from ionic liquids", *Dalton Trans.*, 7, pp. 723-727 (2007).

[34] Z. Li, Z. Jia, Y. Luan and T. Mu: "Ionic liquids for synthesis of inorganic nanomaterials", *Curr. Opin. Solid State Mater. Sci.*,12, pp. 1-8 (2008).

[35] J. Fernandez, X. Paredes, F. M. Gacino, M. J. P. Comunas and A. S. Pensado: "Pressure-viscosity behaviour and film thickness in elastohydrodynamic regime of lubrication of ionic liquids and other base oils", *Lubr. Sci.*, 26, pp. 449-462 (2014).

[36] T. Regueira, L. Lugo and J. Fernández; "Ionic liquids as hydraulic fluids: comparison of several properties with those of conventional oils", *Lubr. Sci.*, 26, pp. 488-499 (2014).

[37] I. Otero, E. R. López, M. Reichelt, M. Villanueva, J. Salgado and J. Fernández: "Ionic Liquids Based on Phosphonium Cations All Neat Lubricants or Lubricant Additives for a Steel/Steel Contact", *ACS Appl. Mater. Interfaces*., 6, pp. 13115-13128 (2014).

[38] F. L. Sánchez, I. Otero, E. R. López and J. Fernández, "Tribological Properties of Two Bis(trifluoromethylsulfonyl)-imide-Based Ionic Liquids on Steel/Steel Contact", *Tribol. T.*, 57, pp. 637-646 (2014).

[39] I. R. Collins, M. J. Earle, S. P. Exton, N. V. Plechkova and K. R. Seddon: "Ionic liquids and uses thereof", *PCT Int. Appl. WO 2006111712A2*, 2006.

[40] M. Blesic, M. Swadźba-Kwaśny, J. D. Holbrey, J. N. Canongia-Lopez, K. R. Seddon and L. P. N. Rebelo: "New catanionic surfactants based on 1-alkyl-3-methylimidazolium alkylsulfonates, $[C_nH_{2n+1}mim][C_mH_{2m+1}SO_3]$: mesomorphism and aggregation", *Phys. Chem. Chem. Phys.*, 11, pp. 4260-4268 (2009).

[41] J. Lu, F. Yan and J. Texter: "Advanced applications of ionic liquids in polymer science", *Prog. Polymer Sci.*, 34, pp. 431-448 (2009).

[42] M. Blesic, A. Lopes, E. Melo, Z. Petrovski, N. V. Plechkova, J. N. Canongia-Lopez, K. R. Seddon and L. P. N. Rebelo: "On the Self-Aggregation and Fluorescence Quenching Aptitude of Surfactant Ionic Liquids", *J. Phys. Chem. B*, 112, pp. 8645-8650 (2008).

[43] N. A. Smirnova and E. A. Safonova: "Micellization in solutions of ionic liquids", *Colloid J.*, 74, pp. 254-265 (2012).

[44] M. Blesic, M. H. Marques, N. V. Plechkova, K. R. Seddon, L. P. Rebelo and A. Lopes: "Self-aggregation of ionic liquids: micelle formation in aqueous solution", *Green Chem.*, 9, pp. 481-490 (2007).

[45] N. Cheng, P. Yu, T. Wang, X. Sheng, Y. Bi, Y. Gong and L. Yu: "Self-Aggregation of New Alkylcarboxylate-Based Anionic Surface Active Ionic Liquids: Experimental and Theoretical Investigations", *J. Phys. Chem. B*, 118, pp. 2758-2768 (2014).

[46] J. Bowers, C. P. Butts, P. J. Martin and M. C. Vergara-Gutierrez: "Aggregation behaviour of aqueous solutions of ionic liquids", *Langmuir*, 20, pp. 2191-2198 (2004).

[47] K. S. Rao, P. S. Gehlot, T. J. Trivedi and A. Kumar: "Self-assembly of new surface active ionic liquids based on Aerosol-OT in aqueous media", *J. Colloid Interface Sci.*, 428, pp. 267-275 (2014).

[48] P. D. Galano and O. A. El Seoud: "Ionic Liquid-Based Surfactants: Synthesis, Molecular Structure, Micellar Properties and Applications", in *Ionic Liquid-Based Surfactant Science: Formulation, Characterization, and Applications* (Eds. B. K. Paul, S. P. Moulik and W. Kunz), Wiley Series on Surface and Interfacial Chemistry, pp. 63-100, John Wiley & Songs, New Jersey, 2015.

[49] H. Li, C. Yu, R. Chen and J. Li: "Novel ionic liquid-type Gemini surfactants: Synthesis, surface property and antimicrobial activity", *Colloids Surf. A*, 395, pp. 116-124 (2012).

[50] C. Ghatak, V. Govind-Rao, S. Mandal, S. Ghosh and N. Sarkar: "An Understanding of the Modulation of Photophysical Properties of Curcumin inside a Micelle Formed by an Ionic Liquid: A New Possibility of Tunable Drug Delivery System", *J. Phys. Chem. B*, 116, pp. 3369-3379 (2012).

[51] X. Q. An and J. Shen: "Ionic Liquid Microemulsions and Applications", in *Ionic Liquid-Based Surfactant Science: Formulation, Characterization, and Applications* (Eds. B. K. Paul, S. P. Moulik and W. Kunz), Wiley Series on Surface and Interfacial Chemistry, pp. 359-374, John Wiley & Songs, New Jersey, 2015.

[52] D. Guzmán-Lucero, P. Flores, T. Rojo and R. Martínez-Palou: "Ionic Liquids as Demulsifiers of Water-in-Crude Oil Emulsions: Study of the Microwave Effect", *Energy Fuels*, 24, pp. 3610-3615 (2010).

[53] S. Lago, H. Rodríguez, M. K. Khoshkbarchi, A. Soto and A. Arce: "Enhanced oil recovery using the ionic liquid trihexyl(tetradecyl)phosphonium chloride: phase behaviour and properties", *RSC Adv.*, 2, pp. 9392-9397 (2012).

[54] H. S. Xia, J. Yu, Y. Y. Jiang, I. Mahmood and H. Z. Liu: "Physicochemical Features of Ionic Liquid Solutions in the Phase Separation of Penicillin(II): Winsor II Reversed Micelle", *Ind. Eng. Chem. Res.*, 46, pp. 2112-2116 (2007).

[55] M. J. Trujillo-Rodríguez, P. González-Hernández and V. Pino: "Analytical Applications of Ionic Liquid-Based Surfactants in Separation Science", in *Ionic Liquid-Based Surfactant Science: Formulation, Characterization, and Applications* (Eds. B. K. Paul, S. P. Moulik and W. Kunz), Wiley Series on Surface and Interfacial Chemistry, pp. 475-502, John Wiley & Songs, New Jersey, 2015.

[56] J. Zhang: "Ionic Liquid-Based Microemulsions", in *Ionic Liquid-Based Surfactant Science: Formulation, Characterization, and Applications* (Eds. B. K. Paul, S. P. Moulik and W. Kunz), Wiley Series on Surface and Interfacial Chemistry, pp. 325-342, John Wiley & Songs, New Jersey, 2015.

[57] S. Livi, J. F. Gérard and J. Duchet-Rumeau: "Ionic Liquids: Surfactant Agents for Layered Silicates", in *Ionic Liquid-Based Surfactant Science: Formulation, Characterization, and Applications* (Eds. B. K. Paul, S. P. Moulik and W. Kunz), Wiley Series on Surface and Interfacial Chemistry, pp. 503-516, John Wiley & Songs, New Jersey, 2015.

[58] B. Bhushan: "Introduction to Nanotechnology", in *Springer Handbook of Nanotechnology* (Ed. B. Bhushan), pp.

1-12, Springer-Verlag Berlin Heidelberg, 2004.

[59] R. M. Brydson and C. Hammond: “Generic methodologies for nanotechnology: classification and fabrication”, in *Nanoscale Science and Technology* (Eds. R. W. Kelsall, I. W. Hamley, M. Geoghegan), pp. 1-55, John Wiley & Sons. Leeds, 2005.

[60] *Wichlab* (2016). Retrieved June 2016, from http://www.wichlab.com/research/

[61] *Nanotechnology Timeline* (2016). Retrieved June 2016, from http://www.nano.gov/timeline

[62] R. Zsigmondy and H. Siedentopf: “Uber Sichtbarmachung und Größenbestimmung ultramikoskopischer Teilchen, mit besonderer Anwendung auf Goldrubingläser”, *Ann. Phys.*, 315, pp. 1-39 (1902).

[63] J. L. Liu and S. Bashir: “Nanomaterials and Their Application” in *Advanced Nanomaterials and Their Applications in Renewable Energy* (Eds. J. L. Liu, and S. Bashir), pp. 1-50, Elsevier, 2015.

[64] T. J. Park, G. C. Papaefthymiou, A. J. Viescas, A. R. Moodenbaugh and S. S. Wong: “Size-Dependent Magnetic Properties of Single-Crystalline Multiferroic $BiFeO_3$ Nanoparticles”, *Nano Lett.*, 7, pp. 766-772 (2007).

[65] G. Audoit, J. S. Kulkarni, M. A. Morris and J. D. Holmes: “Size dependent thermal properties of embedded crystalline germanium nanowires”, *J. Mater. Chem.*, 17, pp. 1608-1613 (2007).

[66] J. P. Salvetat, J. M. Bonard, M. H. Thomson, A. J. Kulik, L. Forró, W. Benoit and L. Zuppiroli: “Mechanical properties of carbon nanotubes”, *Appl. Phys. A*, 69, pp. 255-260 (1999).

[67] I. Moreels, K. Lambert, D. Smeets, D. De Muynck, T. Nollet, J. C. Martins, F. Vanhaecke, A. Vantomme, C. Delerue, G. Allan and Z. Hens: “Size-Dependent Optical Properties of Colloidal PbS Quantum Dots”, *ACS Nano*, 3, pp. 3023-3030 (2009).

[68] C. N. R. Rao, G. U. Kulkarni, P. J. Thomas and P. Edwards: “Size-Dependent Chemistry: Properties of Nanocrystals”, *Chem. Eur. J.*, 8, pp. 28-35 (2008).

[69] J. O. Joswig and M. J. Springborg: "Size-dependent structural and electronic properties of Ti_n clusters (n≤100)", *Phys. Condens. Matter*, 19, pp. 106207-106224 (2007).

[70] S. Barcikowski, A. Hahn, A. Kabashin and B. Chichkov: "Properties of nanoparticles generated during femtosecond laser machining in air and water", *Appl. Phys. A*, 87, pp. 47-55 (2007).

[71] P. He, H. T. Liu, Z. Y. Li, Y. Liu, X. D. Xu and J. H. Li: "Electrochemical deposition of silver in room-temperature ionic liquids and its surface-enhanced raman scattering effect", *Langmuir*, 20, pp. 10260-10267 (2004).

[72] P. Y. Chen and I. W. Sun: "Electrochemistry of Cd(II) in the basic 1-ethyl-3-methylimidazolium chloride/tetrafluoroborate room temperature molten salt", *Electrochim. Acta*, 45, pp. 3163-3170 (2000).

[73] P. Y. Chen and I. W. Sun: "Electrochemical study of copper in a basic 1-ethyl-3-methylimidazolium tetrafluoroborate room temperature molten salt", *Electrochim. Acta* , 44, pp. 441-450 (1999).

[74] M. H. Yang and I. W. Sun: "Electrodeposition of antimony in a water-stable 1-ethyl-3-methylimidazolium chloride tetrafluoroborate room temperature ionic liquid", *J. Appl. Electrochem.*, 33, pp. 1077-1084 (2003).

[75] J. F. Huang and I. W. Sun: "Electrodeposition of PtZn in a Lewis acidic $ZnCl_2$–1-ethyl-3-methylimidazolium chloride ionic liquid", *Electrochim. Acta*, 49, pp. 3251-3258 (2004).

[76] J. F. Huang and I. W. Sun: "Fabrication and surface functionalization of nanoporous gold by electrochemical alloying/dealloying of Au–Zn in an Ionic Liquid, and the Self-Assembly of L-Cysteine Monolayers", *Adv. Funct. Mater.*,15, pp. 989-994 (2005).

[77] J. F. Huang and I. W. Sun: "Formation of nanoporous platinum by selective anodic dissolution of PtZn surface alloy in a lewis acidic zinc chloride-1-ethyl-3-methylimidazolium chloride ionic liquid", *Chem. Mater.*,16, pp. 1829-1831 (2004).

[78] Y. Wang and H. Yang: "Synthesis of CoPt nanorods in ionic liquids", *J. Am. Chem. Soc.*, 127, pp. 5316-5317 (2005).

[79] Y. Wang and H. Yang: "Oleic acid as the capping agent in the synthesis of noble metal nanoparticles in imidazolium-based ionic liquids", *Chem. Commun.*, pp. 2545-2547 (2006).

[80] K. Binnemans: "Ionic liquid crystals", *Chem. Rev.*,105, pp. 4148-4204 (2005).

[81] A. Taubert: "CuCl nanoplatelets from an ionic liquid-crystal precursor", *Angew. Chem. Int. Ed.*, 43, pp. 5380-5382 (2004).

[82] A. Taubert, P. Steiner and A. Mantion: "Ionic liquid crystal precursors for inorganic particles: phase diagram and thermal properties of a CuCl nanoplatelet precursor", *J. Phys. Chem. B*, 109, pp. 155421-15547 (2005).

[83] A. Taubert: "(Sub)micron CaF_2 cubes and hollow rods from ionic liquid emulsions", *Acta Chim. Slov.*, 52, pp. 168-170 (2005).

[84] A. Arce, A. Soto, E. Rodil and B. Rodriguez-Cabo: "Process for preparation of nanoparticles in ionic liquids", *PCT Int. Appl. WO 2012013852A2*, 2012.

[85] B. Rodríguez-Cabo, E. Rodil, H. Rodríguez, A. Soto and A. Arce: "Direct Preparation of Sulfide Semiconductor Nanoparticles from the Corresponding Bulk Powders in an Ionic Liquid", *Angew. Chem. Int. Ed.*, 51, pp. 1424-1427 (2012).

[86] B. Rodríguez-Cabo, E. Rodil, A. Soto and A. Arce: "Preparation of metal oxide nanoparticles in ionic liquid medium", *J. Nanopart. Res.*, 14, pp. 938-947 (2012).

[87] B. Rodríguez-Cabo, I. Rodríguez-Palmeiro, R. Rodil, E. Rodil , A. Arce and A. Soto "Synthesis of AgCl nanoparticles in ionic liquid and their application in photodegradation of Orange II", *J. Mater. Sci.*, 50, pp. 3576-3585 (2015).

[88] W. J. Stark: "Nanoparticles in Biological Systems", *Angew. Chem. Int. Ed.*, 50, pp. 1242-1258 (2011).

[89] T. K. Nguyen, H. T. T. Duong, R. Selvanayagam, C. Boyer and N. Barraud: "Iron oxide nanoparticle-mediated hyperthermia stimulates dispersal in bacterial biofilms and enhances antibiotic efficacy", *Sci. Rep.*, 5, pp. 1-15 (2015).

[90] C. A. Fromen, G. R. Robbins, T. W. Shen, M. P. Kai , J. P. Y. Ting and J. M. DeSimone: "Controlled analysis of nanoparticle charge on mucosal and systemic antibody responses following pulmonary immunization", *Proc. Natl. Acad. Sci. U.S.A.*, 112, pp. 488-493 (2015).

[91] S. S. Lee, W. Song, M. Cho, H. L. Puppala, P. Nguyen, H. Zhu, L. Segatori and V. L. Colvin: "Antioxidant Properties of Cerium Oxide Nanocrystals as a Function of Nanocrystal Diameter and Surface Coating", *ACS Nano*, 7, pp. 9693-9703 (2013).

[92] R. Savaliya, D. Shah, R. Singh, A. Kumar, R. Shanker, A. Dhawan and S. Singh: "Nanotechnology in Disease Diagnostic Techniques", *Curr. Drug Metab.*, 16, pp. 645-661 (2015).

[93] B. S Sekhon: "Food nanotechnology – an overview", *Nanotechnol. Sci. Appl.*, 3, pp. 1-15 (2010).

[94] M. Karkare, *Nanotechnology: Fundamentals and Applications*, I. K. International, New Delhi, 2008.

[95] R. Dastjerdi and M. Montazer: "A review on the application of inorganic nano-structured materials in the modification of textiles: Focus on anti-microbial properties", *Colloids Surf. B*, 79, pp. 5-18 (2010).

[96] M. S. Lowry, D. R. Hubble, A. L. Wressell, M. S. Vratsanos, F. R. Pepe and C. R. Hegedus: "Assessment of UV-permeability in nano-ZnO filled coatings via high throughput experimentation", *J. Coat. Technol. Res.*, 5, pp. 233-239 (2008).

[97] A. A. Rempel: "Nanotechnologies. Properties and applications of nanostructured materials", *Russ. Chem. Rev.*, 76, pp. 435-461 (2007).

[98] R. Jin: "The impacts of nanotechnology on catalysis by precious metal nanoparticles", *Nanotechnol. Rev.*, 1, pp. 31-56 (2012).

[99] M. Zäch, C. Hägglund, D. Chakarov and B. Kasemo: "Nanoscience and nanotechnology for advanced energy systems", *Curr. Opin. Solid State Mater. Sci.*, 10, pp. 132-143 (2006).

[100] Y. S. Hu, R. Demir-Cakan, M. M. Titirici, J. O. Müller, R.

Schlögl, M. Antonietti and J. Maier: “Superior Storage Performance of a Si@SiOx/C Nanocomposite as Anode Material for Lithium-Ion Batteries”, *Angew. Chem. Int. Ed.*, 47, pp. 1645 -1649 (2008).

[101] J. K. Lee, K. B. Smith, C. M. Hayner and H. H. Kung: “Silicon nanoparticles–graphene paper composites for Li ion battery anodes”, *Chem. Commun.*, 46, pp. 2025-2027 (2010).

[102] A. Star, V. Joshi, S. Skarupo, D. Thomas and J. C. P. Gabriel: “Gas Sensor Array Based on Metal-Decorated Carbon Nanotubes”, *J. Phys. Chem. B*, 110, pp. 21014-21020 (2006).

[103] T. Bora and J. Dutta: “Applications of Nanotechnology in Wastewater Treatment-A Review.”, *J. Nanosci. Nanotechnol.*, 14, pp. 613-626 (2014).

[104] J. L. Wang and L. J. Xu: “Advanced Oxidation Processes for Wastewater Treatment: Formation of Hydroxyl Radical and Application”, *Crit. Rev. Env. Sci.*, 42, pp. 251-325 (2012).

[105] N. Xu, Z. Shi, Y. Fan, J. Dong, J. Shi and M. Z. C. Hu: “Effects of particle size of TiO_2 on photocatalytic degradation of methylene blue in aqueous suspensions”, *Ind. Eng. Chem. Res.*, 38, pp. 373-379 (1999).

[106] C. Martínez, M. Fernández, J. Santaballa and J. Faria: “Kinetics and mechanism of aqueous degradation of carbamazepine by heterogeneous photocatalysis using nanocrystalline TiO_2, ZnO and multi-walled carbon nanotubes–anatase composites”, *Appl. Catal., B*, 102, pp. 563-571 (2011).

[107] Y Chen, K. Wang and L. Lou: “Photodegradation of dye pollutants on silica gel supported TiO_2 particles under visible light irradiation”, *J. Photochem. Photobiol. A*, 163, pp. 281-287 (2004).

[108] C. Lizama, J. Freer, J. Baeza and H. D. Mansilla: “Optimized photodegradation of Reactive Blue 19 on TiO_2 and ZnO suspensions”, *Catal. Today*, 76, pp. 235-246 (2002).

[109] S. Murgolo, F. Petronella, R. Ciannarella, R. Comparelli, A. Agostiano, M. Curri and G. Mascolo “UV and solar-based photocatalytic degradation of organic pollutants by nano-sized TiO_2 grown on carbon nanotubes”, *Catal. Today*, 240, pp. 114-124 (2015).

[110] S. K. Maeng, K. Cho, B. Jeong, J. Lee, Y. Lee, C. Lee, K. J. Choi and S. W. Hong: "Substrate-immobilized electrospun TiO_2 nanofibers for photocatalytic degradation of pharmaceuticals: The effects of pH and dissolved organic matter characteristics", *Water Res.*, 86, pp. 25-34 (2015).

[111] C. Karunakaran, R. Dhanalakshmi, G. Manikandan and P. Gomathisankar: "Photodegradation of carboxylic acids on Al_2O_3 and SiO_2 nanoparticles", *Indian J. Chem. Sec. A*, 50, pp.163-170 (2011).

[112] Y. Badr, M. A. El-Wahed and M. Mahmoud: "Photocatalytic degradation of methyl red dye by silica nanoparticles", *J. Hazard. Mater.*, 154, pp. 245-253 (2008).

[113] N. Daneshvar, D. Salari and A. Khataee: "Photocatalytic degradation of azo dye acid red 14 in water on ZnO as an alternative catalyst to TiO_2", *J. Photochem. Photobiol. A*, 162, pp. 317-322 (2004).

[114] G. Zhang, Y. Gao, Y. Zhang and Y. Guo "Fe_2O_3-pillared rectorite as an efficient and stable Fenton-like heterogeneous catalyst for photodegradation of organic contaminants", *Environ. Sci. Technol.*, 44, pp. 6384-6389 (2010).

[115] P. Wang, B. Huang, X. Zhang, X. Qin, H. Jin, Y. Dai, Z. Wang, J. Wei, J. Zhan, S. Wang, J. Wang and M. H. Whangbo: "Highly efficient visible-light plasmonic photocatalyst Ag@AgBr" *Chem. Eur. J.*, 15, pp. 1821-1824 (2009).

[116] Y. Xu, H. Xu, H. Li, J. Xia, C. Liu and L. Liu: "Enhanced photocatalytic activity of new photocatalyst Ag/AgCl/ZnO", *J. Alloy Compd.*, 509, pp. 3286-3292 (2011).

[117] J. Shu, Z. Wang, G. Xia, Y. Zheng, L. Yang and W. Zhang: "One-pot synthesis of AgCl@Ag hybrid photocatalyst with high photocatalytic activity and photostability under visible light and sunlight irradiation", Chem. Eng. J., 252, pp. 374-381 (2014).

[118] H. Gatemala, C. Thammacharoen and S. Ekgasit: "3D AgCl microstructures selectively fabricated via Cl^--induced precipitation from $[Ag(NH_3)_2]$", *Cryst. Eng. Comm.*, 16, pp. 6688-6696 (2014).

[119] H. Xu, H. Li, J. Xia, S. Yin, Z. Luo, L. Liu and L. Xu:

"One-pot synthesis of visible-light-driven plasmonic photocatalyst Ag/AgCl in ionic liquid*", ACS Appl. Mater. Inter.*, 3, pp. 22-29 (2011).

[120] G. Li, K. H. Wong, X. Zhang, C. Hu, J. C. Yu, R. C. Y. Chan and P. K. Wong: "Degradation of Acid Orange 7 using magnetic AgBr under visible light: the roles of oxidizing species", *Chemosphere*, 76, pp. 1185-1191 (2009).

[121] P. Wang, B. Huang, X. Qin, X. Zhang, Y. Dai, J. Wei and M- H. Whangbo: "Ag@AgCl: a highly efficient and stable photocatalyst active under visible light", *Angew. Chem. Int.* Ed., 47, pp. 7931-7933 (2008).

[122] P. Wang, B. Huang, X. Zhang, X. Qin, Y. Dai, Z. Wang, and Z. Lou: "Highly efficient visible light plasmonic photocatalysts Ag@Ag(Cl, Br) and Ag@AgCl-AgI", *Chem. Cat. Chem.*, 3, pp. 360-364 (2011).

[123] B. Rodríguez-Cabo, I. Rodríguez-Palmeiro, R. Rodil, E. Rodil, A. Arce and A. Soto: "Photocatalytic degradation of methyl orange, methylene blue and rhodamine B with AgCl nanocatalyst synthesised from its bulk material in the ionic liquid $[P_{6\,6\,6\,14}]Cl$". *Water Sci. Tech.* Accepted, September 2016.

[124] S. U. S. Choi: "Enhancing Thermal Conductivity of Fluids with Nanoparticles" in *Developments and Applications of Non-Newtonian Flows* (Eds. D. A. Siginer, and H. P. Wang), vol. 231, pp. 99-105, ASME, New York, 1995.

[125] R. Taylor, S. Coulombe, T. Otanicar, P. Phelan, A. Gunawan, W. Lv, G. Rosengarten, R. Prasher and H. Tyagi: "Small particles, big impacts: A review of the diverse applications of nanofluids", *J. Appl. Phys.*, 113, pp. 1-19 (2013).

[126] S. Mukherjee and S. Paria: "Preparation and Stability of Nanofluids-A Review", *IOSR Journal of Mechanical and Civil Engineering*, 9, pp. 63-69 (2013).

[127] Y. Li, J. Zhou, S. Tung, E. Schneider and S. Xi: "A review on development of nanofluid preparation and characterization", *Powder Technol.*, 196, pp. 89-101 (2009).

[128] C. A. Nieto de Castro, M. J. V. Lourenço, A. P. C.

Ribeiro, E. Langa, S. I. C. Vieira, P. Goodrich and C. Hardacre: "Thermal Properties of Ionic Liquids and IoNanofluids of Imidazolium and Pyrrolidinium Liquids", *J. Chem. Eng. Data*, 55, pp. 653-661 (2010).

[129] C. A. Nieto de Castro, A. P. C. Ribeiro, S. I. C. Vieira, J. M. P. Franca, M. J. V. Lourenco, F. V. Santos, S. M. S. Murshed, P. Goodrich and C. Hardacre: "Synthesis, Properties and Physical Applications of IoNanofluids" in *Ionic Liquids - New Aspects for the Future* (Ed. J.Kadokawa), pp. 165-193, InTech, 2013.

[130] S. M. S. Murshed and C. A. Nieto de Castro: "Superior thermal features of carbon nanotubes-based nanofluids – A review", *Renew. Sust. Energ. Rev.*, 37, pp. 155-167 (2014).

[131] J. M. P. Franca, F. Reis, S. I. C. Vieira, M. J. V. Lourenço, F. J. V. Santos, C. A. Nieto de Castro and A. A. H. Pádua: "Thermophysical properties of ionic liquid dicyanamide (DCA) nanosystems", *J. Chem. Thermodynamics*, 79, pp. 248-257 (2014).

[132] J. M. P. Franca, S. I. C.Vieira, M. J. V. Lourenco, S. M. S.Murshed and C.A. Nieto de Castro: "Thermal Conductivity of $[C_4mim][(CF_3SO_2)_2N]$ and $[C_2mim][EtSO_4]$ and Their IoNanofluids with Carbon Nanotubes: Experiment and Theory", *J. Chem. Eng. Data*, 58, pp. 467-476 (2013).

[133] A. G. M. Ferreira, P. N. Simões, A. F. Ferreira, M. A. Fonseca, M. S. A. Oliveira and A. S. M. Trino: "Transport and thermal properties of quaternary phosphonium ionic liquids and IoNanofluids", *J. Chem. Thermodyn.*, 64, pp. 80-92 (2013).

[134] B. Wang, X. Wang, W. Lou and J. Hao: "Rheological and Tribological Properties of Ionic Liquid-Based Nanofluids Containing Functionalized Multi-Walled Carbon Nanotubes", *J. Phys. Chem. C*, 114, pp. 8749-8754 (2010).

[135] T. C. Paul, A. K. M. M. Morshed, E. B. Fox and J. A. Khan: "Thermal performance of Al_2O_3 Nanoparticle Enhanced Ionic Liquids (NEILs) for Concentrated Solar Power (CSP) applications", *Int. J. Heat Mass Transfer*, 85, pp. 585-594 (2015).

[136] T. C. Paul, A. K. M. M. Morshed and J. A. Khan: "Effect of Nanoparticle Dispersion on Thermophysical Properties of

Ionic Liquids for its Potential Application in Solar Collector", *Procedia Eng.*, 90, pp. 643-648 (2014).

[137] M. Swadźba-Kwaśny, L. Chancelier, S. Ng, H. G. Manyar, C. Hardacre and P. Nockemann: "Facile *in situ* synthesis of nanofluids based on ionic liquids and copper oxide clusters and nanoparticles", *Dalton Trans.*, 41, pp. 219-227 (2012).

[138] B. Wang, X. Wang, W. Lou and J. Hao: "Ionic liquid-based stable nanofluids containing gold nanoparticles", *J. Colloid Interface Sci.*, 362, pp. 5-14 (2011).

[139] I. Rodríguez-Palmeiro, B. Rodríguez-Cabo, E. Rodil, A. Arce, J. M. Saiz-Jabardo and A. Soto: "Synthesis and characterization of highly concentrated AgI-[$P_{6,6,6,14}$]Cl ionanofluids", *J. Nanopart. Res.*, 15, pp. 1-8 (2013).

[140] K. V. Wong and O. De Leon, "Applications of Nanofluids: Current and Future", *Adv. Mech. Eng.*, 519659, pp. 1-11 (2010).

[141] X. Q. Wang and A. S. Mujumdar: "A review on Nanofluids - Part II: Experiments and Applications", *Braz. J. Chem. Eng.*, 25, pp. 631-648 (2008).

[142] W. J. Minkowycz, E. M. Sparrow and J. P. Abraham, *Nanoparticle Heat Transfer and Fluid Flow*, Advances in Numerical Heat Transfer (Eds. W. J. Minkowycz, E. M. Sparrow, and J. P. Abraham), CRC Press (Taylor & Francis Group), Boca Raton, Florida, 2013.

[143] E. C. Donaldson, G. V. Chilingarian and T. F. Yen, *Enhanced oil recovery, II: processes and operations* (Eds. E. C. Donaldson, G. V. Chilingarian, and T. F. Yen), Elsevier, Amsterdam, 1989.

[144] J. L. Salager, *Recuperación mejorada del petróleo* (Cuaderno FIRP S357-C) (Ed. J. L. Salager), Universidad de los Andes, Mérida-Venezuela, 2005.

[145] J. G. Speight, *Enhanced oil recovery methods for heavy oil and tar sands*, GULF Publishing Company, Houston, 2009.

[146] V. Alvarado and E. Manrique: "Enhanced Oil Recovery: An Update Review", *Energies*, 3, pp. 1529-1575 (2010).

[147] A. Shah, R. Fishwick, J. Wood, G. Leeke, S. Rigby and

M. Greaves: “A review of novel techniques for heavy oil and bitumen extraction and upgrading”, *Energy Environ. Sci.*, 3, pp. 700-714 (2010).

[148] J. J. Sheng, *Modern chemical enhanced oil recovery. Theory and practice*, Elsevier, Amsterdam, 2011.

[149] I. Lazar, I. G. Petrisor and T. F. Yen: “Microbial enhanced oil recovery (MEOR)”, *Petrol. Sci. Technol.*, 25, pp. 1353-1366 (2007).

[150] M. Fanun, *Microemulsions: Properties and Applications* (Ed. M. Fanun), CRC Press (Taylor & Francis Group), Boca Raton, Florida, 2008.

[151] P. A. Winsor, *Solvent Properties of Amphiphilic Compounds*, Butherworth & Co., London, 1954.

[152] J. L. Salager, J. C. Morgan, R. S. Schechter, W. H. Wade and E. Vasquez: “Optimum Formulation of Surfactant/Water/Oil Systems for Minimum Interfacial Tension or Phase Behaviour”, *Soc. Petrol. Eng. J.*, 19, pp. 107-115 (1979).

[153] J. Gross and G. Sadowski: “Perturbed-Chain SAFT: An Equation of State Based on a Perturbation Theory for Chain Molecules”, *Ind. Eng. Chem. Res.*, 40, pp. 1244-1260 (2001).

[154] J. Gross and G. Sadowski: “Application of the Perturbed-Chain SAFT Equation of State to Associating Systems”, *Ind. Eng. Chem. Res.*, 41, pp. 5510-5515 (2002).

[155] J. P. Wolbach and S. I. Sandler: “Using Molecular Orbital Calculations To Describe the Phase Behaviour of Cross-associating Mixtures”, *Ind. Eng. Chem. Res.*, 37, pp. 2917-2928 (1998).

[156] M. S. Benzagouta, I. M. Al Nashef, W. Karnanda and K. Al-Khidir: “Ionic liquids as novel surfactants for potential use in enhanced oil recovery”, *Korean J. Chem. Eng.*, 30, pp. 2108-2117 (2013).

[157] A. Z. Hezave, S. Dorostkar, S. Ayatollahi, M. Nabipour and B. Hemmateenejad: “Dynamic interfacial tension behaviour between heavy crude oil and ionic liquid solution (1-dodecyl-3-methylimidazolium chloride ([C_{12}mim][Cl]+ distilled or saline water/heavy crude oil)) as a new

surfactant", *J. Mol. Liquid*, 187, pp. 83-89 (2013).

[158] A. Z. Hezave, S. Dorostkar, S. Ayatollahi, M. Nabipour and B. Hemmateenejad: "Effect of different families (imidazolium and pyridinium) of ionic liquids-base surfactants on interfacial tension water/crude oil system", *Fluid Phase Equil.*, 360, pp. 139-145 (2013).

[159] S. Sakthivel, S. Velusamy, R. L. Gardas and J. S. Sangwai: "Use of Aromatic Ionic Liquids in the Reduction of Surface Phenomena of Crude Oil–Water System and their Synergism with Brine", *Ind. Eng. Chem. Res.*, 54, pp. 968-978 (2015).

[160] S. Sakthivel, S. Velusamy, R. L. Gardas and J. S. Sangwai: "Adsorption of aliphatic ionic liquids at low waxy crude oil–water interfaces and the effect of brine", *Colloids Surf. A*, 468, pp. 62-75 (2015).

[161] S. Sakthivel, P. K. Chhotaray, S. Velusamy, R. L. Gardas and J. S. Sangwai: "Synergistic effect of lactam, ammonium and hydroxyl ammonium based ionic liquids with and without NaCl on the surface phenomena of crude oil/water system", *Fluid Phase Equil.*, 398, pp. 80-97 (2015).

[162] J. F. B. Pereira, R. Costa, N. Foios and J. A. P. Coutinho: "Ionic liquid enhanced oil recovery in sand-pack columns", *Fuel*, 134 pp. 196-200 (2014).

[163] A. Z. Hezave, S. Dorostkar, S. Ayatollahi, M. Nabipour and B. Hemmateenejad: "Investigating the effect of ionic liquid (1-dodecyl-3-methylimidazolium chloride ($[C_{12}mim][Cl]$)) on the water/oil interfacial tension as a novel surfactant", *Colloids Surf. A*, 421, pp. 63-71 (2013).

[164] M. S. Bin-Dahbag, A. A. Al Quraishi, M. S. Benzagouta, M. M. Kinawy, I. M. Al Nashef and E. Al Mushaegeh: "Experimental Study of Use of Ionic Liquids in Enhanced Oil Recovery", *J. Pet. Environ. Biotechnol.*, 4, pp. 165-171 (2014).

[165] M. S. Bin-Dahbag, A. A. Al Quraishi and M. S. Benzagouta: "Efficiency of ionic liquids for chemical enhanced oil recovery", *J. Petrol. Explor. Prod. Technol.*, 5, pp. 353-361 (2015).

[166] S. Gou, T. Yin, L. Yan and Q. Guo: "Water-soluble complexes of hydrophobically modified polymer and surface

active imidazolium-based ionic liquids for enhancing oil recovery", *Colloids Surf. A*, 471 pp. 45-53 (2015).

[167] S. Palchowdhury and B. L. Bhargava: "Ionic Liquids at Nonane–Water Interfaces: Molecular Dynamics Studies", *J. Phys. Chem. B*, 118, pp. 13930-13939 (2014).

[168] S. Sakthivel, R. L. Gardas and J. S. Sangwai: "Effect of Alkyl Ammonium Ionic Liquids on the Interfacial Tension of the Crude Oil-Water System and Their Use for the Enhanced Oil Recovery Using Ionic Liquid-Polymer Flooding", *Energy Fuels*, 30, pp. 2514-2523 (2016).

[169] A. Mohsenzadeh, Y. Al-Wahaibi, A. Jibril, R. Al-Hajri and S. Shuwa: "The novel use of Deep Eutectic Solvents for enhancing heavy oil recovery", *J. Pet. Sci. Eng.*, 130, pp. 6-15 (2015).

[170] A. Mohsenzadeh, Y. Al-Wahaibi, R. Al-Hajri and B. Jibril: "Effects of concentration, salinity and injection scenario of ionic liquids analogue in heavy oil recovery enhancement", *J. Pet. Sci. Eng.*, 133, pp. 114-122 (2015).

[171] I. Rodríguez-Palmeiro, O. Rodríguez, A. Soto and C. Held: "Measuring and PC-SAFT modelling three-phase behaviour", *Phys. Chem. Chem. Phys.*, 17, pp. 1800-1810 (2015).

[172] I. Rodríguez-Escontrela, I. Rodríguez-Palmeiro, O. Rodríguez, A. Arce and A. Soto: "Phase behaviour of the surfactant ionic liquid trihexyltetradecylphosphonium bis(2,4,4-trimethylpentyl)phosphinate with water and dodecane", *Colloids Surf., A*, 480, pp. 50-59 (2015).

[173] I. Rodríguez-Palmeiro, I. Rodríguez-Escontrela, O. Rodríguez, A. Arce and A. Soto: "Characterization and interfacial properties of the surfactant ionic liquid 1-dodecyl-3-methylimidazolium acetate for enhanced oil recovery", *RSC Adv.*, 5, pp. 22178-22187 (2015).

[174] I. Rodríguez-Escontrela, I. Rodríguez-Palmeiro, O. Rodríguez, A. Arce and A. Soto: "Liquid-liquid-liquid equilibria for water + $[P_{6\ 6\ 6\ 14}]$[DCA] + dodecane ternary system", *Fluid Phase Equilibr.*, 405, pp. 124-131 (2015)

[175] I. Rodríguez-Escontrela, I. Rodríguez-Palmeiro, O. Rodríguez, A. Arce and A. Soto: "Characterization and phase

behaviour of the surfactant ionic liquid tributylmethyl-phosphonium dodecylsulfate for enhanced oil recovery", *Fluid Phase Equilibr.*, 417, pp. 87-95 (2016).

USC
UNIVERSIDADE
DE SANTIAGO
DE COMPOSTELA

APPENDIX: RESUMEN
(Summary, in Spanish)

USC
UNIVERSIDADE
DE SANTIAGO
DE COMPOSTELA

En los últimos años, la comunidad científica ha puesto sus ojos en los líquidos iónicos (ILs) como una familia de compuestos con un enorme potencial. Son sus prometedoras propiedades las que han llevado a los investigadores a plantearse su uso en múltiples aplicaciones. Estos disolventes de diseño podrían sustituir a los disolventes orgánicos convencionales en diferentes procesos, haciéndolos medioambientalmente más sostenibles. Una de las características que requiere mayor atención es la presencia de diferentes dominios en la estructura de estas sales. De ese modo, las regiones con alta densidad de carga en los iones crean una red polar, mientras que las partes con baja densidad de carga permanecen separadas constituyendo dominios apolares (las regiones apolares están presentes en las cadenas alquílicas de los iones, que son especialmente significativas en el caso de los ILs surfactantes, SAILs). La presencia de estos dominios polares y apolares implica la existencia de diferentes tipos de interacciones, tanto en el seno de los ILs como en sus mezclas con otros compuestos.

El objetivo de esta Tesis, presentada como compendio de artículos, es el aprovechamiento de esta particular segregación en dominios de los ILs, específicamente en el caso de los SAILs, para el desarrollo de nuevas aplicaciones. Concretamente, se ha estudiado la capacidad de estas sales para sintetizar nanopartículas y nanofluidos mediante un método simple de disolución-reprecipitación. Además, se ha evaluado la capacidad de estas sales para mejorar los métodos de Extracción Mejorada del Petróleo que utilizan surfactantes.

A continuación se resumen los diferentes artículos que constituyen la Tesis.

Síntesis de nanopartículas de AgCl en líquido iónico, y su aplicación para la fotodegradación de naranja de β-naftol.

Los tintes industriales presentes en muchos efluentes representan una seria amenaza para el medio ambiente. Hoy en día estos tintes se emplean en numerosos procesos como la fabricación de textiles, plásticos, papel, teñido de pieles, fabricación de cosméticos o tecnología de alimentos. Con el incremento en el uso de fibras, ha aumentado la producción de nuevos tintes sintéticos, más estables químicamente y por

tanto más resistentes a los procesos de degradación convencionales. Entre ellos, los tintes tipo "azo" representan el 50% de los tintes empleados, fundamentalmente en la industria textil. Es por ello que en los últimos años los esfuerzos se han centrado en el tratamiento de este tipo de contaminantes mediante una serie de métodos de entre los cuales se hayan: procesos de adsorción, sistemas Fenton, tratamientos biológicos, degradación fotocatalítica, micro-filtración o coagulación/floculación. Los métodos fotocata-líticos constituyen unos de los más innovadores y con mayor potencial, a la vez que medioambientalmente más sostenibles. Existe un interés creciente en el uso de nanopartículas de diferente naturaleza (carbono, plata, óxidos metálicos, etc) como catalizadores. En el caso de los haluros de plata, se han usado sobretodo *composites*, no habiéndose estudiado el uso de nanopartículas de cloruro de plata hasta el momento.

El objetivo de este trabajo es sintetizar nanopartículas de cloruro de plata, AgCl, y tras su caracterización analizar su validez para la degradación del tinte naranja de β-naftol o naranja II (tinte tipo "azo") bajo radiación ultravioleta (UV). Se estudia el efecto de varios parámetros como la concentración del tinte, la carga de nanopartículas y el pH de la disolución acuosa.

Experimental

Síntesis y caracterización de las nanopartículas de AgCl

Las nanopartículas de AgCl se sintetizaron empleando un método de disolución/reprecipitación, obteniéndose una disolución transparente con una concentración de sólidos del 10% en masa. Con el objetivo de confirmar la presencia de las nanopartículas en la disolución, se analizó la misma mediante espectroscopia UV-visible (UV-vis). Se empleó microscopía electrónica de transmisión (TEM) para determinar el tamaño y la forma de las nanopartículas.

En una siguiente etapa, las nanopartículas se precipitaron mediante la adición de etanol. Con el fin de confirmar la estructura del nanomaterial, descartando cualquier proceso de transformación durante la síntesis y precipitación, las nanopartículas obtenidas se analizaron mediante difracción de rayos X (PXRD). Finalmente, con el objeto de conocer la superficie de las nanopartículas, se

analizaron también mediante microscopía electrónica de barrido (SEM).

Estudio de la fotodegradación catalítica de naranja de β-naftol con las nanopartículas de AgCl

Los experimentos de fotodegradación se llevaron a cabo partiendo de una disolución *stock* de naranja de β-naftol. Para llevar a cabo los experimentos, las muestras se agitaron en presencia de las nanopartículas bajo radiación UV durante un tiempo fijo en tubos de ensayo de Pyrex, midiéndose la absorbancia UV-vis tanto de la muestra inicial como de la tratada. Además, se analizó una muestra de la fase líquida obtenida después del proceso fotocatalítico mediante cromatografía líquida acoplada a un espectrómetro de masas con analizadores de cuadrupolo y de tiempo de vuelo (LC-Q-TOF-MS), con el objeto de identificar los nuevos productos formados.

Para analizar el efecto de la radiación UV y del fotocatalizador se realizaron experimentos empleando solamente radiación UV sin catalizador, y viceversa. Para determinar el efecto del tamaño del fotocatalizador se realizó un experimento empleando AgCl comercial de tamaño volumétrico. Por otro lado, para comparar el efecto de este fotocatalizador con otros nanomateriales comúnmente utilizados, se realizaron experimentos empleando nanopartículas comerciales de Ag, ZnO y TiO_2, bajo las mismas condiciones experimentales.

Para obtener la cinética del proceso de degradación se desarrolló un experimento tomando muestras del líquido en diferentes tiempos. Se analizaron las diferentes muestras mediante espectroscopia UV-vis, para determinar la concentración de tinte con el tiempo.

La influencia de la concentración de tinte y de la carga de nanopartículas también se estudió, empleando para ello diferentes valores de concentración inicial naranja de β-naftol y diferentes cargas de fotocatalizador.

El pH es un parámetro a tener en cuenta, ya que las aguas residuales contienen además del tinte otros compuestos que pueden hacer variar la acidez o basicidad de las mismas. Por lo tanto, se llevaron a cabo experimentos alterando el pH inicial de la disolución (empleando para ello

ácido sulfúrico e hidróxido sódico), manteniendo las mismas condiciones de agitación magnética y de radiación UV.

Resultados y discusión

Caracterización de las nanopartículas

El análisis de rayos X confirmó la estructura cúbica del AgCl. El espectro de absorbancia UV mostró el pico característico del AgCl a 300 nm, no hallándose indicios de Ag (cuyo pico aparecería a los 400 nm). Las imágenes obtenidas en el SEM mostraron aglomerados cúbicos de pequeñas nanopartículas (que se corresponde con estructuras previamente encontradas por otros autores), mientras que las imágenes del TEM (previas a la formación de los aglomerados cúbicos) indicaron la presencia de nanopartículas esféricas del rango de 5-20 nm de diámetro.

Evaluación de la actividad fotocatalítica

En un primer experimento, partiendo de una concentración de tinte de 100 ppm y usando una carga de nanopartículas de 1 $g \cdot L^{-1}$, después de 30 min de agitación bajo radiación UV, el análisis de espectroscopia UV-visible confirmó una degradación del 79.2%. También se ha comprobado que, después de 5 usos, la composición de las nanopartículas permanece invariable (no se observa presencia de Ag).

La radiación UV sobre la superficie del fotocatalizador genera huecos y electrones. Estos electrones son capaces de producir en un primer lugar O_2^-, y a continuación H_2O_2, que puede degradar el tinte. Se identificaron los productos de la fotodegradación a distintos tiempos de reacción mediante LC-Q-TOF-MS, proponiéndose un mecanismo de reacción para el proceso.

Al emplear el fotocatalizador en tamaño volumétrico se obtiene una disminución de la efectividad (42.2%). Esto es debido a la menor superficie específica del sólido volumétrico en comparación con las nanopartículas. De manera análoga, al usar luz solar en vez de radiación UV, se alcanza tan solo un 20.4% de degradación. El uso únicamente de radiación UV sin ningún tipo de catalizador ofreció un valor de degradación de 24.4%. Por tanto, el efecto combinado de nanopartículas de AgCl bajo radiación UV resulta eficaz para la degradación de naranja de β-naftol, obteniendo mejores resultados que

con otros nanocatalizadores (29.4% para Ag, 50.4% para TiO_2 y 62.5% para ZnO).

Efecto de la concentración inicial de tinte y de fotocatalizador

Al aumentar la concentración inicial de tinte disminuye la eficiencia de la degradación. Además, para una concentración inicial de tinte dada, una mayor carga de nanopartículas implica una mayor degradación. Para una carga de nanopartículas de 1 g L^{-1} (seleccionada para el resto de los ensayos) el proceso de degradación es fotocatalítico, mientras que a concentraciones mayores de nanopartículas el proceso se debe principalmente a la adsorción y no tanto a la fotodegradación.

Efecto del pH en la disolución inicial

Los resultados obtenidos para un pH ácido son similares que para el pH natural de la disolución. Sin embargo, al aumentar el pH a 9, el porcentaje de degradación aumenta hasta alcanzar un 96.7%, disminuyendo bruscamente cuando el medio se vuelve muy básico.

Conclusiones

La obtención de nanopartículas de AgCl es posible mediante un simple método de disolución/reprecipitación que utiliza únicamente el sólido volumétrico y el IL $[P_{6\ 6\ 6\ 14}]Cl$, evitando por tanto el uso de disolventes orgánicos. Se obtuvo una alta concentración de pequeñas nanopartículas (<20 nm) en forma de agregados cúbicos.

Las nanopartículas obtenidas se emplearon en la fotodegradación del tinte naranja de β-naftol, consiguiéndose resultados prometedores. No se ha observado la formación de plata metálica durante el proceso de fotodegradación. Partiendo de una concentración de 100 ppm de tinte, y de 1 g·L^{-1} de nanopartículas, tras 30 min bajo radiación UV se alcanza una degradación del tinte del 79.2%. La efectividad del proceso se debe a la acción combinada de las nanopartículas y de la radiación UV, ya que ambos efectos por separado implican menores valores de degradación. Con las nanopartículas de AgCl se obtienen mejores resultados que con otras nanopartículas comúnmente empleadas. El proceso de degradación responde a una cinética de pseudo primer orden, con un valor de la constante de 0.0451 min^{-1} y

los productos finales de la degradación son pequeños ácidos dicarboxílicos y dióxido de carbono.

La tasa de degradación aumenta al disminuir la concentración inicial de tinte o al aumentar la carga de nanopartículas, alcanzándose una degradación prácticamente completa (≥99.9%) para cualquier muestra con menos de 100 ppm de tinte y usando 10 $g \cdot L^{-1}$ tras 30 min de radiación UV. Sin embargo, para altas concentraciones de catalizador la eliminación del tinte por adsorción prevalece sobre la fotodegradación. Se ha comprobado que un valor de pH entorno a 9 aumenta la efectividad del proceso. Finalmente, se ha comprobado la reciclabilidad de las nanopartículas usándolas 5 veces, sin observar pérdidas significativas en su actividad (partiendo de un 79.2% de degradación, se alcanza un valor constante del 63-64% a partir del cuarto ciclo).

Síntesis y caracterización de ionanofluidos de AgI–$[P_{6\,6\,6\,14}]Cl$ de alta concentración

Los haluros de plata se han empleado en numerosas aplicaciones. Entre ellos el yoduro de plata, AgI, ha destacado por ser un electrolito sólido altamente conductor (especialmente cuando el tamaño de partícula es menor que 140 nm), con aplicación en baterías de estado sólido, sensores químicos o sembrado de nubes. Su estructura experimenta cambios a presión atmosférica con la temperatura. De ese modo, mientras que a temperatura ambiente coexisten las estructuras β–AgI y γ-AgI, a 420.15 K hay una transición mediante la cual aparece la forma α-AgI.

La síntesis de nanopartículas de AgI se lleva comúnmente a cabo mediante reacción química entre dos precursores, siendo $AgNO_3$ y KI los más habituales. En los últimos años, los ILs están mostrando su efectividad para la síntesis de muy diversos tipos de nanomateriales a través de diferentes técnicas. En la mayoría de los casos, los ILs actúan como medio de reacción o como agente estabilizante, pero también se han empleado como generadores de micelas en el seno de las cuales se obtienen las nanopartículas. En el caso específico de las nanopartículas de AgI, los ILs en combinación con disolventes orgánicos, han sido utilizados en lo fomación de micelas como medio de síntesis de este nanomaterial a partir de sólido volumétrico de AgI.

El objetivo de este trabajo es probar si el método de síntesis de nanopartículas utilizado anteriormente es válido también para la síntesis de ionanofluidos estables. Esto eliminaría la necesidad de usar disolventes orgánicos en la síntesis. En concreto se pretenden sintetizar ionanofluidos de diferentes concentraciones consistentes en nanopartículas de AgI en el seno del IL cloruro de trihexil(tetradecil)fosfonio, $[P_{6\,6\,6\,14}]Cl$. Los ionanofluidos se caracterizan mediante la determinación de varias propiedades físicas, térmicas y eléctricas.

Experimental

Síntesis de los ionanofluidos (nanopartículas de AgI en $[P_{6\,6\,6\,14}]Cl$)

Se añadieron diferentes cantidades de sólido volumétrico de AgI a un balón con el IL $[P_{6\,6\,6\,14}]Cl$, consiguiendo mezclas de diferentes concentraciones.

Caracterización de los ionanofluidos

Se midieron las propiedades físicas del IL y de los ionanofluidos de distintas concentraciones. Para la densidad e índice de refracción se varió la temperatura desde 293.15 a 323.15 K. Las medidas de conductividad eléctrica se realizaron hasta los 358.15 K. Para obtener los valores de viscosidad, fue necesario comprobar el comportamiento Newtoniano de los ionanofluidos llevando a cabo experimentos en un reómetro. Una vez comprobado, se realizaron medidas desde 295.15 a 343.15 K. El calor específico se determinó desde 298.15 a 473.15 K.

Caracterización de las nanopartículas

Para la caracterización de las nanopartículas fue necesario precipitarlas y extraerlas del IL. Se analizó el sólido obtenido mediante PXRD para comprobar la estructura de las nanopartículas, y mediante TEM para determinar su tamaño y forma. La absorbancia UV-vis fue también medida. El tamaño y distribución de las nanopartículas se determinó mediante dispersión dinámica de luz (DLS), determinándose su radio hidrodinámico analizando su movimiento Browniano.

Resultados y discusión

La primera evidencia de la formación de los ionanofluidos fue la coloración amarillenta de las dispersiones (a mayor concentración de nanopartículas mayor coloración). Para concentraciones hasta el 50% en peso, el valor de la concentración fue estimado durante la preparación, ya que no se observó sólido precipitado tras la síntesis. No se observó esta dispersión completa cuando se intentó sintetizar ionanofluido al 60% en peso de AgI. En el resto de los casos, los ionanofluidos resultaron claros y estables (sin observar precipitación incluso tras varios meses).

Los valores de densidad e índice de refracción obtenidos de los ionanofluidos indicaron una disminución lineal al aumentar la temperatura, y un aumento al aumentar la concentración de nanopartículas.

En el caso de la viscosidad, tanto el IL como los ionanofluidos presentaron comportamiento Newtoniano. No se observó variación en la viscosidad en el rango de concentraciones de 1-20% en peso con respecto al IL puro. Sin embargo, esta propiedad aumentó drásticamente a concentraciones elevadas, y especialmente en las temperaturas más bajas. Como era de esperar, los valores de viscosidad disminuyeron con el aumento de la temperatura.

Se esperaba un incremento en la conductividad eléctrica de los ionanofluidos con el aumento de la concentración de AgI. Sin embargo, se ha encontrado que los valores de conductividad aumentaron al aumentar la concentración hasta el 20% en peso, y a partir de esa concentración se produjo una disminución. Este comportamiento puede explicarse debido al aumento de la viscosidad de los ionanofluidos con mayor concentración de nanopartículas. Una menor movilidad de los iones asociada al aumento de la viscosidad pudo llevar a valores más bajos de conductividad eléctrica.

En el caso del calor específico, los valores aumentaron ligeramente al aumentar la temperatura. Sin embargo, debido a que el calor específico del AgI es menor que él del IL, un aumento en la concentración de AgI implicó una disminución en el calor específico de los ionanofluidos.

La caracterización de las nanopartículas se llevó a cabo partiendo de la muestra al 20% de concentración. Se halló el

pico de absorbancia del UV-vis a 355 nm, lo cual se corresponde con valores bibliográficos.

Debido a que el AgI es un semiconductor de banda directa, se pudo calcular su energía de banda directa, obteniéndose un valor de 3.49 eV a λ_{max}. Con ese valor, se realizó una primera estimación del tamaño de las nanopartículas mediante la ecuación de Brus, obteniéndose un valor del diámetro de partícula de aproximadamente 3.5 nm. Las medidas realizadas en el ZetaSizer proporcionaron tanto el tamaño medio de las nanopartículas como la distribución de tamaños. Los valores obtenidos resultaron coherentes con la estimación inicial. Del mismo modo, las imágenes obtenidas mediante TEM corroboraron tanto el tamaño de partícula (entre 2 y 4 nm) como la estrecha distrución de tamaños.

Finalmente, se analizó la estructura de las nanopartículas de AgI obtenidas mediante PXRD, revelando la existencia de yodargirita, la estructura cristalina hexagonal correspondiente a la fase β-AgI, lo que implica que no hubo ningún cambio estructural durante la transformación de sólido volumétrico a nanopartícula.

Conclusiones

La síntesis de ionanofluidos de AgI en el IL $[P_{6\ 6\ 6\ 14}]Cl$ es posible mediante un método de disolución/reprecipitación que evita el uso de altas presiones o temperaturas, así como de disolventes volátiles. Esta técnica permite obtener ionanofluidos estables con elevadas concentraciones de nanopartículas de hasta el 50% en peso.

Tanto la densidad como el índice de refracción aumentan con la concentración de nanopartículas, y disminuyen ligeramente con la temperatura, mientras que el calor específico se comporta de manera opuesta, disminuyendo con la concentración de nanopartículas y aumentando ligeramente con la temperatura.

La reducida conductividad eléctrica del IL (elegido por su capacidad de estabilizar nanopartículas) puede ser compensada aumentando la concentración de nanopartículas de AgI dispersas en él, pero teniendo en cuenta que se ha obtenido un máximo de esta propiedad a una concentración del 20% en peso. Este hecho puede deberse a la reducción de

la mobilidad de iones con el aumento de la viscosidad que se da a altas concentraciones.

Los estudios de PXRD corroboraron la estructura hexagonal de las nanopartículas (β-AgI) que constituyen los ionanofluidos. Dichas nanopartículas son esféricas, bien definidas y no aglomeradas, con una distribución de tamaños entre 2 y 4 nm.

Medida y modelización empleando PC-SAFT del comportamiento de fases de sistemas trifásicos

El conocimiento acerca de los diagramas de fase ternarios de sistemas de equilibrio líquido-líquido es crucial para los procesos de extracción. Los sistemas ternarios con miscibilidades parciales y siendo los tres componentes líquidos a una presión y temperatura dada fueron clasificados por Treybal en cuatro tipos. Los sistemas Treybal I, II y III se caracterizan por la existencia de uno, dos o tres pares de componentes puros parcialmente miscibles, respectivamente, mientras que los sistemas Treybal IV implican la formación de fases sólidas. El equilibrio de tres fases líquidas puede ocurrir cuando las tres regiones inmiscibles de un sistema tipo III se solapan. Sin embargo, no siempre es necesario la presencia de tres pares parcialmente miscibles, ya que existen ejemplos de sistemas con solo un par inmiscible en los que a ciertas concentraciones presentan tres fases líquidas en equilibrio.

Dentro de los sistemas ternarios, aquellos que están formados por agua-aceite-surfactante son de gran importancia desde un punto de vista industrial debido a su aplicación en la Extracción Mejorada de Petróleo (EOR). El comportamiento de fases de este tipo de sistemas puede visualizarse con facilidad a través de la clasificación de Winsor. El comportamiento correspondiente a los sistemas Winsor tipo III (que implica la existencia de una región trifásica, rodeada de tres regiones bifásicas) está asociado a valores mínimos de la tensión interfacial entre las fases acuosa y orgánica, condición requerida en los procesos de EOR con surfactantes. A pesar del gran interés que despierta esta aplicación, la obtención rigurosa de los diagramas ternarios es complicada y tediosa, por lo que la posibilidad de predecir el comportamiento de este tipo de sistemas, en especial de los formados por agua-aceite-surfactante, podría resultar tremendamente ventajosa.

En este trabajo, se pretenden estudiar sistemas del tipo agua (o salmuera) + aceite + surfactante, empleando *n*-dodecano como aceite, y dos ILs (bis(trifluorometil-sulfonil)imida de 1-decil-3-metilimidazolio, $[C_{10}mim][NTf_2]$, y bis(trifluorometil-sulfonil)imida de 1-dodecil-3-metilimida-zolio, $[C_{12}mim][NTf_2]$) como surfactantes. Dado que ambos ILs son inmiscibles en agua y *n*-dodecano, los sistemas ternarios correspondientes son clasificados como Treybal tipo III. Debido a la estructura de estos ILs, en la que una larga cadena alquílica está unida a cabeza polar en el catión, son sustancias anfifílicas y potencialmente surfactantes. Teniendo en mente una posible aplicación en EOR, se pretenden estudiar los diagramas de equilibrio de fases de estos sistemas en busca de diagramas Winsor tipo III con una microemulsión media equilibrada en su contenido en agua y aceite, que lleven a una reducción de la tensión interfacial. Se pretende además predecir los datos obtenidos mediante la ecuación de estado PC-SAFT (*Perturbed-Chain Statistical Associating Fluid Theory*). Esta ecuación fue desarrollada por Gross y Sadowski. Es una teoría de perturbación en la que se asume que los fluidos están formados por cadenas de esferas rígidas para el cálculo de la energía de Helmholtz residual, considerando términos de dispersión y de asociación.

Experimental

Para determinar los diagramas de fases de los sistemas ternarios agua + $[C_nmim][NTf_2]$ (*n*=10, 12) + *n*-dodecano se introdujo una composición conocida de los componentes en celdas de equilibrio encamisadas, con agitación mecánica para asegurar el contacto entre fases, y posteriormente se cesó la agitación para permitir la adecuada separación de las mismas. Se tomó una muestra de cada una de las fases en equilibrio para medir su composición y sus propiedades físicas (concretamente densidad y viscosidad), así como la tensión interfacial entre ellas. Las concentraciones de agua y *n*-dodecano de cada fase fueron determinadas mediante cromatografía de gases, obteniendo la concentración de IL por diferencia.

Para evaluar el comportamiento de agregación de ambos ILs en agua a 298.15 K fue empleado el método de las tensiones superficiales. El tamaño de las microgotas presentes en la fase rica en IL fue determinado mediante microscopía óptica y confocal.

Para la predicción de los datos mediante el modelo PC-SAFT se obtuvieron únicamente datos de componenetes puros obtenidos de la bibliografía. Únicamente en el caso del $[C_{12}mim][NTf_2]$, el tamaño y diámetro de los segmentos, así como la energía de dispersión fueron obtenidos mediante ajuste de datos experimentales de densidad del IL puro en un rango de temperaturas desde 288.15 a 348.15 K.

Resultados y discusión

Se estudió el comportamiento de fases para los sistemas agua + $[C_{10}mim][NTf_2]$ + *n*-dodecano, y agua + $[C_{12}mim][NTf_2]$ + *n*-dodecano, a presión atmosférica, tanto a 298.15 como a 348.15 K.

Los valores de solubilidad mutua entre los ILs y el agua obtenidos coinciden con valores previamente publicados. La solubilidad en agua dismunuye al aumentar la longitud de la cadena alquílica, *n*, alcanzando un mínimo para *n*=8, y aumentando para un mayor número de carbonos. El mismo comportamiento puede observarse para la serie *n*=6-10 para los ILs $[C_nmim][BF_4]$. Además, la solubilidad mutua aumenta con la temperatura. En el caso del *n*-dodecano, su solubilidad en los ILs estudiados aumenta con la temperatura, y está en concordancia con los valores bibliográficos.

En la evaluación del comportamiento de agregación de los ILs en agua se obtuvieron resultados diferentes para cada uno de ellos. En el caso del $[C_{10}mim][NTf_2]$ no se detectó la formación de micelas, en consonancia con los resultados previamente publicados. Sin embargo para el $[C_{12}mim][NTf_2]$, se observó una disminución inicial de la tensión superficial con la concentración de IL, seguida de un valor constante, lo que indica la formación de micelas. La concentración correspondiente a ese punto de ruptura se corresponde con la cmc, resultando ser 0.06 mM. Ambos ILs reducen drásticamente el valor de la tensión superficial del agua. Sin embargo, mientras que el catión $[C_{12}mim^+]$ es capaz de formar micelas, con el catión $[C_{10}mim^+]$ aparece inmiscibilidad antes de su formación.

Los diagramas obtenidos para los sistemas ternarios se corresponden, según la clasificación de Treybal, con sistemas tipo III. Además, pueden ser clasificados como Winsor tipo III, con una región trifásica rodeada de dos regiones bifásicas (la región bifásica inferior es despreciable), así como con un

dominio monofásico. La región trifásica consta de tres fases en equilibrio: una fase rica en surfactante (IL), una fase rica en agua y una tercera rica en *n*-dodecano. Sin embargo, con ambos ILs, las fases ricas en surfactante obtenidas contienen gran cantidad de IL, siendo más denso que el agua y el n-dodecano, por lo que dicha fase aparece en la parte inferior de los sistemas. Las fases ricas en IL fueron también analizadas mediante microscopía óptica y confocal, observándose gotas del rango de 1-3 μm para el $[C_{12}mim][NTf_2]$, y de inferior tamaño en el caso del $[C_{10}mim][NTf_2]$.

La determinación de la densidad y la viscosidad de las fases, así como de las tensiones interfaciales entre ellas, se realizó teniendo en mente una posible aplicación en EOR. Las dos primeras gobiernan la movilidad del fluido en el interior del pozo, de tal modo que si la presencia del IL aumenta la viscosidad de la fase acuosa se reduciría la presencia de digitaciones, favoreciendo el proceso. De igual modo, el proceso se vería favorecido alcanzándose tensiones interfaciales aceite/agua reducidas. De nuevo, el efecto de la temperatura fue analizado, realizando las medidas a 298.15 y 348.15 K. Además, debido a la presencia de sales en el pozo, el mismo estudio fue realizado sustituyendo el agua por salmuera (disolución acuosa de NaCl al 4% en peso). El $[C_{12}mim][NTf_2]$ provoca tensiones interfaciales más bajas, debido a su mayor carácter anfifílico. Para ambos ILs, la tensión interfacial agua/IL disminuye con la temperatura y con la adición de NaCl. Sin embargo, en el caso de la tensión interfacial IL/*n*-dodecano no se ve afectada por la temperatura. Se ha encontrado un comportamiento similar para las interfases de los sistemas de tres fases. Las tensiones interfaciales fase acuosa/fase rica en IL, y fase rica en *n*-dodecano/fase acuosa disminuyen con la temperatura y con la adición de sal, siendo el efecto de la sal más acusado a temperaturas más altas. Sin embargo, el efecto de ambas variables es despreciable para la tensión interfacial entre fase rica en *n*-dodecano/fase rica en IL.

Los resultados predichos mediante PC-SAFT muestran gran concordancia con los resultados experimentales. Los valores de la desviación media absoluta entre los obtenidos mediante PC-SAFT y los experimentales en los sistemas a 298.15 K son del mismo orden de magnitud (0.001-0.003) que las incertidumbres de las medidas experimentales. Al aumentar la temperatura, las desviaciones aumentan ligeramente. Pese a ello, la predicción es bastante buena, con

valores de desvío de 0.012 para el sistema con $[C_{10}mim][NTf_2]$ y de 0.020 para el sistema con $[C_{12}mim][NTf_2]$. Además, esos valores de desviación pueden ser fácilmente reducidos introduciendo un valor del parámetro k_{ij} en el par (*n*-dodecano/IL), alcanzando unos valores de 0.005 y 0.006 para el $[C_{10}mim][NTf_2]$ y $[C_{12}mim][NTf_2]$ respectivamente para un valor de k_{ij} de 0.008.

Conclusiones

En este trabajo se han determinado propiedades termodinámicas y comportamiento de fases de sistemas agua (o salmuera) + aceite + surfactante, empleando *n*-dodecano como aceite y dos ILs como surfactantes ($[C_{10}mim][NTf_2]$ y $[C_{12}mim][NTf_2]$). Todos los sistemas (a 298.15 y 348.15 K) revelaron un comportamiento Treybal tipo III, pudiendo ser además clasificados como Winsor tipo III, en los que se alcanza una región trifásica formada por una fase rica en IL, una fase con exceso de agua y otra con exceso de aceite, sin la adición de cosurfactantes. Pudo observarse que las tensiones interfaciales disminuyeron al aumentar el tamaño de la cadena alquílica del catión del IL, al aumentar la temperatura, y en presencia de sal.

Algunos de los resultados obtenidos (como la elevada tensión interfacial entre aceite y agua en todos los casos, así como el elevado contenido de IL en el vértice del triángulo de tres fases) indican que los ILs estudiados no son los mejores candidatos para ser empleados en EOR.

Sin embargo, se pudo predecir satisfactoriamente el comportamiento de fases mediante el modelo PC-SAFT, sin más que utilizar parámetros de los componentes puros. Esto puede significar un gran avance en EOR, ya que permitiría hacer un barrido rápido y barato de posibles ILs para esta aplicación.

Caracterización y propiedades interfaciales del líquido iónico surfactante acetato de 1-dodecil-3-metilimidazolio para recuperación mejorada de petróleo

La extracción de petróleo presenta una serie de dificultades debido a las distintas resistencias que el crudo se encuentra al fluir a través del pozo. Las técnicas de EOR se emplean para vencer esas resistencias. Hoy en día los esfuerzos se

concentran en los métodos químicos, basados en la adición de aditivos de diferente naturaleza, para mejorar las prestaciones de la inundación con agua y su capacidad para empujar el crudo al exterior del pozo. En la mayor parte de los casos, los mejores resultados se obtienen mediante la combinación de diferentes productos, combinando así sus efectos. La adición de surfactantes es uno de los métodos más prometedores pero la obtención de un surfactante óptimo es el cuello de botella de esta aplicación.

Dentro de las ventajas que presentan los ILs, hay que destacar su condición de disolventes de diseño. Sus propiedades pueden ser modificadas, mediante la elección de sus iones, y dirigidas hacia una aplicación concreta. En los últimos años se ha producido una revolución en el estudio de los SAILs cuya estructura está formada por una parte hidrofóbica (generalmente una larga cadena alquílica) y una hidrofílica (una cabeza polar iónica). La posibilidad de emplear estos compuestos en EOR ha empezado a estudiarse recientemente. Su habilidad para este fin se evalúa en términos de reducción de la tensión interfacial entre crudo y agua, pero también en el comportamiento de fases de los sistemas formados por agua + aceite + surfactante (que debe resultar Winsor tipo III para la formación de una microemulsión equilibrada en contenido de agua y aceite), experimentos de adsorción en materiales similares al lecho del pozo y experimentos de inundación de lecho.

En este trabajo se sintetiza un nuevo SAIL miscible con agua mediante la combinación del catión 1-dodecil-3-metilimidazolio [$C_{12}mim^{+}$] y del anión acetato, [OAc^{-}]. Se evalúa su comportamiento como surfactante mediante la caracterización de la tensión superficial y conductividad eléctrica en disolución acuosa, obteniendo su cmc y parámetros relacionados. Como primer paso para la propuesta de este SAIL para EOR, se realizan medidas de tensión interfacial dinámica entre disoluciones acuosas del IL y crudo. Se analiza el efecto de diferentes variables importantes en el proceso (concentración de surfactante, temperatura o salinidad del agua), así como el efecto de la adición de aditivos alcalinos, con el objetivo de definir una formulación óptima que lleve a reducciones drásticas de la tensión interfacial.

Experimental

El SAIL acetato de 1-dodecil-3-metilimidazolio, [C_{12}mim][OAc] se sintetizó mediante una reacción de metátesis de un único paso entre el bromuro de 1-dodecil-3-metilimidazolio, [C_{12}mim]Br, y acetato potásico, KOAc. Tras purificación, se comprobó su pureza mediante cromatografía iónica (para la determinación de bromuro residual) y se determinó su contenido en agua por valoración en coulómetro Karl-Fischer.

Para el estudio del comportamiento de agregación del SAIL en agua se prepararon disoluciones acuosas con diferentes concentraciones. Para la determinación de la cmc se realizaron medidas de la tensión superficial empleando el método de plato de Wilhelmy, así como medidas de la conductividad eléctrica. Para el estudio de la tensión interfacial entre el crudo y la disolución acuosa del IL se realizaron medidas de tensiones interfaciales dinámicas empleando un tensiómetro de gota giratoria.

Resultados y discusión

Agregación en agua

El comportamiento de agregación en agua del SAIL se evaluó en términos de tensión superficial y conductividad eléctrica, medidas a diferentes concetraciones de SAIL. La tensión superficial, medida a 298.15 K, disminuye al aumentar la concentración de SAIL, y luego permanece constante. La concentración en ese punto, correspondiente a la cmc, resultó 0.81 mM. Se obtuvieron también otros parámetros, como la tensión superficial en la cmc (36.8 $mN \cdot m^{-1}$), el pC_{20} (3.27), que es el logaritmo negativo de la concentración necesaria para reducir la tensión superficial del disolvente en 20 mN m^{-1}, o el ratio cmc/C_{20} (1.50). La concentración de surfactante de exceso en la superficie, Γ_m, y el área mínima por molécula de surfactante en la superficie, a^s_m, pudieron obtenerse a partir de los datos experimentales, resultando ser 7.53 μmol m^{-2} y 0.22 nm^2, respectivamente. Se han comparando los resultados obtenidos con valores bibliográficos de SAILs con el mismo catión y diferentes aniones (cloruro, bromuro y yoduro). El valor de la cmc del [C_{12}mim][OAc] es un orden de magintud menor que en todos los demás SAILs. El valor de la tensión superficial en la cmc es menor que para el Br^- o el Cl^-, pero mayor que para el I^-. El valor del pC_{20} es mayor en el [C_{12}mim][OAc] que en los demás casos, indicando una mayor

eficiencia en la adsorción del surfactante en la interfase. El valor del ratio cmc/C_{20} es significativamente menor, siguiendo la tendencia $OAc^- < Cl^- < Br^- < I$. Esto implica que el anión acetato favorece la micelización sobre la adsorción más que los haluros. La concentración de surfactante de exceso en la superficie, Γ_m, es mayor para el acetato, y por lo tanto, el área mínima por molécula de surfactante en la superficie, a^s_m, es menor, indicando un mayor empaquetamiento del surfactante en la interfase agua/aire. En el caso de a^s_m, la tendencia es $Cl^- > Br^- > I^- > OAc^-$.

Los valores de conductividad eléctrica se midieron a 288.15, 298.15 y 308.15 K, ajustando los datos experimentales mediante regresión de mínimos cuadrados no lineal con el modelo propuesto por Carpena, con el objeto de determinar la cmc y las pendientes antes y después de la cmc. El grado de ionización de micela en torno a la cmc, α, fue calculado como la relación entre esas dos pendientes, mientras que el grado de unión del contraión, β, es igual a $1-\alpha$. Es habitual que exista cierta diferencia entre los valores de la cmc obtenidos por diferentes métodos (el valor obtenido mediante conductividad eléctrica resultó 0.46 mM a 298.15 K). El grado de ionización obtenido es próximo a la unidad, indicando un grado de unión de los iones acetato bajo (al contrario de lo que ocurre para los haluros). A partir de los valores de la cmc y de α, pudo calcularse la energía de Gibbs de micelización, ΔG^0_{mic}, resultando ser negativa (proceso espontáneo) para todas las temperaturas, aumentando ligeramente (resultando menos espontáneo) al aumentar la temperatura en el rango estudiado. Además, los valores en el caso del acetato son similares que para el cloruro, disminuyendo para el bromuro y yoduro. En diferentes estudios se ha relacionado el efecto de diferentes contraiones sobre la micelización con su capa de hidratación. Se ha comprobado que existe una correlación lineal lo suficientemente buena como para afirmar que que la variación en ΔG^0_{mic} depende de la variación en la hidratación del contraión.

Tensión interfacial dinámica en sistemas crudo/disoluciones acuosas de SAIL

El valor de la tensión interfacial entre el crudo empleado (*Saharan Blend)* y el agua resultó ser de 19.2 $mN \cdot m^{-1}$. Como punto de partida, se evaluó el efecto de la concentración de SAIL, preparando disoluciones acuosas de 500, 2000 y 4000

ppm de SAIL, y realizando experimentos de tensiones interfaciales dinámicas a 298.15 K y presión atmosférica. La tensión interfacial de equilibrio disminuyó al aumentar la concentración de SAIL, alcanzando valores de 6.91, 2.92 y 2.08 $mN \cdot m^{-1}$ respectivamente. Esos valores coinciden con los mínimos obtenidos, excepto para la disolución de 2000 ppm, cuyo mínimo alcanzó 2.77 $mN \cdot m^{-1}$. Esta misma tendencia (reducción de la tensión interfacial con la concentración, pero con una reducción de la eficiencia en la disminución a partir de cierta concentración) fue encontrada para otros ILs en la bibliografía. Se seleccionó una concentración de SAIL de 2000 ppm para el resto de experimentos, como óptimo entre reducción en la tensión interfacial y gasto de surfactante.

La salinidad de la fase acuosa tiene gran influencia sobre la tensión interfacial en los sistemas crudo/agua. Por este motivo, se realizaron varios experimentos variando la salinidad de la fase acuosa (concentración de NaCl) desde 0 al 4% en peso, manteniendo la concetración de SAIL constante a 2000 ppm. Los resultados obtenidos indicaron una clara disminución de la tensión interfacial con el aumento de la salinidad (desde 2.92 a 1.54 $mN \cdot m^{-1}$ con 1000 ppm de NaCl), pero en el rango de concentraciones de 2000 a 40000 ppm de NaCl las tensiones interfaciales de equilibrio alcanzaron valores similares (estabilizándose en torno a 1.2 $mN \cdot m^{-1}$). Todos los perfiles de tensión interfacial dinámica mostraron valores mínimos entre 0.4 y 0.8 $mN \cdot m^{-1}$ en el rango de concentraciones de 2000 a 40000 ppm de NaCl. Este límite en la reducción de la tensión interfacial con la salinidad fue encontrado en la bibliografóa para el SAIL cloruro de 1-dodecilpiridinio, $[C_{12}py]Cl$, a mayores concentraciones de NaCl.

Para analizar el efecto de la temperatura, se realizaron medidas de tensión interfacial dinámica entre el crudo y la disolución acuosa de SAIL (2000 ppm) a 298.15, 318.15 y 338.15 K. Para ver el efecto conjunto de temperatura y salinidad sobre la tensión interfacial, los experimentos fueron realizados empleando agua destilada y salmuera (4% en peso de NaCl) para preparar las distintas disoluciones acuosas de SAIL. Los resultados mostraron que el efecto de la temperatura es totalmente distinto en presencia o en ausencia de sal. Mientras que en para la disolución con agua destilada la tensión interfacial de equilibrio disminuye al aumentar la temperatura en el rango estudiado, pasando de 2.92 a 0.81 $mN \cdot m^{-1}$, en el caso de la salmuera aumenta desde

1.20 a 2.03 $mN \cdot m^{-1}$. Los perfiles de tensión interfacial dinámica también resultaron diferentes en agua destilada o salmuera, siendo para ésta última perfiles que aumentan con el tiempo y presentando un mínimo que aumenta con el aumento de la temperatura desde 0.51 a 1.70 $mN \cdot m^{-1}$. Este comportamiento es común a otros SAILs de acuerdo a la información bibliográfica.

Por último, se analizó el efecto de la presencia de álcalis en la disolución, ya que es sabido que los álcalis reaccionan con compuestos presentes en el crudo generando surfactantes *in situ*. Para ello, se llevaron a cabo una serie de experimentos empleando una disolución de $[C_{12}mim][OAc]$ (2000 ppm) en salmuera (4% en peso de NaCl) variando la concentración de NaOH (0, 0.5, 1.0 y 1.5% en peso) a 298.15 K. Los resultados muestran una disminución en la tensión interfacial de equilibrio al aumentar la concentración de NaOH (desde 1.2 a 0.30, 0.25 y 0.11 $mN \cdot m^{-1}$ para concentraciones de 0.5, 1.0 y 1.5% en peso de NaOH, respectivamente). Además, los perfiles de tensión interfacial dinámica presentaron una forma tipo "V", alcanzando un valor de la tensión interfacial mínimo de 0.10, 0.11 y 0.05 $mN \cdot m^{-1}$ para las concentraciones de NaOH de 0.5, 1.0 y 1.5%, respectivamente. Teniendo en cuenta que el valor de la tensión interfacial entre el crudo y el agua pura fue de 19.2 $mN \cdot m^{-1}$, se ha conseguido una reducción de la tensión interfacial de dos o tres órdenes de magnitud. Para profundizar sobre el efecto de los álcalis, se ha evaluado la presencia de Na_2CO_3. Se ha obtenido igualmente una reducción en la tensión interfacial, pero el efecto de la concentración de éste álcali no resultó claro (alcanzándose valores en el rango de 0.69-0.81 $mN \cdot m^{-1}$ para tensiones interfaciales de equilibrio, y de 0.29-0.32 $mN \cdot m^{-1}$ para las tensiones interfaciales mínimas). En cualquier caso, se obtuvieron mejores resultados empleando NaOH.

Conclusiones

El comportamiento de agregación del SAIL $[C_{12}mim][OAc]$ se evaluó, en términos de tensión superficial y conductividad eléctrica, comparándolo con otros SAILs con el mismo catión pero con aniones haluro. El $[C_{12}mim][OAc]$ presentó, en general, cmc más baja, mejor tendencia de micelización sobre la adsorción en la interfase, y menor espontaneidad para la

micelización. El efecto de contraión puede ser explicado en términos de sus radios de hidratación.

Se midieron las tensiones interfaciales dinámicas entre disoluciones acuosas de [C_{12}mim][OAc] y crudo para diferentes formulaciones y condiciones. Los resultados obtenidos han sido prometedores, alcanzando valores de reducción en la tensión interfacial muy significativos, y presentando las formulaciones utilizadas gran estabilidad en presencia de sal y álcalis.

Los trabajos previos encontrados en bibliografía donde se utilizan SAILs para reducir la tensión interfacial agua/crudo concluyen que estos compuestos son prometedores en el campo de EOR. Sin embargo, en muchos de ellos, los resultados de tensión interfacial obtenidos están lejos de ser ultra-bajos. En este trabajo se ha mostrado que la combinación del SAIL [C_{12}mim][OAc] con álcalis es importante para alcanzar una mayor reducción en la tensión intefacial. Las grandes posibilidades que ofrecen los ILs debido a su versatilidad y adaptabilidad, deben ser combinadas con otros aspectos habitualmente considerados en EOR para alcanzar formulaciones óptimas.

Como conslusiones globales, hay que destacar que los SAILs possen propiedades únicas que los convierten en compuestos atractivos para ser empleados en numerosas de aplicaciones. Concretamente, se ha probado con éxito su aplicabilidad en la síntesis de nanopartículas e ionanofluidos, así como su potencial uso para la mejora de métodos de EOR basados en surfactantes.